Investigation of Phyto-, Endo-, and Syntheto-cannabinoids in the Management of
Osteoarthritis Pain and Inflammation in Rats

by

Holly T.A. Philpott

Submitted in partial fulfilment of the requirements
for the degree of Master of Science

at

Dalhousie University
Halifax, Nova Scotia
November 2017

For my lab mother, Allison

Table of Contents

List of Tables

List of Figures

Abstract

The most prevalent form of joint disease, osteoarthritis (OA), is characterised by joint destruction, pain, and intermittent inflammation. It has recently emerged that OA is also associated with damage to the sensory nerves innervating these joints which leads to vasomotor dysfunction and neuropathic pain. Chronic pain associated with OA is the number one reason for patients to visit their physician, and is thought to be linked to neuropathy, inflammation and the degenerative changes that occur within OA joints. The ineffectiveness of currently used analgesics in providing symptom relief for OA patients suggests the need for novel therapeutic discoveries to help those affected by this disease.

Cannabinoids are a family of molecules that have been widely shown to decrease pain and inflammation and show promise in combatting OA-associated pain and inflammation. These compounds were first isolated from the *Cannabis sativa* plant, and similar compounds have since been identified within our bodies. This endocannabinoid system is the body's natural pain-modulating system and has been shown to be upregulated within the joints of OA patients. Targeted activation of the endocannabinoid system via locally-delivered compounds into the joint may help to enhance analgesia and reduce inflammation, while minimising the production of psychoactive side-effects traditionally associated with systemic cannabinoid use.

The aim of this thesis was to investigate the therapeutic potential of a phytocannabinoid, an endocannabinoid, and a synthetocannabinoid, administered locally into the knee, to manage OA inflammation and pain.

List of Abbreviations and Symbols Used

2-AG	2-Arachidonoylglycerol
5-HT$_{1A}$	5-Hydroxytryptamine receptor type 1A
ACEA	Arachidonyl-2-chloroethylamide
ACL	Anterior cruciate ligament
AEA	Anandamide
ALS	Amyotrophic Lateral Sclerosis
ANOVA	Analysis of variance
ARRIVE	Animal Research: Reporting of *In Vivo* Experiments
ATF-3	Activating transcription factor-3
BL	Baseline
Ca^{2+}	Calcium
CB$_1$R	Cannabinoid receptor type 1
CB$_2$R	Cannabinoid receptor type 2
CBD	Cannabidiol
CBG	Cannabigerol
CBN	Cannabinol
CGRP	Calcitonin gene-related peptide
CNS	Central nervous system
CONTRA	Contralateral
COX	Cyclooxygenase
CPP	Conditioned place preference
DAG	Diacylglycerol

DAGL	Diacylglycerol lipase
DAMP	Damage-associated molecular pattern
DRG	Dorsal root ganglia
EAE	Experimental autoimmune encephalomyelitis
ECS	Endocannabinoid system
ESAM	Endothelial cell-selective adhesion molecule
FAAH	Fatty acid amide hydrolase
FCA	Freund's Complete Adjuvant
GADPH	Glyceraldehyde-3-phosphate dehydrogenase
GPR18	G protein receptor 18
GPR55	G protein receptor 55
GPCR	G protein coupled receptor
hr	Hour
i.artic.	Intraarticular
i.p.	Intraperitoneal
i.v.	Intravenous
ICAM1	Intercellular adhesion molecule 1
ICAM2	Intercellular adhesion molecule 2
IFN-γ	Interferon-gamma
IL-1α	Interleukin-1 alpha
IL-1β	Interleukin-1 beta
IL-6	Interleukin-6
IVM	Intravital microscopy

JAM	Junctional adhesion molecule
LASCA	Laser speckle contrast analysis
LCL	Lateral collateral ligament
LSD	Least significant difference
MAGL	Monoacylglycerol lipase
MAP	Mean arterial pressure
MCL	Medial collateral ligament
MIA	Sodium monoiodoacetate
min	Minute(s)
MRI	Magnetic resonance imaging
MS	Multiple Sclerosis
NAPE	N-Acylphosphatidylethanolamines
NS	Not significant
NSAID	Non-steroidal antiinflammatory drug
OA	Osteoarthritis
PAG	Periaqueductal gray
PCL	Posterior cruciate ligament
PEA	Palmitoylethanolamide
PECAM1	Platelet endothelial cell adhesion molecule 1
PG	Prostaglandin
PNS	Peripheral nervous system
PU	Perfusion unit
RA	Rheumatoid arthritis

s.c.	Subcutaneous
sec	Second(s)
SEM	Standard error of the mean
SP	Substance P
TCA	Tricyclic antidepressant
TRP	Transient receptor potential
TRPV1	Transient receptor potential vanilloid 1
VCAM1	Vascular cell adhesion molecule 1
VEH	Vehicle
Δ^9-THC	Delta-9-Tetrahydrocannabinol
WB	Weight bearing
WT	Withdrawal threshold

Acknowledgements

First and foremost, I would like to thank my supervisor Dr. Jason J. McDougall. Thank you very much for your continued support and guidance, your mentorship over the past two years has been fundamental to my success in graduate school and in the completion of this thesis.

I would also like to acknowledge and thank the past and current members of the McDougall Lab with whom I have worked with. Most importantly, I would like to thank Allison Reid for her help throughout all aspects of this project and my time in the lab, I will be forever grateful. To Milind Muley and Melissa O'Brien, your support, help, and friendship have been greatly appreciated and treasured. Your work ethic and passion for science is inspiring and highly motivating.

I would like to acknowledge the members of my advisory and defense committees, Dr. Jim Fawcett, Dr. Melanie Kelly, and Dr. Christian Lehmann, all of whom, through constructive feedback and support, have helped shape this thesis.

Additionally, I would also like to thank everyone in the Department of Pharmacology for a fantastic few years. Specifically, graduate student coordinators, Dr. Kishore Pasumarthi and Dr. Ryan Pelis, as well as Luisa Vaughan, Sandi Leaf, and Cheryl Bailey for all they do in the administration office.

Last, but certainly not least, I would like to thank my amazing family and friends for their constant support and encouragement over the course of my studies.

Chapter 1: Introduction

1.1 Overview

Osteoarthritis (OA) is one of the most prominent musculoskeletal conditions, and is characterised by joint destruction, pain, and chronic fluctuations in inflammation. Chronic pain is the most debilitating symptom for OA patients, and severely decreases their ability to function during daily activities. Current therapies are not effective at relieving pain and often come with unwanted side effects; therefore, the development of new therapies is required. Chronic pain sufferers are the largest users of medical cannabis (marijuana) for their symptoms, but use can be limited by the psychoactive effects.

Three types of cannabinoids exist: phytocannabinoids, which are compounds extracted from the cannabis plant; endocannabinoids, which are compounds made by the body to form a natural pain-regulating system; and synthetocannabinoids, which are compounds synthetically made to mimic the endocannabinoids. The use of cannabinoid compounds has been shown to decrease pain and inflammation in preclinical studies.

This project was focused on establishing the role of locally administered cannabinoid and cannabinoid-modulating compounds in relieving pain and inflammation in a preclinical OA model. Additionally, the role that cannabinoid compounds have on OA disease progression and joint nerve damage was explored. Targeted and local activation of the endocannabinoid system may help to improve symptom relief and slow disease progression, while limiting the psychoactive effects associated with many cannabinoid compounds.

1.2 Anatomy of the human knee joint

The knee joint consists of the tibiofemoral and patellofemoral articulations. Synovial joints are highly moveable and are characterised by the presence of a synovial membrane and a joint cavity which is filled with synovial fluid. This fluid is secreted by the inner synovial membrane, and fills the joint space to provide lubrication for smooth biomechanical action of the joint. Synovial fluid also provides a conduit for the delivery of nutrients and oxygen to the internal structures of the joint via an intricate network of blood vessels. Synoviocytes secrete hyaluronic acid and lubricin, which form a viscous fluid providing frictionless movement between the bones of the joint. Additionally, the knee joint includes accessory muscles, internal and extraarticular ligaments, tendons, menisci, and bursae which aid in joint stability and function. The knee joint is classified as a complex hinge joint due to movement being largely restricted to one plane, but with strong accessory ligaments rotational or pivotal movement can be performed. The primary movements of the knee joint are described as flexion, extension, internal (medial) and external (lateral) rotation. The knee joints permit controlled movement to facilitate daily activities such as walking, running, and stair climbing, all of which require interactions between components of the musculoskeletal, nervous, and vascular systems.

The knee joint is comprised of three bones: the femur, patella, and tibia. There are five accessory ligaments: the anterior cruciate ligament (ACL), the posterior cruciate ligament (PCL), the medial collateral ligament (MCL), the lateral collateral ligament (LCL), and the patellar ligament (Figure 1.1). A second bone found in the lower leg, the fibula, provides stability to the knee joint by being an attachment point for the LCL, but is not directly part of the articulation. The cruciate ligaments, ACL and PCL, and the

collateral ligaments, MCL and LCL, aid in stabilising the joint during movement (*e.g.*

extension, flexion, preventing the knee from overextending, and limiting axial rotation).

The patellar ligament and accessory tendons at the front of the knee help stabilise the

patella. The posterior of the knee joint is reinforced by the oblique popliteal and arcuate

popliteal ligaments.
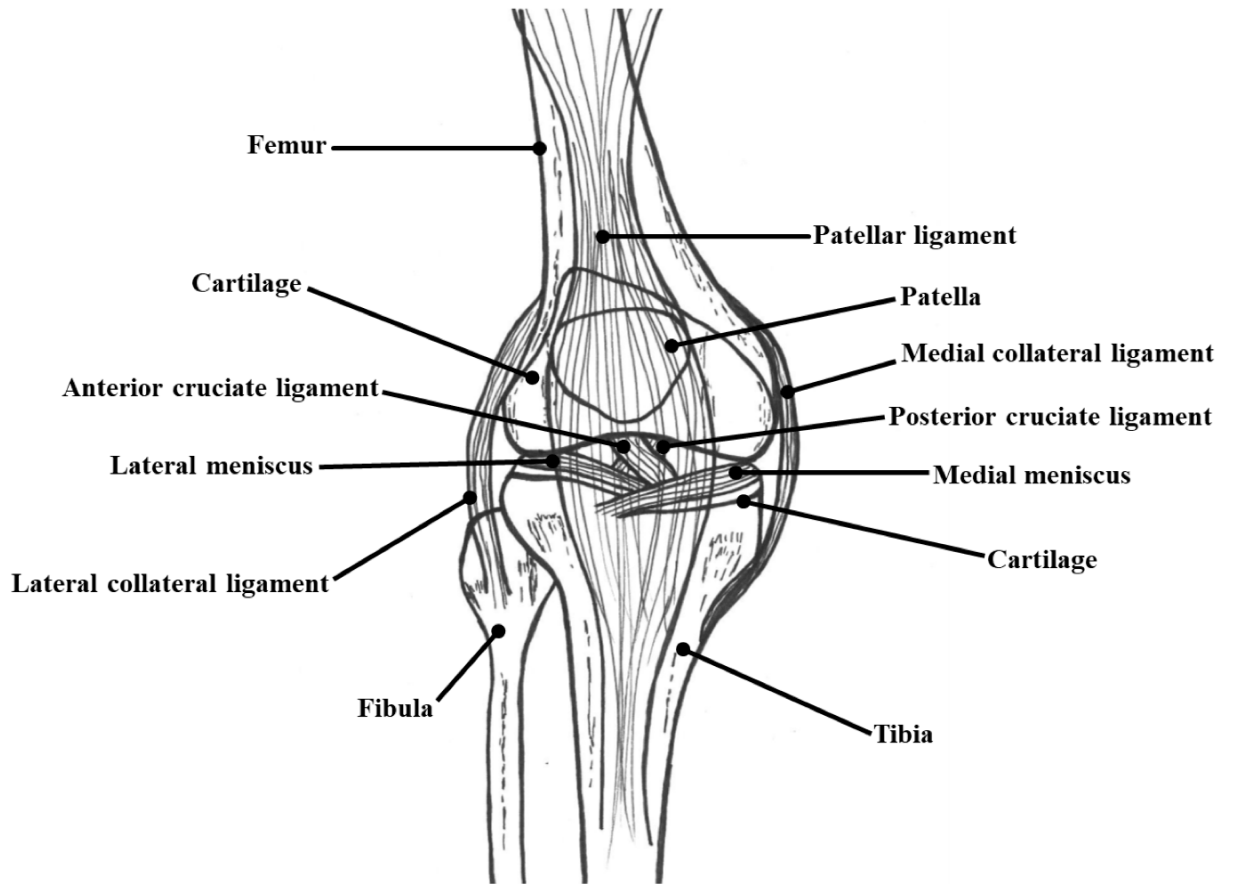
Figure 1.1 Anatomy of the human knee joint. (Original artwork).

The articular capsule surrounds the joint and is composed of an outer fibrous layer,

which is avascular, and an inner membranous layer called the synovial membrane. The

knee also contains two crescent-shaped disks, one medial and one lateral, called menisci.

Their main functions are load bearing and stability. The medial meniscus is anchored more securely than the lateral meniscus and undergoes less displacement during flexion and rotation. The menisci provide shock absorption, prevent capsule and synovial impingement, and provide some joint lubrication. Additionally, the surfaces of the femur and tibia are coated with cartilage, a fibrous, collagenous matrix providing extra joint cushioning.

1.2.1   Knee joint vasculature

In humans, as well as in rodents, the knee joint vasculature originates from branches of the femoral artery and vein, called the genicular, popliteal, and saphenous branches (Figure 1.2). The femoral artery branches just above the knee into the popliteal artery and the descending genicular artery, which further divides into the saphenous branch. The popliteal artery travels down the posterior of the knee joint and branches into five genicular branches, which are responsible for supplying the synovium, menisci, and ligaments of the knee joint. The different anatomical parts of the knee joint have different vascular supply. As discussed previously, the synovial membrane is highly vascular, whereas cartilage and ligaments are not. Only the outer layers of the joint ligaments (epiligament) as well as the outer portion of the menisci closest to the synovium (outer third), contain blood vessels.

Descending branch of
lateral femoral circumflex

Highest genicular

Musculoarticular branch
of highest genicular

Saphenous branch of
highest genicular

Lateral superior genicular

Medial superior genicular

Lateral inferior genicular

Medial inferior genicular

Fibular branch

Anterior recurrent tibial branch

Anterior tibial branch
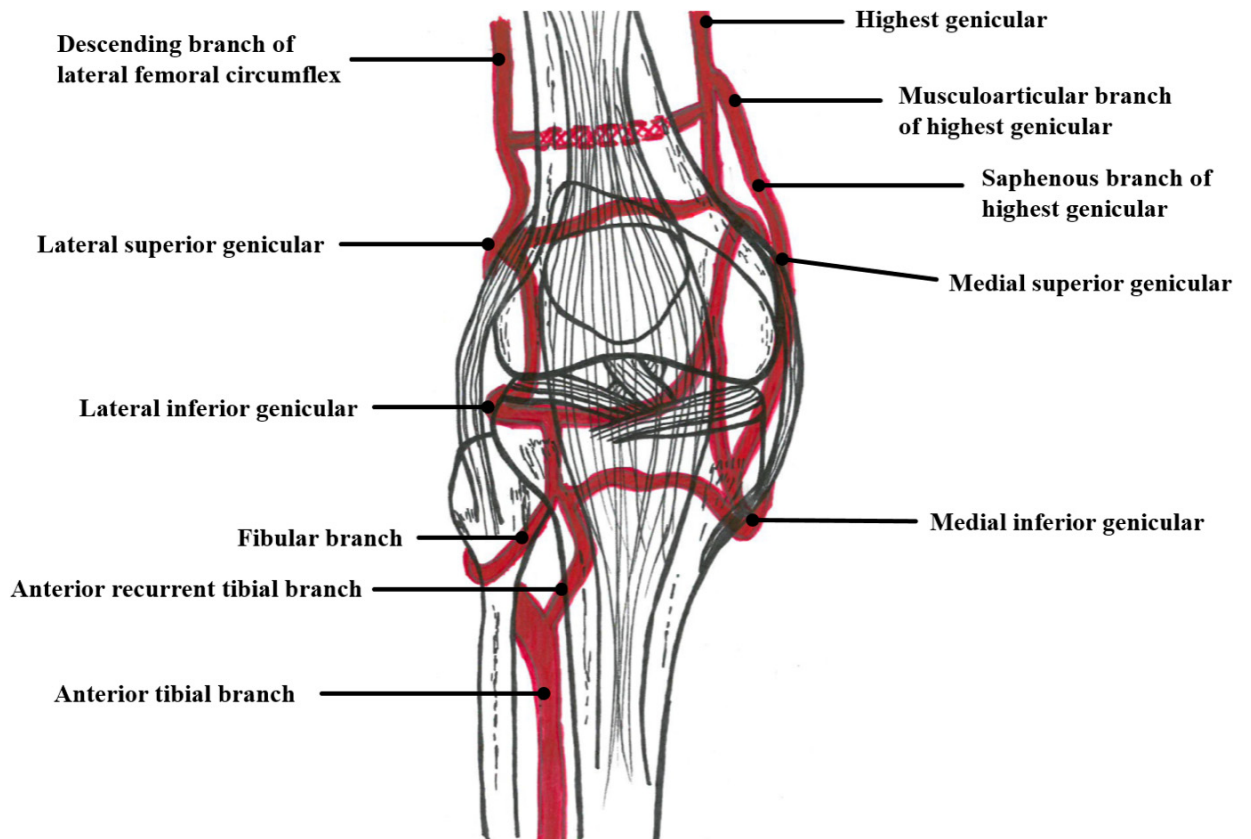
Figure 1.2 Vasculature of the human knee joint. (Original artwork).

1.2.2 Knee joint neuroanatomy

Proper knee joint locomotion requires sophisticated organisation and communication between the peripheral nervous system (PNS) and central nervous system (CNS). Both efferent and afferent neurones are responsible for generating these neuronal messages. The knee joint is innervated by contributions from the femoral, sciatic, tibial, and common peroneal nerves. These branches originate from the lumbar plexus of the spinal cord (L2-L6) in both rodents (Catre & Salo, 1999) and (L2-L5) humans (Agur & Dalley, 2013). The saphenous nerve is one of the largest and longest branches of the femoral nerve. It courses down the medial aspect of the leg next to the saphenous artery.

The saphenous nerve divides into an infrapatellar branch, medial articular branch, and a terminal branch which continues to the medial aspect of the ankle and foot. It innervates the medial and anterolateral skin below the patella, and the anterior inferior knee capsule.
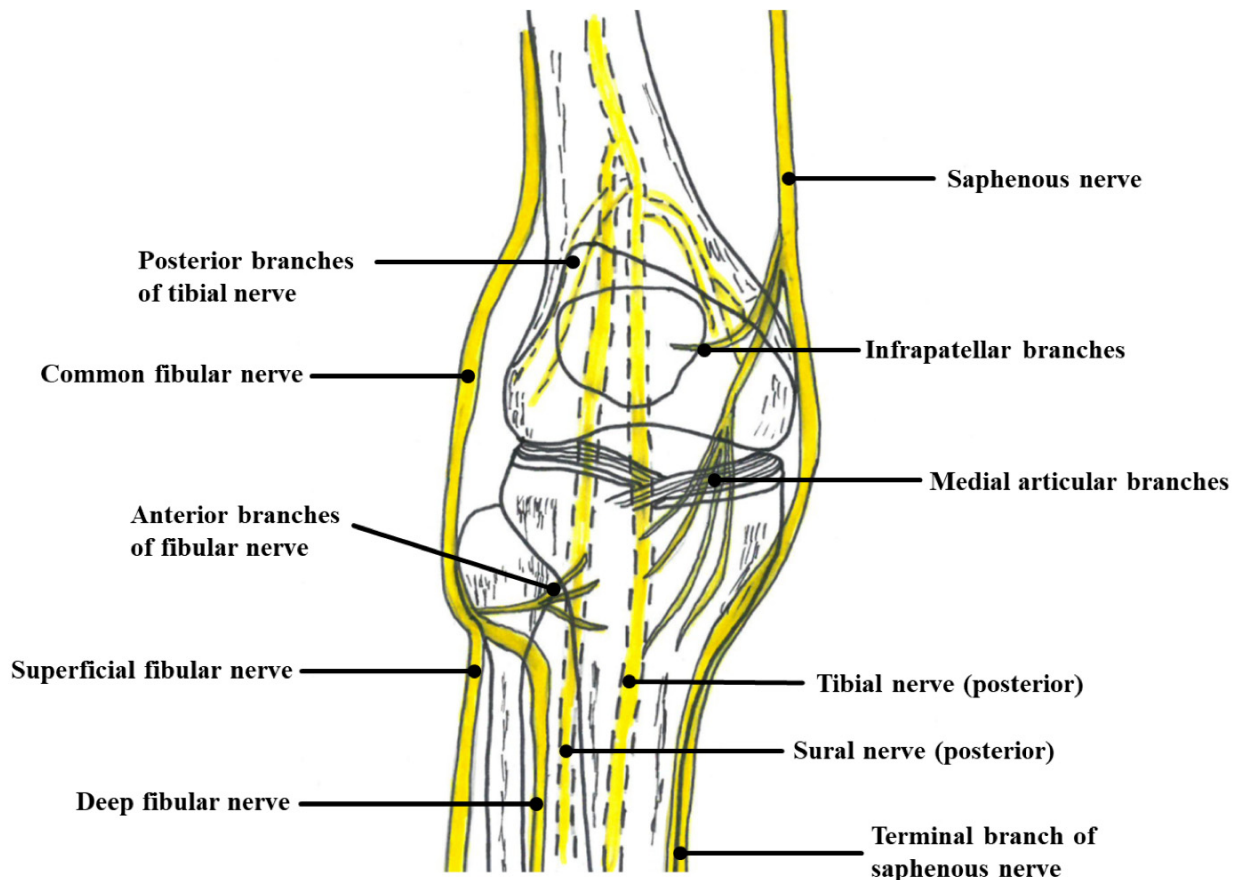
Figure 1.3: Innervation of the human knee joint. (Original artwork).

The origin of joint sympathetic efferent fibres arise from the lumbar plexus and terminate near joint blood vessels (Catre & Salo, 1999) where they are responsible for normal vasomotor control and responses in healthy joints (McDougall *et al.,* 1994; McDougall *et al.,* 1995; Karimian *et al.,* 1995; McDougall, 2001). Sensory information is transmitted by afferent fibres, which relay information regarding proprioception,

movement, and nociception to the CNS. Primary joint afferents can be subdivided into four classes: Aα, Aβ, Aδ, and C fibres (Table 1.1).

Table 1.1 Afferent innervation of the human knee joint

Fibre Type	Sensory Fibre Class	Diameter	Myelination	Conduction Velocity	Function	Location
Aα	**I**	10-18µm	Yes	70-120 (m/s)	Proprioception	Ligaments
Aβ	**II**	5-13µm	Yes	20-70 (m/s)	Proprioception	Capsule Ligaments Muscles
Aδ	**III**	1-5µm	Yes, thinly	2.5-20 (m/s)	Nociception	Capsule Synovium
C	**IV**	<1µm	No	0.5-2.5 (m/s)	Nociception	Capsule Synovium

(Adapted from Mapp, 1995; Krustev *et al.,* 2015)

The joint capsule, ligaments, menisci, periosteum, and subchondral bone are largely innervated by a network of both myelinated and unmyelinated fibres (Schaible *et al.,* 2009). Class I (Aα) are large diameter, myelinated fibres, which primarily innervate the joint ligaments and relay proprioceptive signals. Class II (Aβ) are also large diameter, myelinated fibres which signal proprioceptive information to the CNS, and innervate the joint capsule, ligaments, and muscles. Some of these act as mechanoreceptors, sensitive to pressure and traction. Class III (Aδ) are small diameter, thinly myelinated fibres which conduct nociceptive information. Class IV (C) are small, unmyelinated fibres which innervate the joint, they also transmit nociceptive signals (Freeman & Wyke, 1967; Horner & Dellon, 1994). Classes III and IV contribute to 80% of innervation of the rat synovium (Hildebrand *et al.,* 1991; Schaible *et al.,* 2009). The free nerve endings of the

Aδ and C fibres are distributed throughout the skin, muscle, surface of ligaments, and the joint, however the cartilage has no associated innervation (Schaible *et al.,* 2009). These fibres are classified as polymodal because they can be stimulated by chemical, thermal, and mechanical stimuli. Aδ fibres act as high-threshold mechanoreceptors, which are rapidly conducting and respond to sharp pain, and thermal stimuli, and are responsible for the reflex nociceptive response to acute pain (Hildebrand *et al.,* 1991; Schaible *et al.,* 2009; Trouvin & Perrot, 2017). C fibres are also high-threshold, slow conducting fibres and their activation leads to diffuse dull pain (Hildebrand *et al.,* 1991; Schaible *et al.,* 2009). Normally these afferents are silent but can be activated by joint inflammation, increased intraarticular (i.artic.) pressure, local chemical changes (*e.g.* neuropeptide release) or lesions, leading to subsequent plasticity changes in the periphery and centrally (Hildebrand *et al.,* 1991; Arendt-Nielsen, 2017; Trouvin & Perrot, 2017). This causes pain thresholds to lower and these nociceptors begin to relay information to the central nervous system. The information encodes heightened pain intensities (hyperalgesia) as well as pain sensations in response to normally innocuous stimuli (allodynia) (Schaible & Schmidt, 1985; Neugebauer & Schaible, 1988; Schaible & Schmidt, 1988).

1.3 Arthritis

Arthritis is the most prominent musculoskeletal disease and the number one cause of disability worldwide. Although arthritis is commonly thought to be a disease of the elderly population, it can affect people at any age. In Canada, arthritis affects 1 in every 6 people over the age of 15 (Arthritis Society of Canada, 2013). There are a number of factors that increase one's risk of developing arthritis, such as gender, age, genetics,

history of traumatic joint injury, and co-morbidities such as obesity. The average cost of arthritis to the Canadian economy is extremely high at $33 billion, and is predicted to double within the next 20 years (Brooks, 2006; The Arthritis Society of Canada, 2013), this is largely due to increased health care costs and loss of productivity among arthritis sufferers. Furthermore, the generic term "arthritis" is not a single disease, but rather a collection of over 100 different forms of disease that affect the musculoskeletal system. Each type of arthritis has a unique aetiology, pathophysiology and is, therefore, treated differently. Some types of arthritis affect only one joint but some can cause a polyarthritis, affecting many synovial joints, with the most common being weight-bearing joints such as the hips, knees, and ankles. Commonly shared symptoms are joint pain, stiffness, loss of function, swelling, and chronic fatigue. The two most common types of arthritis are osteoarthritis (OA) and rheumatoid arthritis (RA) (Figure 1.4).
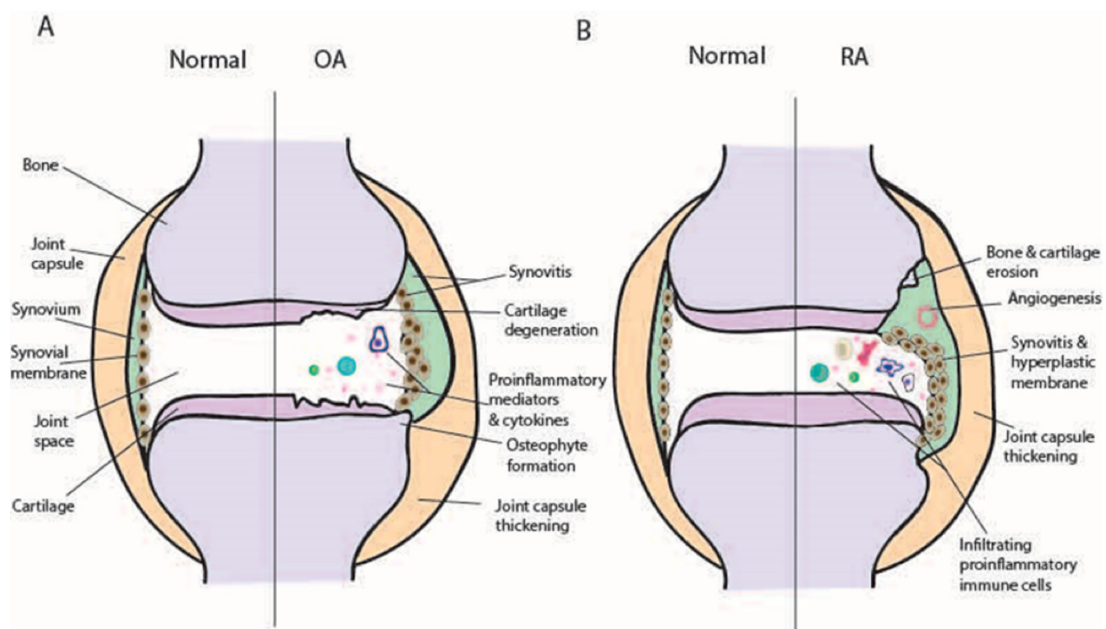
Figure 1.4 Illustration comparing the pathology of knee joints with osteoarthritis (A) and rheumatoid arthritis (B). (Adapted from Philpott & McDougall, 2017).

1.3.1 Rheumatoid arthritis (RA)

RA is a chronic, systemic autoimmune disease which is characterised by recurrent inflammatory flares within the joint, or many joints (Scott *et al.,* 2010). RA typically affects the small joints in the hands and feet, but can also manifest in non-articular organs such as the eyes, heart, and lungs (Krustev *et al.,* 2015). RA inflammatory flares are associated with high levels of hyperaemia, oedema, infiltrating immune cells, and increased release of proinflammatory mediators (Fernandes *et al.,* 2002; Krustev *et al.,* 2015). The chronic inflammation can eventually lead to the development of pain and the erosion of the cartilage and bones (McInnes & Schett, 2007).

1.3.2 Osteoarthritis (OA)

OA is a multifactorial disease, which involves many different pathological contributors, and is classified as a painful and degenerative disease of the synovial joints. Similar to other forms of arthritis, the prevalence of OA increases with age and is more common in women than in men (Aigner *et al.,* 2004). Other risk factors for OA include age, a history of joint trauma, altered biomechanics, and obesity (Felson, 2004). As the knee joint ages, the ligaments loosen and the cartilage eburnates which increases shear forces within the joint (Sokoloff, 1987). Major and minor injuries to the knee from sport or work that requires a lot of kneeling or heavy lifting have been shown to predispose people to knee OA (Felson & Chaisson, 1997; Jensen & Eenberg, 1996; Kujala *et al.,* 1995), by altering joint biomechanics. Congenital or developmental abnormalities, can also cause malalignment and improper loading of the joints (Harris, 1986; Wedge *et al.,* 1991; Felson, 2004). OA generally affects large, weight-bearing joints like the hip and

knee, but can also appear in the ankle joints and hands. Common clinical features of OA
are joint degeneration, dysfunction, and pain (Table 1.2).

Table 1.2 American College of Rheumatology: Knee OA Classification Criteria

Clinical Observations: knee pain most days of the month plus 3 from list below
1. Crepitus on active joint motion 2. Morning stiffness (lasting > 30 min) 3. Age > 38 years 4. Bony enlargement upon physical examination of joint 5. Bony tenderness upon physical examination of joint 6. No palpable warmth
Clinical Observations + Radiographic Evidence: knee pain most days of the month, osteophytes on joint margins, plus 1 from list below
1. Crepitus on active joint motion 2. Morning stiffness (lasting > 30 min) 3. Age > 38 years

(Adapted from Wu *et al.,* 2005)

OA was traditionally referred to as an arthrosis, thought to primarily affect the
articular cartilage of the joint, where the joint erodes over time due to chronic wear and
tear. However, recent evidence shows that OA disease progression is driven by chronic
low-grade inflammatory processes (Sokolove & Lepus, 2013; Robinson *et al.,* 2016). The
pathogenesis of OA also becomes increasingly complex due to the presence of multiple
structural and pain phenotypes, all of which has led to the subcategorisation of different
OA patients. Some patient populations have erosive or hypertrophic OA and can
experience differing pain phenotypes including inflammatory, degenerative, or
neuropathic pain as well as experience fluctuations in joint inflammation (Bierma-
Zeinstra & Verhagen, 2011).

1.3.2.1 Inflammation in osteoarthritis

In OA, inflammation or synovitis, is marked by the appearance of joint swelling, hyperaemia, stiffness, pain, and the infiltration of proinflammatory mediators into the joint space. Imaging studies using magnetic resonance imaging (MRI) have suggested an association between the presence of synovitis and OA progression (Krasnokutsky *et al.,* 2011; Felson *et al.,* 2003; Roemer *et al.,* 2011). Increased synovial inflammation was noted in 43% of OA patients and was associated with more severe preoperative pain and loss of function scores (Scanzello *et al.,* 2011) as well as increased joint destruction (Scanzello *et al.,* 2011; Torres *et al.,* 2006; Scanzello & Goldring, 2012). The degree of immune cell infiltration and inflammation is heterogeneous between OA patients (Benito *et al.,* 2005) and appears in lower levels when compared to RA patients (Nettelbladt & Sundblad, 1959; Sohn *et al.,* 2012). Overexpression and infiltration of inflammatory cells and mediators are increased in early, compared to late, OA (Benito *et al.,* 2005), suggesting that inflammation is predictive of OA progression and that an important period of time may exist where antiinflammatory interventions may be highly effective for the prevention of end-stage OA (Robinson *et al.,* 2016).

During synovitis, hyperplasia of the cells of the synovial lining allow inflammatory mediators to infiltrate (Sokolove & Lepus, 2013). OA tissues and synovial fluid have abnormally high levels of plasma proteins, complement mediators, cytokines, and neuropeptides (Nettelbladt & Sundblad, 1959; Sohn *et al.,* 2012; Gobezie *et al.,* 2007), none of which are found in normal joints (Goldring *et al.,* 2011). Additionally, elevated serum levels of the inflammatory marker C-reactive protein is predictive of OA disease progression (Pelletier *et al.,* 2001).

When joint tissues are damaged and the extracellular matrix breaks down, damage-associated molecular patterns (DAMPs) are produced and activate innate inflammatory processes involving mast cells and macrophages (Robinson *et al.,* 2016) which in turn produce an abundance of mediators that subsequently lead to the further development of synovitis and joint destruction (Sokolove & Lepus, 2013; Orlowsky & Kraus, 2015). The complement cascade can be activated by DAMPs and components of apoptotic joint debris can chemoattract proinflammatory leukocytes to further potentiate inflammation and promote tissue damage. The pathogenesis of OA has been linked to this pathway in both humans and rodents (Wang *et al.,* 2011). Inhibition of complement activation, both genetically and pharmacologically, significantly reduced OA joint damage in preclinical models (Wang *et al.,* 2011).

Cytokines are involved in OA pathogenesis (Sokolove & Lepus, 2013; Kapoor *et al.,* 2011) and contribute to the development of pain during inflammatory flares. In joint inflammation, they are released from endothelial cells, chondrocytes, fibroblasts, and infiltrating leukocytes. Synovial cytokine concentrations significantly increase (McInnes & Schett, 2007) during inflammation in both OA and RA (Farahat *et al.,* 1993). Furthermore, there exists a relationship between levels of interleukin-1α (IL-1α), interleukin-1β (IL-1β), interleukin-6 (IL-6), and tumor necrosis factor-α (TNF-α) and disease progression in OA patients (Smith *et al.,* 1997). These mediators can dysregulate the homeostatic balance between cartilage synthesis and break down (Saklatvala, 1986; Goldring *et al.,* 1994; Sokolove & Lepus, 2013). Cytokine levels have also been elevated in the sodium monoiodoacetate (MIA) model of OA (Orita *et al.,* 2011). These cytokines are also able to activate and sensitise joint nociceptors (Kidd & Urban, 2001).

Mechanical stress can also induce downstream proinflammatory signalling pathways. *In vitro* studies showed that impact injury induces chondrocyte death and activates stress-induced kinases to upregulate proinflammatory cytokines and chemokines (Ding *et al.,* 2010; Goodwin *et al.,* 2010).

Other immune cell infiltrates are macrophages and mast cells (Dean *et al.,* 1993), but also a small number of T cells and B cells (Bondeson *et al.,* 2010) which regulate adaptive immunity. Macrophages in OA joints produce cytokines which contribute to cartilage breakdown and osteophyte formation. Activated mast cells are present in synovial tissues and high levels have been correlated with a higher degree of structural damage and synovitis (de Lange-Brokaar *et al.,* 2012).

Prostaglandins and leukotrienes are lipid mediators that have been detected in OA joints and are involved in disease pathology by promoting inflammation and by stimulating cytokine production, apoptosis, and angiogenesis (Martel-Pelletier *et al.,* 2003). These mediators are produced from arachidonic acid via the cyclooxygenase (COX) pathway that can be induced by inflammation and trauma.

Proinflammatory neuropeptides have been identified in the synovium of RA and OA patients (Gronblad *et al.,* 1988) as well as in animals (Konttinen *et al.,* 1990), where they play an active role in pain modulation and in the regulation of inflammation. They activate inflammatory cells and induce release of cytokines. Inflammatory neuropeptides include substance P (SP), calcitonin gene-related peptide (CGRP), and vasoactive intestinal peptide (VIP) and are stored and released from the terminals of autonomic nerves and slowly conducting joint afferents (McDougall *et al.,* 1997; Ahmed *et al.,* 1993; Heppelmann & Pawlak, 1997). Neuropeptides are known to possess both

proinflammatory and inflammation-resolving activity. For example, CGRP has potent vasodilatory effects and local application accelerated skin wound healing in rats (Khalil & Helme, 1996). In another study, transected ligaments where the ends were left in close proximity were associated with a CGRP-mediated increase in vasodilation, but this was not the case when the transected ligament ends were allowed to retract during healing (McDougall *et al.,* 2000). Under certain physiological conditions neuropeptides might be advantageous in resolving inflammation and repairing trauma.

1.3.2.2 Joint nerve damage

In arthritic joints, the number of free fibres innervating the synovium is greatly reduced and shows abnormal distribution when compared to normal joints (Gronblad *et al.,* 1988; Mapp, 1995). These findings have also been shown in animals (Konttinen *et al.,* 1990; Mapp *et al.,* 1994). In a rabbit surgical ligament transection model, nerve fibres were noted as highly irregular and possessed abnormal characteristics such as swelling and truncation of the fibres, as well as a high expression of neuropeptides. Poor functional recovery in these animals was associated with impaired CGRP release (McDougall *et al.,* 1997; McDougall *et al.,* 2000). Another study showed that intact joint innervation was necessary for MCL repair in rabbits, where animals with nerve transection had poor structural outcomes when compared to control animals (Ivie *et al.,* 2002). Additionally, the structural pathology was correlated with differences in angiogenesis and ligament perfusion (Ivie *et al.,* 2002). In a model of inflammatory arthritis, there were pronounced changes in the staining of CGRP, SP, and VIP fibres over four weeks and this was attributed to nerve fibre sprouting (Buma *et al.,* 2000).

Furthermore, in OA, new nerve growth that accompanies angiogenesis can begin to innervate joint structures which were not normally innervated and could contribute to pain (Mapp & Walsh, 2012).

1.3.2.3 Osteoarthritis pain

Chronic pain is the most common symptom OA patients experience. Pain pathophysiology is complex and the experience of pain is not ubiquitous among patients. Although synovitis has been well correlated with pain outcomes (Baker *et al.*, 2010), both clinical and preclinical findings show that pain is independent of structural modifications within the joint (McDougall *et al.*, 2009; Cedraschi *et al.*, 2013).

Nociceptors in the joint are activated by various physiological stimuli (*e.g.* mechanical, chemical, thermal) and transmit pain signals via dorsal root ganglia (DRG), to the dorsal horn of the spinal cord where they decussate across to the contralateral side and synapse with second order neurones. The signal continues up the spinothalamic tract into the brain stem and thalamus, then relays signals to the hypothalamus, amygdala, periaqueductal grey (PAG), basal ganglia, limbic system, and somatosensory cortex (Costigan *et al.*, 2009) (Figure 1.5).
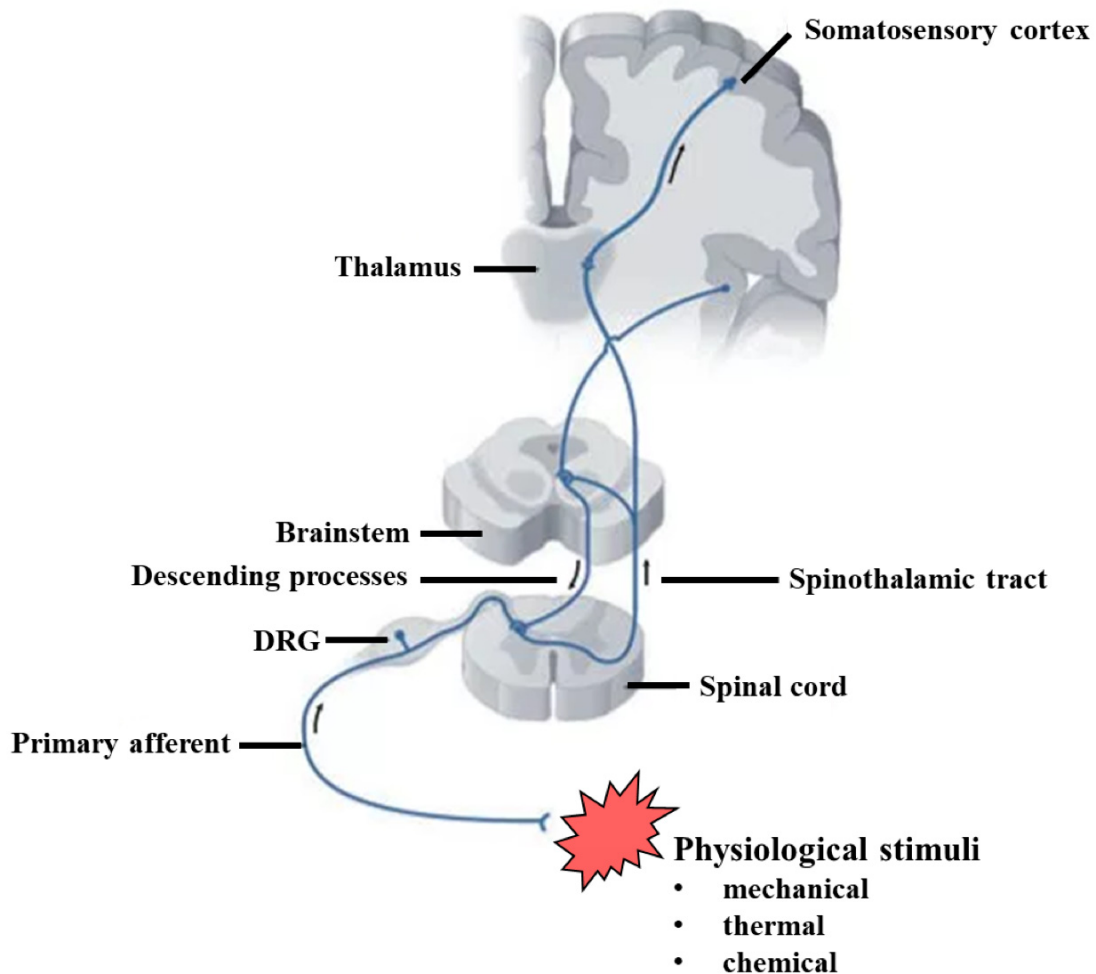
Figure 1.5 Nociceptive pain pathway. (Adapted from Costigan *et al.,* 2009).

The first *in vivo* evidence that mechanoreceptors are located in the rat knee joint was provided by Heppelmann and McDougall (2005). Using single unit electrophysiology recordings from joint primary afferents, they were able to decrease afferent firing rates in response to mechanical rotation of the joint by local application of mechanogated ion channel blockers, amiloride and gadolinium (Heppelmann & McDougall, 2005). Normal joints have an i.artic. subatmospheric pressure between (-2)–(-10)mmHg (Levick, 1979), but during inflammatory flares the pressure can to rise to 20mmHg causing activation of

joint mechanoreceptors. These nociceptors may also be activated by increased pressure in the subchondral bone (Trouvin & Perrot, 2017).

Peripheral inflammation plays a role in the maintenance of joint pain involving the release of inflammatory mediators upon damage to joint tissues (Schaible, 2006; Schaible *et al.,* 2009; Arendt-Nielsen, 2017). These mediators attempt to aid in healing, but instead begin to activate intracellular signal transduction pathways in nociceptor terminals which subsequently increases expression of ion channels on the nerve terminal (Costigan *et al.,* 2009). The threshold for activation is reduced and membrane excitability increases, causing changes in responsiveness (Costigan *et al.,* 2009; Latremoliere &Woolf, 2009). Innocuous stimuli can now produce pain and noxious stimuli can now produce an exaggerated pain response. Neurones now have amplified responsiveness in transmission of nociceptive information, which is called peripheral sensitisation (Figure 1.6) and is usually restricted to the site of injury or inflammation (Costigan *et al.,* 2009; Latremoliere & Woolf, 2009).
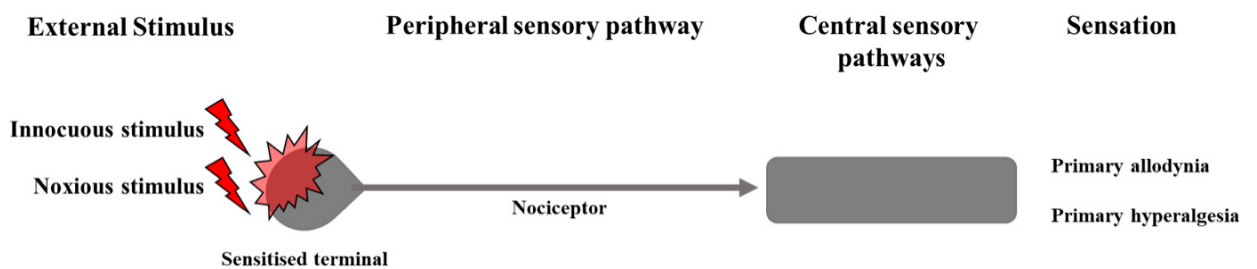
Figure 1.6 Pain mechanisms related to peripheral sensitisation. (Adapted from Costigan *et al.,* 2009).

Central sensitisation (Figure 1.7) differs from peripheral sensitisation in the incorporation of novel sensory inputs to the pathways, which transmit nociceptive information by fibres that do not normally transmit pain (*e.g.* low-threshold mechanoreceptors Aβ fibres) (Costigan *et al.,* 2009; Latremoliere & Woolf, 2009). Also, inappropriate signalling of nociceptive specific neurones, which start to respond to innocuous and noxious stimuli. It is common to see patients with pain in one region which spreads to another (*e.g.* people with knee OA having pain in the ankle or foot). Additionally, in one study it was reported that up to 70% of knee OA patients included had at least one somatosensory abnormality such as thermal hypoaesthesia, tactile hypoaesthesia or hyperalgesia, and pressure hyperalgesia (Wylde *et al.,* 2012; Trouvin & Perrot, 2017). Studies conclude that one-third of patients with painful OA have a neuropathic component that could augment central pain processing (Dimitroulas *et al.,* 2014; Moreton *et al.,* 2015). In pathological conditions such as OA, when central sensitisation occurs, pain can spontaneously arise and spread beyond the site of injury (Martindale *et al.,* 2007; Latremoliere & Woolf, 2009); these centrally-mediated effects are mainly observed in patients with established OA (Arendt-Nielsen *et al.,* 2010). A high degree of central sensitisation has been linked to high levels of pain (Arendt-Nielsen *et al.,* 2010; Finan *et al.,* 2013), disability, poor quality of life (Imamura *et al.,* 2003), more diffuse pain around the joint (Skou *et al.,* 2014), high levels of proinflammatory cytokines (Lee *et al.,* 2011), and poor outcome after total joint replacement (Lundblad *et al.,* 2008; Wylde *et al.,* 2015).

Central sensitisation can occur from inflammation as well as peripheral and central nerve damage. Both arise from changes in neuronal properties and signalling

within the CNS, where there is a potentiation or amplification in response to increased sensory input.
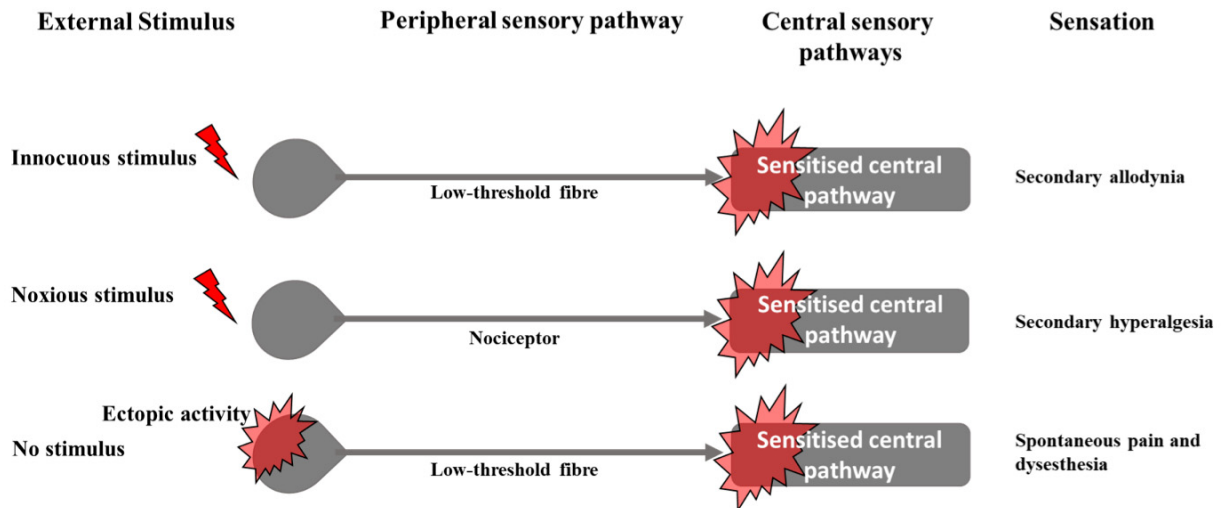
Figure 1.7 Pain mechanisms related to central sensitisation. (Adapted from Costigan *et al.,* 2009).

Changes in nerve fibres include increased membrane excitability by the potentiation of excitatory glutamatergic synapses as well as increased response of NMDA receptors to glutamate (Latremoliere & Woolf, 2009). There is also a decrease in inhibitory transmission and influences from GABAergic and glycinergic receptors in the dorsal horn of the spinal cord (Lin *et al.,* 1996). Additionally, broadening of receptive fields and changes in sensory responses causes spreading of signals and produces pain in non-injured tissue (Latremoliere & Woolf, 2009). Spontaneous action potentials can be generated from injured nerve fibres (Devor & Seltzer, 1999; Djourhi *et al.,* 2006) or activation of receptors by neuropeptide release can lead to a progressive increase in responses to both noxious and innocuous stimuli (Woolf & Thompson, 1991; Woolf *et*

al., 1996; Woolf & Salter, 2000). When changes in excitability occur, it is called "wind-up" and can lead to central sensitisation (Woolf & Thompson, 1991). Peripheral nerve injury and inflammation cause activation of glial cells in the spinal cord. Activated microglia and astrocytes release neurotransmitters, cytokines, and reactive oxygen species (Watkins & Maier, 2002; Romero-Sandoval *et al.,* 2008), which again increases neuronal excitability. These interactions drive and prolong central sensitisation processes (Kawasaki *et al.,* 2004; Ji *et al.,* 2009).

Many receptor systems have been identified in the joint and contribute to the generation, and exacerbation or inhibition of signals from noxious stimuli (Krustev *et al.,* 2015). These include the opioid system (Mousa *et al.,* 2007), serotonin receptor system (Bardin, 2011), cannabinoid system (LaPorta *et al.,* 2013; Philpott & McDougall, 2017), and TRPV1 receptors which may play a significant role in neuropathic pain generation (Baker & McDougall, 2004, Schuelert *et al.,* 2010; Kelly *et al.,* 2015). All of these systems may be targeted for novel pain controlling therapies.

1.3.2.4 Commonly prescribed therapies for OA

There still remains limited options for the treatment of OA. Therapies for OA patients are mainly targeted at pain control and not at prevention or treatment of disease progression (Sokolove & Lepus, 2013) (described in Table 1.2).

First line therapies for OA patients are non-steroidal anti-inflammatory drugs (NSAIDs) or acetaminophen. NSAIDs can be non-selective cyclooxygenase (COX) inhibitors (*e.g.* ibuprofen) or selective (COX-2) inhibitors (*e.g.* celecoxib) which provide relief of inflammation and pain. Acetaminophen also provides modest antiinflammatory

action and analgesia. These treatments are effective in the short-term and are readily available over the counter. OA can also be treated locally by topical preparations. Topical gels and patches (*e.g.* lidocaine, diclofenac, or capsaicin) provide localised pain relief and may be better tolerated than oral therapies (Dray, 2008; van Laar *et al.,* 2012).

Furthermore, injections into the joint of either hyaluronate or corticosteroids have been indicated for treating OA. Injections of synthetic hyaluronates provide the joint with lubrication and pain relief (Ayhan *et al.,* 2014). Corticosteroids are potent antiinflammatory agents and can reduce flares (Dray, 2008; van Laar *et al.,* 2012), but have been linked to cartilage damage and chondrotoxicity after long-term, high dose use (Wernecke *et al.,* 2015).

Second line therapies for patients with severe OA, who are unresponsive to first line therapies, include opioids, tricyclic antidepressants (TCAs), and anticonvulsants. All of these therapies provide potent pain relief, but are contraindicated in elderly populations and for long term use because of their undesirable side effect profiles (described in Table 1.3) and risk of abuse (Dray, 2008; van Laar *et al.,* 2012).

Table 1.3 Commonly prescribed therapies for OA

Drug	Action	Indication	Adverse Events
NSAIDs (*e.g.* Ibuprofen) (*e.g.* Celecoxib)	Antiinflammatory Analgesia	Mild/moderate OA	Cardiovascular events, gastrointestinal bleeding
Acetaminophen	Mild antiinflammatory agent Analgesia	Mild/moderate OA	Hepatotoxicity, cardiovascular events
Topicals (*e.g.* Voltaren)	Localised analgesia	Mild/moderate OA	Skin irritation
Injectables (*e.g.* Hyaluronates) (*e.g.* Corticosteroids)	Synthetic joint lubrication Potent antiinflammatory agent	Moderate/severe OA	Joint damage and neuropathy from repeated injections
Opioids	Potent analgesic	Moderate/severe OA	Nausea, dizziness, constipation, somnolence, tolerance
TCA's	Potent analgesic	Moderate/severe OA with neuropathic-type pain	Sedation, dizziness, blurred vision, constipation
Anti-convulsants	Potent analgesic	Moderate/severe OA with central sensitisation	Sedation, dizziness, blurred vision, constipation

(Dray, 2008; van Laar *et al.,* 2012)

Analgesics currently prescribed for OA target a variety of pain mechanisms but they often fail to provide adequate pain alleviation. Patients also discontinue their medications due to the occurrence of adverse side effects (Sokolove & Lepus, 2013). It has been reported that approximately 60% of OA patients are citing inadequate pain relief (Crichton & Green, 2002), and many are using other ways to manage their symptoms.

These include medicinal cannabis and cannabis compounds (Kalant, 2001; Aggarwal *et al.,* 2009; Fitzcharles & Hauser, 2016), essential oils (Mahboubi, 2017), and exercise (Booth *et al.,* 2017; Cormier *et al.,* 2017).

1.4 Cannabinoids

A class of compounds called cannabinoids are gaining interest as potential novel therapies with the potential to treat a number of ailments, including arthritis. These compounds are extracted from the cannabis plant or are synthetically made to model them.

Cannabis has a long history of use for medicinal purposes. In fact, the earliest documented use of cannabis was in China, and dates back 12,000 years (Li, 1974; Mack, 2001; Russo, 2007). Specifically, the literature indicates that Emperor Shen-Nung self-administered cannabis as an experiment and reported that it alleviated his gout (Li, 1974; Mack, 2001; Russo, 2007). An Egyptian text of herbal medical knowledge called Ebers Papyrus, described cannabis as a remedy for treating pain and inflammation (Dawson, 1934; Zias *et al.,* 1993; Russo, 2007). In the 17th century, it was documented that healers used the roots from the cannabis plant to treat a variety of ailments (Ryz *et al.,* 2017). The roots were boiled in water and then either drank or applied topically for fever, inflammation, pain, infections, burns, and gout or arthritis (Ryz *et al.,* 2017). It wasn't until the 1960's that a bioactive cannabis compound was isolated and synthesised by Gaoni and Mechoulam (1964). The compound was delta-9-tetrahydrocannabinol (Δ^9-THC), which is responsible for the majority of the psychoactive effects of cannabis. Along with Δ^9-THC, cannabidiol (CBD), cannabigerol (CBG), and cannabinol (CBN)

were also synthesised. These compounds were aptly named the phytocannabinoids. Almost 30 years later, two Δ^9-THC responsive receptors were discovered called cannabinoid receptor type 1 (CB_1R) and cannabinoid receptor type 2 (CB_2R) (Matsuda *et al.,* 1990; Munro *et al.,* 1993). Soon thereafter, N-arachidonoylethanolamine (anandamide; AEA) (Devane *et al.,* 1992) and 2-arachidonoyl glycerol (2-AG) (Mechoulam *et al.,* 1995) were discovered to be the endogenous ligands of the cannabinoid receptors and were subsequently classified as the endocannabinoids.

1.4.1 *The endocannabinoid system (ECS)*

The endocannabinoid system (ECS) is an endogenous system that is composed of cannabinoid ligands and their receptors. The ECS is mainly associated with the PNS and CNS, but is also found in other body tissues such as the gut, lung, and blood vessels. This system is responsible for many important tasks in the body linked to cellular homeostasis and communication between both cells and organs (Battista *et al.,* 2012). Elevation and activation of the ECS depends on the physiological or pathological state of the body, and is only "switched on" following inflammation, injury, or during disease (Russo, 2016).

1.4.1.1 *Endocannabinoid ligands: synthesis and degradation*

The ECS has two main endogenous ligands: anandamide (AEA) and 2-arachidonylglycerol (2-AG). The biosynthetic pathways for these ligands involve several different phospholipid derivative precursor molecules and metabolic, and catabolic enzymes (Di Marzo, 2008) (Figure 1.9). Typically, AEA and 2-AG are not stored in cellular vesicles but instead are formed in response to an increase in intracellular calcium

(Ca^{2+}) following cell depolarization or mobilization of internal Ca^{2+} stores, in an "on-demand" fashion. Upon hydrolysis of the phospholipid precursor N-acylphosphatidylethanolamines (NAPE), AEA is formed. Conversely, AEA is inactivated by fatty acid amide hydrolase (FAAH), which cleaves the amide bond of AEA to form arachidonic acid and ethanolamine (Deutsch & Chin, 1993; Di Marzo, 2008). 2-AG is produced by the hydrolysis of diacylglycerols (DAGs) by DAG lipases (DAGL) and inactivated by monoacylglycerol lipase (MAGL) into glycerol and free fatty acids (Deutsch & Chin, 1993; Aigner *et al.,* 2007; Di Marzo, 2008). Following their release from peripheral nerve terminals, the endocannabinoid ligands diffuse retrogradely where they act on cannabinoid receptors located on the same nerve ending.
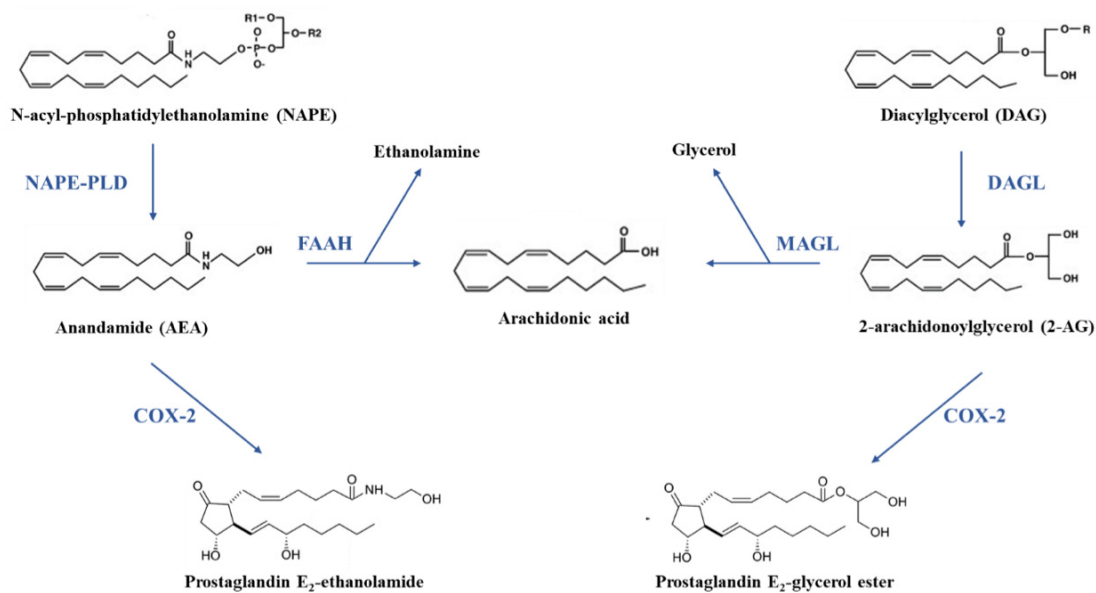
Figure 1.8 Endocannabinoid synthesis and degradation. COX-2, cyclooxygenase 2; DAGL, diacylglycerol lipase; FAAH, fatty acid amide hydrolase; NAPE-PLD, N-acyl-phosphatidylethanolamine phospholipase D. (Adapted from Di Marzo, 2008).

Since AEA and 2-AG are derived from lipid mediators and arachidonic acid, they may also act as substrates for COX-2, which is primarily responsible for the synthesis of prostaglandins (PG) from arachidonic acid (Di Marzo, 2008; Yates & Barker, 2009).

1.4.1.2 Cannabinoid receptors

There exists an interesting receptor profile in the ECS through which the endogenous ligands are able to signal. The ECS has two classical cannabinoid receptors, CB_1R and CB_2R. The CBR's are G-protein-coupled receptors (GPCRs) which have a seven-transmembrane domain and are normally coupled to an inhibitory G-protein (G_i). Upon activation of CB_1R and CB_2R, adenylate cyclase activity and cyclic adenosine monophosphate synthesis are decreased. These actions decrease cation influx which in turn activates potassium efflux (Demuth & Molleman, 2006) causing a decrease in action potentials. Additionally, other receptor systems are known to be associated with the ECS such as the orphan GPCRs, GPR18 and GPR55 as well as the transient receptor potential channels (TRP channels) (Pacher, 2006; Bradshaw *et al.,* 2009; Battista *et al.,* 2012).

1.4.2 Cannabinoids and arthritis

Expanding fields of therapeutic research, as well as the changing legal status regarding cannabis use for medical indications, has brought cannabis and cannabinoid compounds to the forefront of therapeutic investigation. With the widespread distribution of the ECS throughout the body, as well as its many known actions, it is no surprise that cannabinoids have been implicated in many different disease states including arthritis (Fagan & Campbell, 2014; Fernandez-Ruiz *et al.,* 2015; Maccarrone *et al.,* 2015;

Whitting *et al.,* 2015; Fitzcharles & Hauser, 2016). Patients with chronic musculoskeletal disorders are the primary users of medical cannabis. More specifically, 66% of Canadians who are authorised by Health Canada to possess herbal cannabis for medical reasons cite severe arthritis as their diagnosis (Fitzcharles *et al.,* 2014).

1.4.2.1 Localisation of the ECS in joints

There exists a local ECS within the articular joint microenvironment and functional roles for this system have been discovered in the joint tissues of humans (Richardson *et al.,* 2008), as well as animals (Schuelert *et al.,* 2010). Richardson *et al.* (2008) showed that synovial biopsies obtained from patients undergoing total knee arthroplasty revealed that the main components of the ECS (*i.e.* CB_1Rs and CB_2Rs and their ligands AEA and 2-AG) were elevated in arthritic joints. Moreover, there was an increase in the total amount of FAAH and MAGL compared to basal levels in healthy controls. In synovial fluid from both OA and RA patients, AEA and 2-AG were detected, but not in fluid from healthy knee joints (Richardson *et al.,* 2008), further proving that the ECS only engages when needed. *In vitro* studies showed expression of CB_1Rs and CB_2Rs at low levels on fibroblast-like synoviocytes and that these cells also expressed endocannabinoid catabolic enzymes (McPartland, 2008).

Recent preclinical immunohistological evidence indicates that CB_1Rs and CB_2Rs are expressed on neurones which innervate the rat knee joint (McDougall, 2009; Schuelert *et al.,* 2010; McDougall, 2011). Furthermore, CB_2Rs are co-localised with pronociceptive transient receptor potential vanilloid 1 (TRPV1) channels on small diameter neurones, where they act together to modulate joint pain (McDougall, 2009;

Schuelert *et al.,* 2010; McDougall, 2011). In rats, Schuelert *et al.* (2010) were the first to demonstrate that administration of a CB_2R agonist (GW405833) was antinociceptive in normal knee joints, suggesting there is local tonic activation of the ECS. Other *in vivo* studies conducted in MIA-induced OA showed a downregulation of CB_1Rs and CB_2Rs in the ipsilateral lumbar spinal cord of mice (LaPorta *et al.,* 2013), which was interpreted as being due to an increase in local endocannabinoid levels. Additionally, spinal cord levels of 2-AG and AEA, as well as their metabolic enzymes (MAGL and FAAH, respectively), were increased in rats with MIA (Sagar *et al.,* 2010) confirming the involvement of the ECS in the arthritic joint.

1.4.2.2 Effects of cannabinoids on joint inflammation

As discussed previously, a major contributor to degenerative changes within the joint and the progression of rheumatic disease is inflammation (Robinson *et al.,* 2016). Since CB_1Rs and CB_2Rs are expressed on immune cells, vascular smooth muscle and perivascular nerves, cannabinoid compounds and endocannabinoid ligands have the potential to modulate inflammation (Naidu *et al.,* 2010; Ghosh *et al.,* 2013). CB_2R knockout mice express increased levels of proinflammatory biomarkers compared to their wild type counterparts, whereby CB_2Rs have been implicated in the regulation of cytokines, chemokines, neuropeptides, and nitric oxide (Maresz *et al.,* 2007). CB_1Rs are also important regulators of inflammation. In an *in vitro* study, activation of both CB_1Rs and CB_2Rs, rather than just CB_2Rs prevented release of the inflammatory mediator TNF-α during IL-1β-stimulated immune challenge in human astrocytes (Sheng *et al.,* 2004).

Both CB_1R and CB_2R agonists display antiinflammatory actions in preclinical models of acute joint inflammation (Schwarz *et al.,* 1994; Krustev *et al.,* 2014). The two most commonly used models are the carrageenan-induced inflammatory model and the kaolin-carrageenan model. Both are used to reproduce the acute inflammatory flares seen in arthritis patients. The kaolin-carrageenan model induces a more robust inflammatory flare as well as mechanical damage to the joint, when compared to the carrageenan alone. In the carrageenan-induced inflammatory model, oral administration of AEA and the entourage molecule palmitoylethanolamide (PEA) decreased hindpaw oedema and mast cell degranulation (Richardson *et al.,* 1998). Additionally, inhibition of FAAH and MAGL was also able to decrease inflammation (Guindon *et al.,* 2011; Ignatowska-Jankowska *et al.,* 2014). In the kaolin-carrageenan model of acute synovitis, topical administration of a FAAH inhibitor (URB597) reduced joint hyperaemia and leukocyte trafficking (Krustev *et al.,* 2014). Furthermore, upon electrostimulation of the mouse saphenous nerve, an increase in synovial leukocyte trafficking in the knee joint was observed. Administration of URB597 was able to attenuate this neurogenic inflammatory response in mouse knee joints (Krustev *et al.,* 2017).

The major phytocannabinoid CBD administered systemically and orally reduced serum cytokines in collagen-induced inflammatory arthritis (Malfait *et al.,* 2000). Hammell *et al.* (2016) transdermally administered CBD, in the Freund's complete adjuvant (FCA) model of inflammatory arthritis, and found that it decreased knee joint circumference, synovial hypertrophy, and spinal cord immune cell invasion.

The synovium is a major regulator of joint health due to its extensive neurovascular supply. The synovium is also central to joint inflammatory flares because

it is a major source of cytokine production (Maini & Feldmann, 1998). Exposure of naïve

synoviocytes to proinflammatory cytokines lead to an upregulation of CB_1Rs and a

downregulation of CB_2Rs (McPartland, 2008). Other *in vitro* studies demonstrated that

synovial cells from mice with collagen-induced model of inflammatory arthritis,

produced large numbers of TNF-α, a main contributor to arthritic inflammatory flares

(Malfait *et al.,* 2000). In culture, when these synovial cells were treated with CBD they

had less TNF-α production (Malfait *et al.,* 2000). Furthermore, in the same study, CBD

treatment suppressed clinical signs of inflammatory arthritis and the hindpaws of these

mice were protected from joint destruction (Malfait *et al.,* 2000).

1.4.2.3 *Effects of cannabinoids on joint pain*

Cannabinoids and cannabinoid receptors play an important role in modulating OA

pain (LaPorta *et al.,* 2013). In the MIA model of OA, administration of a CB_1R agonist

(arachidonyl-2-chloroethylamide: ACEA) locally to the rat knee joint caused a decrease

in nociceptor firing rate. Additionally, when a CB_1R antagonist was locally administered,

it caused an increase in joint afferent firing rate (Schuelert *et al.,* 2010), suggesting that

activation of CB_1R is antinociceptive. In another study conducted by Schuelert *et al.*

(2011) administration of a FAAH inhibitor locally into the joint of MIA-injected rats

decreased joint pain and mechanonociception. These outcomes were the first to suggest

that there is a modifiable ECS within OA knees which can be used to manage pain

locally.

Cannabinoid compounds have also been found to alleviate pain in inflammatory

models. MAGL inhibition, to increase levels of 2-AG, produced greater analgesia in the

carrageenan-induced paw oedema model when delivered chronically at lower doses, rather than at higher doses (Ghosh *et al.,* 2013), highlighting the ECS adaptation rate in different pathophysiological states. Recently a peripherally restricted FAAH inhibitor (URB937) was developed, which was effective at combatting inflammatory pain; pain behaviour was decreased after intraperitoneal (i.p.) injection but there was no discernable effect on brain levels of FAAH or FAAH activity (Clapper *et al.,* 2010).

The role of CB_2R in joint pain remains controversial with widely varying results. A study by LaPorta *et al.* (2013) demonstrated that mice lacking CB_2Rs exhibited exacerbated responses to mechanical stimulation in the MIA model compared to wild type animals. It has been suggested that CB_2Rs play a role centrally in the modulation of joint nociception because mice overexpressing CB_2Rs in the CNS displayed reduced mechanical allodynia (LaPorta *et al.,* 2013). Conversely CB_1R knockout mice did not have altered mechanical allodynia, suggesting these receptors may not play as large a role (LaPorta *et al.,* 2013). Furthermore, one study found that a specific CB_2R agonist (GW405833) was pronociceptive in OA joints (Schuelert *et al.,* 2010), while other studies have shown that CB_2R agonists produce analgesia (Burston *et al.,* 2013; Vera *et al.,* 2013). Further investigation into the role of CB_2Rs in joint pain control are therefore needed.

1.4.2.4 Neuroprotective effects of cannabinoids

Cannabinoids have been shown to mitigate peripheral nerve damage in several demyelinating diseases; however, their effects on joint neuropathy have not been explored. In a murine sciatic nerve injury model, FAAH and MAGL inhibitors were able

to reverse hindlimb allodynia (Kinsey *et al.,* 2009; Ignatowska-Jankowska *et al.,* 2014). In another sciatic nerve ligation model, as well as in a chronic constriction nerve injury model, a non-selective CB_1R/CB_2R agonist (WIN55-212,2) and an AEA reuptake inhibitor, AM404, also improved behavioural pain outcomes (La Rana *et al.,* 2008). Additionally, in a murine multiple sclerosis (MS) model (Theiler's virus inoculation) synthetic CB_1R and CB_2R agonists improved motor function in the rotarod test and these results correlated with significant spinal cord remyelination (Arevalo-Martin *et al.,* 2003).

1.5   Animal models of OA

OA can be studied preclinically using naturally-progressing models, post-traumatic models (surgically-induced), or chemically-induced models (O'Brien *et al.,* 2017).

1.5.1   *Chemically-induced models*

Chemically-induced models have an advantage over naturally-occurring and surgically-induced models of OA because they are a robust way to rapidly recapitulate aspects of human OA pathophysiology and pain. These models are used in laboratory settings to generate consistent, timely, and cost-effective experiments. The main chemically-induced model of OA is the sodium monoiodoacetate (MIA) model (Bove *et al.,* 2003; O'Brien *et al.,* 2017).

1.5.1.1 Sodium monoiodoacetate (MIA) model of experimental OA

After i.artic. injection, MIA is taken up by chondrocytes and causes a disruption to their homeostatic environment, rendering them unable to produce energy subsequently causing them to die. MIA is an inhibitor of glyceraldehyde-3-phosphate dehydrogenase (GADPH), which is a key enzyme in the glycolysis process, responsible for converting glyceraldehyde-3-phosphate to D-glycerate 1,3,-bisphosphate (Foxall *et al.,* 1984). The MIA model is widely used to investigate the development of OA pathology and pain which occur within 1-2 weeks of induction (Janusz *et al.,* 2001). This model produces cartilage degeneration and subchondral bone loss (Combe *et al.,* 2004). In addition to joint pain and degeneration, MIA also produces acute inflammatory flares similar to those reported by OA patients. In the first few days of the model, there is an increase in infiltrating leukocytes and joint hyperaemia (Bove *et al.,* 2003). By days 5-7, inflammation subsides and remains minimal thereafter. The early inflammatory flare is suspected to drive joint degeneration and damage to joint innervation, thus promoting the development of chronic pain. OA-associated nerve damage has been identified in the MIA model (Thakur *et al.,* 2012; McDougall *et al.,* 2017). Expression of peripheral nerve damage markers have been observed as early as day 3 and upregulation remains at day 14 (Thakur *et al.,* 2012; McDougall *et al.,* 2017). Overall, the advantages of the MIA model include assessment of OA-associated inflammation and inflammatory pain, OA pain with a neuropathic component, and peripheral nerve damage. The structural histopathology of an MIA joint does not fully recapitulate the physical features commonly associated with human OA, which limits joint structure analysis in this model.

1.6 Measuring joint pain and inflammation in animals

1.6.1 Assessing pain

1.6.1.1 Measuring referred pain

As discussed previously, central sensitisation is a form of neuroplasticity which occurs in the CNS. It has been observed in states of acute and chronic inflammation of the joint, and as a consequence of inflammation and nerve damage. Sensitisation is characterised by irregular changes and responses by neurones. This includes increased reactions to noxious stimuli in the injured area as well as increased reactions to stimuli in areas away from the injured area. Furthermore, the threshold of nociceptive neurones projecting to the spinal cord is lowered and the receptive fields are expanded, ultimately resulting in secondary allodynia or referred pain.

Von Frey hair algesiometry uses a sequence of filaments to measure tactile sensitivity and tactile allodynia. Von Frey hair algesiometry is most often used to measure primary allodynia by directly applying the sequence of filaments to the injured or painful area, but can be used to measure secondary allodynia by applying them at a location remote from the injured or painful area. In naïve rats when fine filaments are applied to the plantar surface of the hindpaw there is often no withdrawal response, but rats with MIA-induced OA in the knee joint become sensitive to the von Frey hair stimulation of the paw indicating a secondary allodynic response.

1.6.1.2 Measuring weight bearing deficits

Many OA patients display altered joint biomechanics and kinematics due to pain, degeneration, and swelling. One aspect of altered joint biomechanics is weight bearing

deficits or favouring of the uninjured limb. Weight bearing is used as a measure of spontaneous pain due to inflammation, degeneration, and peripheral sensitisation.

Dynamic incapacitance is assessed by placing unrestrained animals in a chamber with a pressure sensitive floor. Changes in weight borne on the hindlimbs and the amount of paw surface area applied when walking or standing are indicative of pain and altered mechanics (Griffioen *et al.,* 2015; Quadros *et al.,* 2015; O'Brien *et al.,* 2017).

1.6.2 Assessing inflammation

1.6.2.1 Measuring leukocyte trafficking in the joint

One important aspect of the inflammatory response is the recruitment of leukocytes to the site of tissue injury. Leukocytes circulating in the blood will interact with the endothelial cells of the vasculature when passing through areas of inflammation and move from the post-capillary venules out into the tissue to carry out their physiological actions. Assessing these leukocyte-endothelial interactions *in vivo* allows for a robust measurement of inflammation.

Danger signals, or DAMPs, are sent from cells of injured tissues to immune cells of the innate immune system, which then leads to activation and upregulation of proinflammatory mediators. These mediators activate endothelial cells of the microvasculature in the proximity of the inflamed tissue. Circulating leukocytes are then able to recognise these signals on the vascular endothelium and will begin the multistep process of diapedesis and ultimately extravasation.
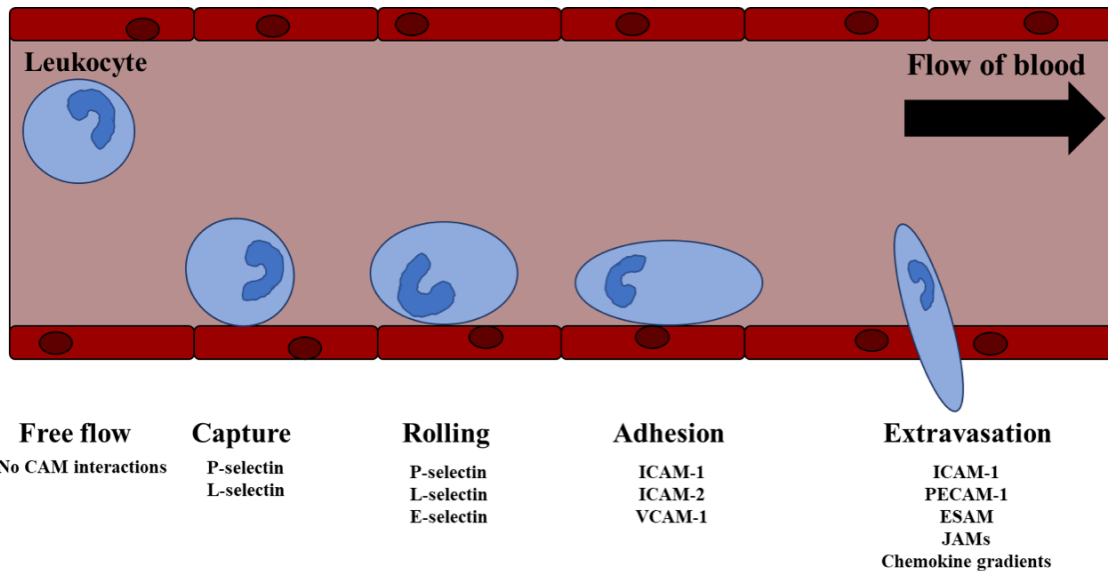
Figure 1.9 Leukocyte extravasation process. (Adapted from Vestweber, 2015).

There are four steps in this process: capture, rolling, adherence, and transmigration. Selectins present on endothelial cells (P-selectin, L-selectin, and E-selectin) mediate capture and subsequent rolling of circulating leukocytes. Slow rolling leukocytes then arrest and firmly adhere to the intimal surface of the venule wall under the influence of intercellular adhesion molecule 1 and 2 (ICAM1 and ICAM2) and vascular cell adhesion molecule 1 (VCAM1). Finally, transmigration is facilitated, either paracellularly or transcellularly, via platelet endothelial cell adhesion molecule 1 (PECAM1), endothelial cell-selective adhesion molecule (ESAM), and junctional adhesion molecules (JAMs). The leukocytes transmigrate out of the vasculature and into the inflamed tissue where they commence a local immune response (Vestweber, 2015).

Both rolling and adhering steps of the extravasation process are important indicators of the amount of inflammation occurring as they precede transmigration of cells into the inflamed area. By using intravital microscopy (IVM), it is possible to

visualise and quantify leukocyte-endothelial interactions occurring *in vivo* within the

knee joint microvasculature. By quantifying leukocyte rolling and adherence, using IVM,

it is possible to assess the degree of joint inflammation as well as assessing the

effectiveness of test compounds on leukocyte kinetics within the joint microcirculation.

1.6.2.2 Measuring knee joint blood flow

Another aspect of inflammation is the increase in blood flow to injured tissue

called hyperaemia. OA patients who experience inflammatory flares and synovitis have

joints that become hyperaemic (Roemer *et al.,* 2011). Measuring changes in blood flow

between arthritic and non-arthritic joints allows for another inflammation assessment.

Using Laser Speckle Contrast Analysis (LASCA) it is possible to measure local blood

flow around the knee joint allowing for the assessment of injured tissue areas and the

efficacy of test compounds to relieve this hyperaemic inflammatory response.

1.6.2.3 Measuring knee joint diameter

Knee joint diameter, used to assess swelling of the joint, is done by measuring the

distance between the medial and lateral femoral condyles. Measuring knee joint diameter

is often used as a diagnostic test to confirm and assess the progression of joint

inflammation. This technique is limited in that local drug administration, either into the

joint cavity or subcutaneously (s.c.), affects the diameter so assessment of the

effectiveness of a peripherally administered treatment is not possible immediately after

injection. Additionally, knee joint diameter increases with age and weight gain over the

development of a model so these factors need to be taken into consideration and controlled for.

1.7 Measuring peripheral nerve damage

As discussed previously, a subset of OA patients experience neuropathic pain which arises from damage to nerves innervating the joint and surrounding area. Assessing peripheral nerve damage in an injured joint allows for a measurement of peripheral neuropathy and can be used to evaluate the efficacy of a test compound on reversing or preventing peripheral nerve damage.

One method used to assess nerve damage is by measuring myelin thickness of nerve fibres. G-ratio values are used to assess demyelination states of a nerve by calculating the internal axonal area relative to the total axonal area of the individual fibres. This provides a morphological measure of global nerve fibre myelination. For studies assessing knee joint nerve damage the saphenous nerve is often used because it is the largest branch of the femoral nerve that innervates the anteromedial aspect of the knee joint (McDougall *et al.,* 2017).

1.8 Objectives and hypotheses

Based on the information provided in this chapter, **we hypothesised that modulating the endocannabinoid system, directly or indirectly, would attenuate OA-associated joint pain and inflammation. Additionally, we hypothesised that blocking early inflammation with prophylactic cannabinoid treatment would prevent the**

subsequent development of joint pain and neuropathy. This project had three main objectives to examine these hypotheses:

Objective 1: *to determine the effects of indirectly modulating the ECS in experimental knee joint OA pain and inflammation.*

Objective 2: *to elucidate the effects of directly modulating the ECS in experimental knee joint OA pain and inflammation.*

Objective 3: *to investigate the effects of a phytocannabinoid in experimental knee joint OA pain, inflammation, and disease progression.*

In the subsequent chapters, these main objectives and hypotheses as well as their additional aims within, will be described further.

Chapter 2: Methods and Materials

2.1 Animals

All experimental protocols were approved by Dalhousie University Committee on the Use of Laboratory Animals, which acts in accordance with the ARRIVE (Animal Research: Reporting of *In Vivo* Experiments) standards put forth by the Canadian Council for Animal Care. Animal care Protocol Numbers: 15-177 and 16-077.

Male Wistar rats (222-404g at time of model induction; Charles River, Quebec, Canada) were housed in pairs in ventilated racks at $22 \pm 2°C$ on a 12:12 hour (hr) light:dark cycle (light-on from 7:00-19:00) in the Carleton Animal Care Facility, Faculty of Medicine, Dalhousie University, Halifax, Nova Scotia, Canada. All animals were allowed at least one week to acclimate after arrival at the facility, before experimental procedures began. Cages were lined with woodchip bedding and animals were provided with Enviro-dri® nesting material and environmental enrichment. Standard lab chow (large, dried pellets) and water were provided *ad libitum*.

2.2 Arthritis Model

2.2.1 Sodium monoiodoacetate (MIA) experimental OA

Animals were deeply anaesthetised (2-4% isoflurane; 100% oxygen at 1L/min) and an acceptable plane of anaesthesia was confirmed by failure to produce a hindpaw pedal withdrawal reflex and an ocular blink reflex. The right (ipsilateral) knee joint was shaved and the area was swabbed with 100% ethanol. An i.artic. injection of 50μl of MIA (3mg in saline) through the infrapatellar ligament was performed. The knee was manually

extended and flexed for 30 seconds (sec) to disperse the MIA solution throughout the

joint space. Animals were returned to their cages and allowed at least 24 hr to recover. In

separate groups of animals, pain was assessed on days 1, 2, 3, 7, 10, 14, and

inflammation was assessed on day 1, following MIA injection.

2.3 Measuring Behavioural Pain

2.3.1 Von Frey hair algesiometry

Von Frey hair algesiometry was used as a measure of secondary allodynia

(referred pain or pain remote from the joint). Alert, unanaesthetised animals were placed

in a Plexiglas chamber (31.5 cm long x 9.5cm wide x 24cm tall) with metal mesh flooring

(Figure 2.1) (Concept Plastics, Dartmouth, Nova Scotia, Canada) which allowed access

to the plantar surface of each hindpaw. Testing began after allowing the animal to

acclimate to the chamber until exploratory behaviour ceased, approximately 10-15

minutes (min). Mechanosensitivity of the ipsilateral hindpaw was assessed using a series

of six von Frey hairs (North Coast Medical, Gilroy, California, USA), which are graded

in bending force (2, 4, 6, 8, 10, 15g). Mechanosensitivity was determined using a

modification of the Dixon's up-down method (Chaplan *et al.,* 1994). Taking care to avoid

the toe pads, a von Frey hair was applied perpendicular to the plantar surface of the

ipsilateral hindpaw until the hair bent; the filament was then held in place for 3 sec. If the

response was positive, the next lower strength hair was applied; if there was a lack of

response, the next higher strength hair was applied up to a cut-off of 15g bending force.

A positive response was classified as a paw withdrawal, shake, or lick or combination

thereof. The withdrawal threshold was calculated using the following formula:

$10^{[Xf+k\delta]}/10{,}000$; where Xf = value (in log units) of the final von Frey hair used, k = tabular value for the pattern of the last 6 positive/negative responses, and δ = mean difference (in log units) between stimuli.

2.3.2 Hindlimb incapacitance

In the same animals hindlimb incapacitance was used as a measure of spontaneous, non-evoked pain. To perform dynamic weight bearing measurements animals were placed in a Perspex chamber (24cm long x 24cm wide x 32cm tall) (model BIO-DWB-AUTO-R, Bioseb, Boulogne, France) with a pressure sensitive floor (Figure 2.2). Hindlimb weight bearing was tracked using proprietary software (Bioseb; Version 1.4.2.92) and recorded using an ImagingSource DFK22AUC03 camera (ImagingSource, Charlotte, NC, USA), over a 3 min period while the animals moved freely around the chamber. Body weight borne on the ipsilateral hindpaw was calculated as a percentage of the total weight borne on both hindlimbs.

2.4 Measuring Joint Inflammation

2.4.1 Knee joint diameter

Knee joint swelling was evaluated by measuring the change in joint diameter (mm) across the joint capsule along the transverse plane of the knee between the femoral chondyles using electronic digital calipers (VWR International, Friendswood, Texas, USA). These measurements were taken at baseline (day 0) and days 1, 2, 3, 7, 10, and 14 post-induction of the MIA model.

2.4.2 Assessment of the synovial microcirculation

2.4.2.1 Surgical preparation

The subsequent surgical preparation of the animals was performed prior to IVM and LASCA recordings of the knee joint vasculature. Animals were deeply anaesthetised by an i.p. injection of urethane (25% solution; 2g/kg in saline). An appropriate surgical plane of anaesthesia was confirmed by failure to stimulate a hindpaw pedal withdrawal reflex and ocular blink reflex. A longitudinal incision was made along the ventral skin of the neck and a blunt dissection technique was used to expose the trachea which was cannulated with PE-200 tubing to permit clear, unrestricted breathing. Next, the right carotid artery was blunt dissected away from surrounding tissue and isolated from the vagus nerve. The carotid was then cannulated with PE-30 tubing filled with heparinised saline (1U/ml). The cannula was attached to an in-line pressure transducer attached to a differentially amplified blood pressure monitor (World Precision Instruments, Sarasota, FL, USA) to allow for continuous monitoring of mean arterial pressure (MAP). None of the compounds tested throughout this project had any significant effect on the animals MAP throughout the respective experiments. The right jugular vein was also blunt dissected away from surrounding tissue and then cannulated with PE-20 tubing filled with heparinised saline (1U/ml) to allow for intravenous (i.v.) administration of rhodamine-6G. The jugular vein was only cannulated if it was not possible to perform a tail vein injection of rhodamine 6G using a 30-gauge needle. The right knee joint was immobilised using a brace made in-lab and the joint capsule was exposed by surgically removing a small ellipse of overlying skin and superficial fascia (<1cm long; <0.5cm

wide). Physiological buffer (135mM NaCl, 20mM NaHCO3, 5mM KCl, 1mM MgSO4*7H2O, pH =7.4) (37°C) was immediately and continuously perfused over the exposed joint.

2.4.2.2 Intravital microscopy (IVM)

IVM was used to assess leukocyte-endothelial interactions within the microcirculation of the knee joint, as described previously (Andruski *et al.,* 2008). After surgical preparation was complete, the synovial microcirculation was visualised under incident fluorescent light using a Leica DM2500 microscope with an HCX APO L 20X objective and an HC Plan 10X eyepiece, and a Leica DFC 3000 camera (Leica Microsystems Inc., Ontario, Canada) giving a final magnification of 200X (Figure 2.3). Leukocyte staining was achieved by i.v. administration of 0.05% rhodamine 6G (0.05mg in 10ml saline). Rhodamine 6G accumulates in the mitochondria of leukocytes (Gear, 1972; Baatz *et al.,* 1995), and has an absorption rate between 440 and 570 nm, which peaks at 530nm (Brackmann, 1986). The excitation of rhodamine 6G is dependent on concentration and solvent used, and emits between 550 and 620nm (Zehentbauer, 1986). Straight, unbranched post-capillary venules (15μm-50μm in diameter) overlying the knee joint capsule were chosen for visualisation and three leukocyte trafficking videos per time point were captured for 1 min duration each.

Two different measures of leukocyte-endothelial interactions were used to assess articular inflammation: (i) rolling leukocytes, which were defined as positively-stained cells travelling slower than the surrounding blood flow. The number of rolling leukocytes to pass an arbitrary line perpendicular to the venule in 1 min were counted, and (ii)

adherent leukocytes, which were defined as positively-stained cells that remained

stationary for a minimum of 30 sec within a 100μm portion of the venule were counted.

2.4.2.3   *Laser speckle contrast analysis (LASCA)*

The same animals that underwent IVM knee joint microvasculature assessments

were also assessed by LASCA here. Knee joint blood flow was measured by LASCA

using a PeriCam PSI System (Figure 2.4) (Perimed Inc., Ardmore, PA, USA). Blood flow

in the exposed knee joint was recorded over 1 min at a working distance of 10cm with a

frame capture rate of 25 images per sec using a laser at wavelength of 785 nm. All

images captured were averaged to generate 1 perfusion image per sec using dedicated

software (PIMSoft, Version 1.5.4.8078). At the end of the experiment rats were

euthanised and a dead scan of the knee was taken as a "biological zero" value. This value

was subtracted from all experimental time point measurements to account for any optical

noise in the tissue. Perfusion images were analysed offline where mean blood perfusion

in a manually defined region of interest approximating the knee joint area was calculated.

To normalise for MAP differences between animals, the mean perfusion values were

used to calculate vascular conductance using the equation $C = Q/P$, where C is

conductance, Q is mean perfusion, and P is MAP. Vascular conductance values were

assigned arbitrary units called perfusion units (PU) (Boas & Dunn, 2010).

2.5   Evaluating Peripheral Nerve Damage

2.5.1   *G ratio analysis of the saphenous nerve*

A small segment (approximately 5mm) of the saphenous nerve was isolated

proximal to the ipsilateral knee joint, excised, and placed in 2.5% glutaraldehyde (diluted

with 0.1M sodium cacodylate buffer), and stored at 4°C for at least one week. Sodium

cacodylate (cacodylic acid, sodium salt trihydrate) is dissolved in distilled water (dH_20)

and then the pH is adjusted to 7.3 with 0.2M hydrochloric acid (HCl), the stock solution

is then diluted to 0.1M just prior to use. The nerve samples were then removed from the

fixative and rinsed three times with 0.1M sodium cacodylate buffer. Samples were fixed

in 1% osmium tetroxide for 2 hr, rinsed with distilled water, and then placed in 0.25%

uranyl acetate (4°C) overnight. The samples were dehydrated in a graduated series of

acetone (50%, 70%, 95%, and finally 100%). The samples were then dried in 100%

acetone for 10 min. Epon araldite resin was utilised to mount the samples. The samples

were placed in a 3:1 ratio of dried 100% acetone to resin for 3 hr, followed by a 1:3 ratio

of dried 100% acetone to resin overnight. Next the samples were placed in 100% Epon

araldite resin for 3 hr and cured in an oven at 60°C for 48 hr. Finally, using an LKB

Huxley ultramicrotome with a diamond knife, the samples were sectioned into 100 nm

thick slices. Cross-sectional slices (approximately 4-5) of the nerves were placed onto a

copper wire grid consisting of 300 individual squares per inch (each square measuring

83μm x 58μm) and then stained with 2% aqueous uranyl acetate for 10 min and finally

lead citrate for 4 min. All processing and sectioning of the samples was completed by

Mary Ann Trevors in the Electron Microscopy Lab, Dalhousie University, Halifax, Nova

Scotia, Canada.

For analysis, the copper wire grids containing the saphenous nerve sections were

inserted into a JEOL JEM 1230 transmission electron microscope (JEOL Corp. Ltd.,

Tokyo, Japan). The microscope was set at a voltage of 80.0 kV, and images were

captured at 2500X using a Hamamatsu ORCA-HR digital camera (Hamamatsu

Photonics, Hamamatsu City, Japan). One nerve cross-section image was visually

partitioned into nine quadrants and three images were captured (from quadrants one, five,

and nine) per sample (Figure 2.5). Myelin thickness for all fibres per sample was assessed

using the G-ratio plugin (version 1.0) on ImageJ processing software (ImageJ bundled

with 64-bit Java 1.6.0_24). The G-ratio, a measure of myelin thickness, was calculated

using the equation $G = \sqrt{\dfrac{a}{A}}$ where a is the internal axonal area, and A is the total

axonal area of the fibre. The higher the G-ratio the higher the degree of nerve

demyelination.

2.6 Materials

2.6.1 Reagents

Table 2.1 List of Reagents

Reagent	Source	Description
Cremophor	Sigma Aldrich (St. Louis, Missouri, USA)	• Emulsifying solvent
Dimethyl sulfoxide (DMSO)	Sigma Aldrich (St. Louis, Missouri, USA)	• Polar aprotic solvent
Gluteraldehyde	Electron Microscopy Sciences (Hatfield, Pennsylvania, USA)	• Component of tissue fixative solution
Heparin	Sandoz Canada Inc. (Boucherville, Quebec, CA)	• Anticoagulant
Isoflurane	CDMV (Dartmouth, Nova Scotia, CA)	• Anesthetic • 1-chloro-2,2,2-trifluoroethyldifluoromethyl ether

2.6.1 Reagents

Table 2.2 List of Reagents continued

Reagent	Source	Description
Magnesium sulfate (MgSO4)	EMD Millipore (Chicago, Illinois, USA)	• Component of physiological buffer solution (pH=7.4)
Potassium chloride (KCl)	Dalhousie Central Stores (Halifax, Nova Scotia, Canada)	• Component of physiological buffer solution (pH=7.4)
Saline (0.9% Sodium chloride)	Dalhousie Central Stores (Halifax, Nova Scotia, Canada)	• Component of drug vehicle • Component of heparinized saline solution
Sodium bicarbonate (NaHCO3)	Dalhousie Central Stores (Halifax, Nova Scotia, Canada)	• Component of physiological buffer solution (pH=7.4)
Sodium cacodylate buffer (1.0M)	Electron Microscopy Sciences (Hatfield, Pennsylvania, USA)	• Component of tissue fixative solution
Sodium chloride (NaCl)	Dalhousie Central Stores (Halifax, Nova Scotia, Canada)	• Component of physiological buffer solution (pH=7.4)
Sodium monoiodoacetate (MIA)	Sigma Aldrich (St. Louis, Missouri, USA)	• Inducer of an experimental OA model • GAPDH inhibitor
Rhodamine-6G	Sigma Aldrich (St. Louis, Missouri, USA)	• Nuclei and mitochondria binding fluorophore
Urethane	Sigma Aldrich (St. Louis, Missouri, USA)	• Anesthetic • Ethyl carbamate

2.6.2 Drugs

Table 2.3 List of Drugs

Drug	Source	Description
AM281	Cayman Chemicals (Ann Arbor, Michigan, USA)	• CB1 receptor antagonist • 1-(2,4-dichlorophenyl)-5-(4-iodophenyl)-4-methyl-N-4-morpholinyl-1H-pyrazole-3-carboxamide
AM630	Cayman Chemicals (Ann Arbor, Michigan, USA)	• CB2 receptor antagonist • 6-iodo-2-methyl-1-(2-morpholin-4-ylethyl)indol-3-yl]-(4-methoxyphenyl)methanone
Cannabidiol (CBD)	Tocris Bioscience (Bio-Techne, Abingdon, UK)	• Phytocannabinoid • 2-[(1*R*,6*R*)-3-methyl-6-(1-methylethenyl)-2-cyclohexen-1-yl]-5-pentyl-1,3-benzenediol
JWH133	Tocris Bioscience (Bio-Techne, Abingdon, UK)	• CB2 receptor agonist • (6aR,10aR)-3-(1,1-Dimethylbutyl)-6a,7,10,10a-tetrahydro-6,6,9-trimethyl-6H-dibenzo[b,d]pyran
KML29	MedChem Express USA (Monmouth Junction, New Jersey, USA)	• MAGL inhibitor • 4-[*Bis*(1,3-benzodioxol-5-yl)hydroxymethyl]-1-piperidinecarboxylic acid 2,2,2-trifluoro-1-(trifluoromethyl)ethyl ester
SB-366791	Sigma Aldrich (St. Louis, Missouri, USA)	• TRPV1 antagonist • N-(3-methoxyphenyl)-4-chlorocinnamide

2.6.3 Equipment

Table 2.4 List of Equipment

Device	Model	Manufacturer
Blood Pressure Monitor with In-line Pressure Transducer	BP-1	World Precision Instruments (Sarasota, Florida, USA)
Blood Perfusion Imager	PeriCam PSI *Normal Resolution* with PimSoft Software	Perimed Inc. (Ardmore, Pennsylvania, USA)
Dynamic Weight Bearing System	BIO-DWB-AUTO-R for rats with DFK22AUC03 camera with Bioseb software version 1.4.2.92	DWB system and software from Bioseb (Boulogne, France) Camera from ImagingSource (Charlotte, North Carolina, USA)
Digital Caliper	62379-531	VWR International (Friendswood, Texas, USA)
Intravital Microscope	Leica DM2500 microscope with HCX APO L 20X objective and HC Plan 10X eyepiece, and Leica DFC 3000 camera (final magnification 200X)	Leica Microsystems Inc. (Concord, Ontario, Canada)
Temperature Control Monitor and Heating Pad	TC1000	CWE Inc. (Ardmore, Pennsylvania, USA)
Transmission Electron Microscope (TEM)	JEOL JEM 1230 and Hamamatsu ORCA-HR digital camera	TEM from JEOL Corp. Ltd. (Tokyo, Japan) Hamamatsu Photonics (Hamamatsu City, Japan)
Von Frey Chamber	Custom made	Concept Plastics Inc. (Dartmouth, Nova Scotia, Canada)
Von Frey Hairs	Semme Weinstein Microfilaments	North Coast Medical (Gilroy, California, USA)

2.7 Statistical analyses and data presentation

All data are expressed as mean values ± standard error of the mean (SEM). All data were tested for Gaussian distribution by the Kolmogorov-Smirnov test. For each comparison, if all experimental groups passed the normality test, then the appropriate parametric statistical test was used for analysis. If one or more groups were not normally distributed, then the corresponding non-parametric statistical test was used for analysis. Statistical analyses differed between studies and are stated in the corresponding figure legend. All analyses were performed, and all graphs were generated, using GraphPad Prism 6.0 (La Jolla, California, USA). A $P<0.05$ was considered statistically significant. For each comparison, n is equal to the number of animal subjects in each experimental cohort.

2.7 Figures
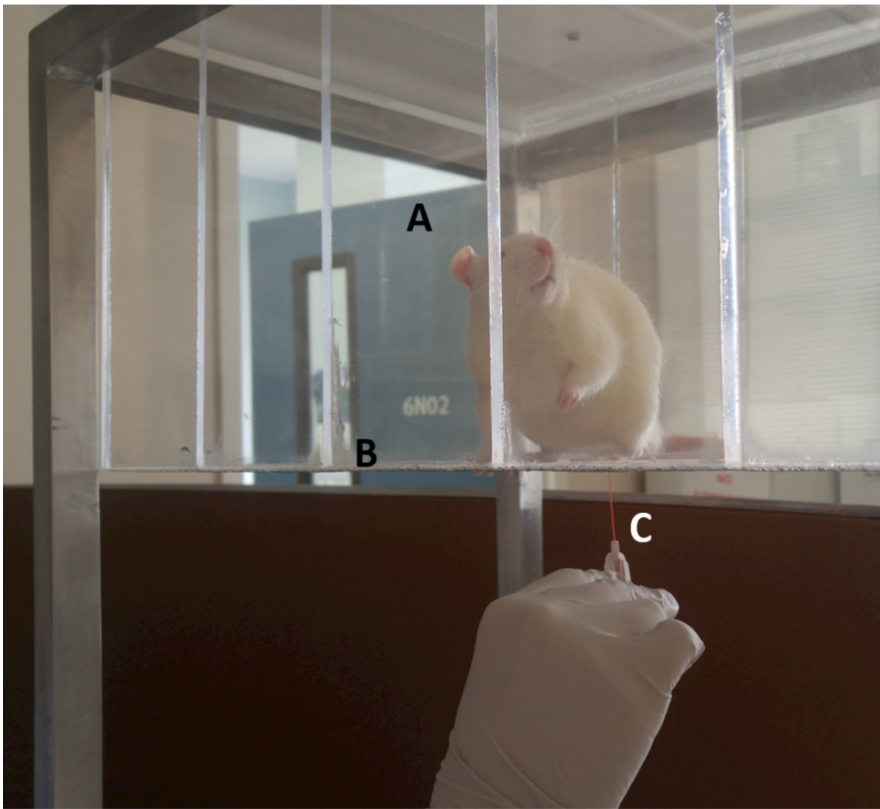
A. Plexiglas chamber for animal
B. Metal mesh flooring
C. Von Frey hair monofilament (1 of series of 6)

Figure 2.1 Photograph of Von Frey algesiometry apparatus and setup.
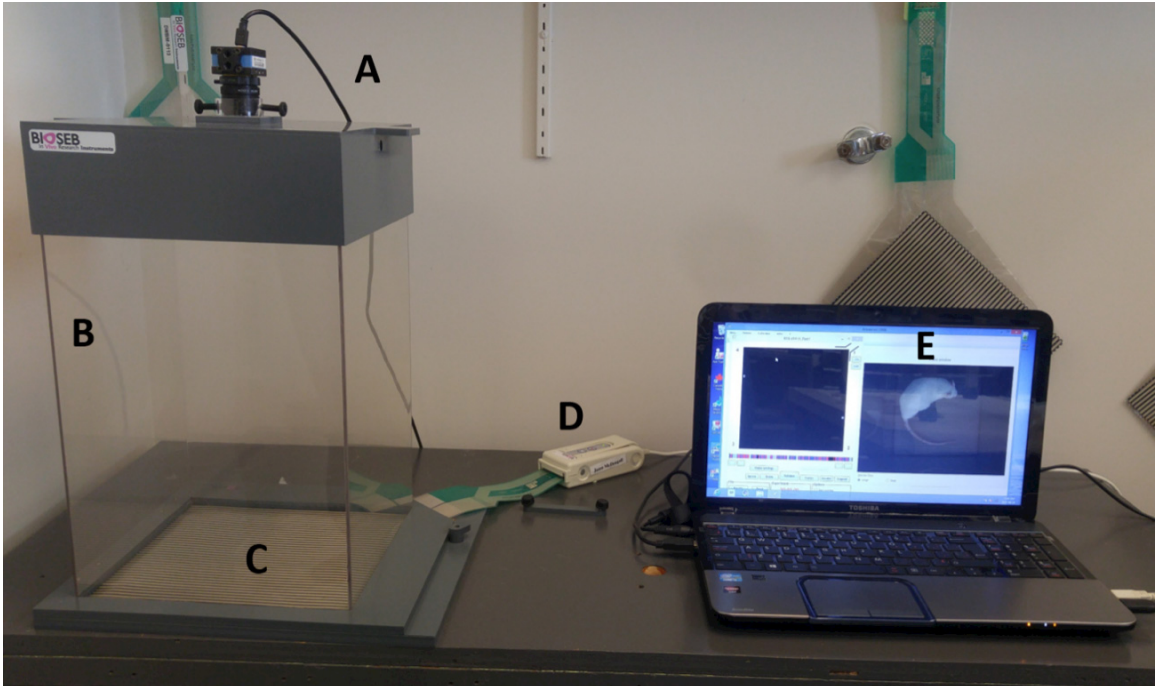
A. DFK22AUC03 camera
B. Perspex chamber for animal
C. Sensor pad
D. Handle input to Bioseb software
E. Bioseb software for capture and analysis

Figure 2.2 Photograph of Dynamic Incapacitance apparatus and setup.
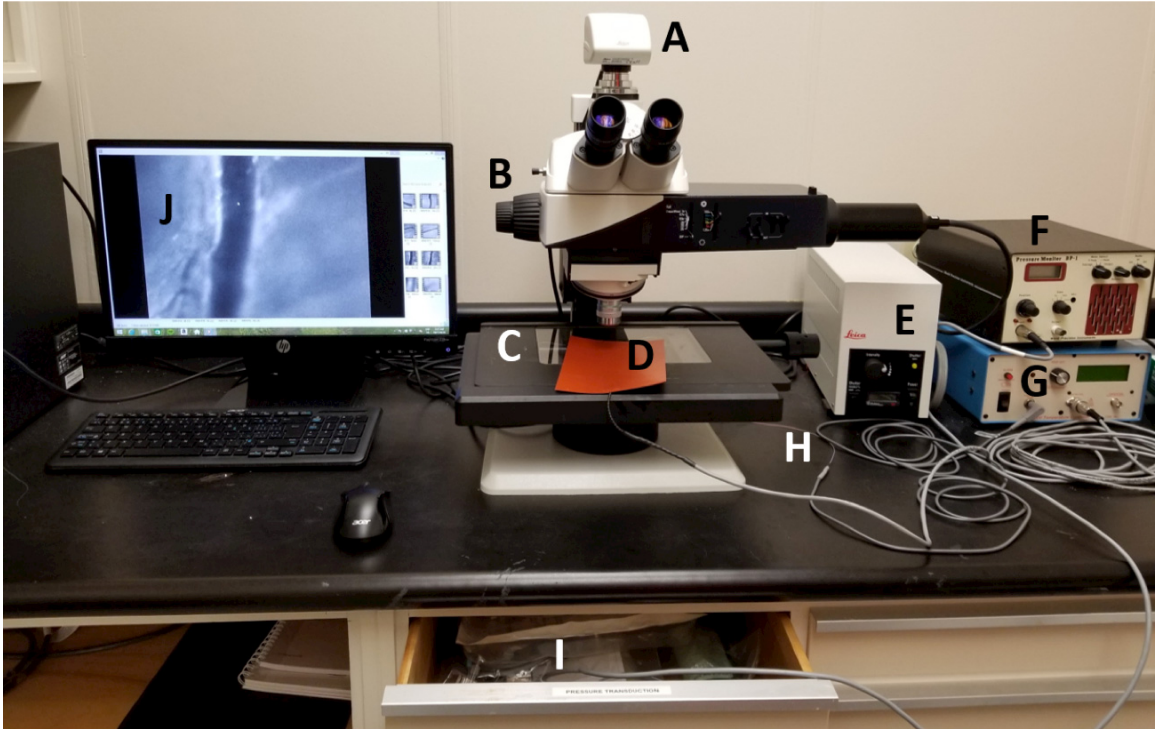
A. Leica DFC 3000 camera
B. Leica DM2500 microscope
C. Stage for animal
D. Temperature control heating pad
E. Leica light source
F. Blood Pressure Monitor
G. Temperature control monitor
H. Temperature probe
I. Pressure Transducer
J. PC with LAS Suite Software for capture and analysis

Figure 2.3 Photograph of Intravital Microscopy (IVM) set up
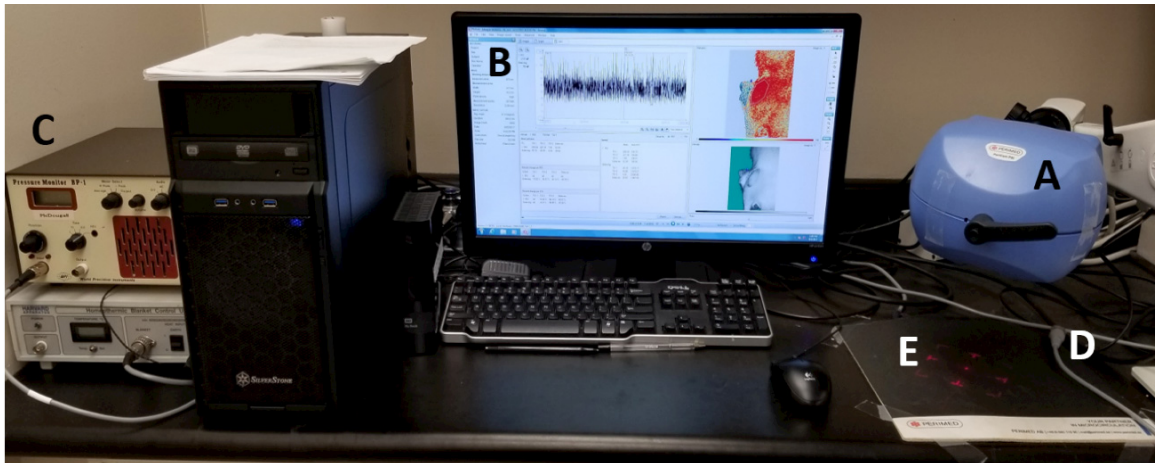
A. Pericam PSI blood flow imager
B. PIMSoft recording software
C. Blood pressure monitor
D. Pressure transducer
E. Stage for animal

Figure 2.4 Photograph of Laser Speckle Contrast Analysis (LASCA) setup.
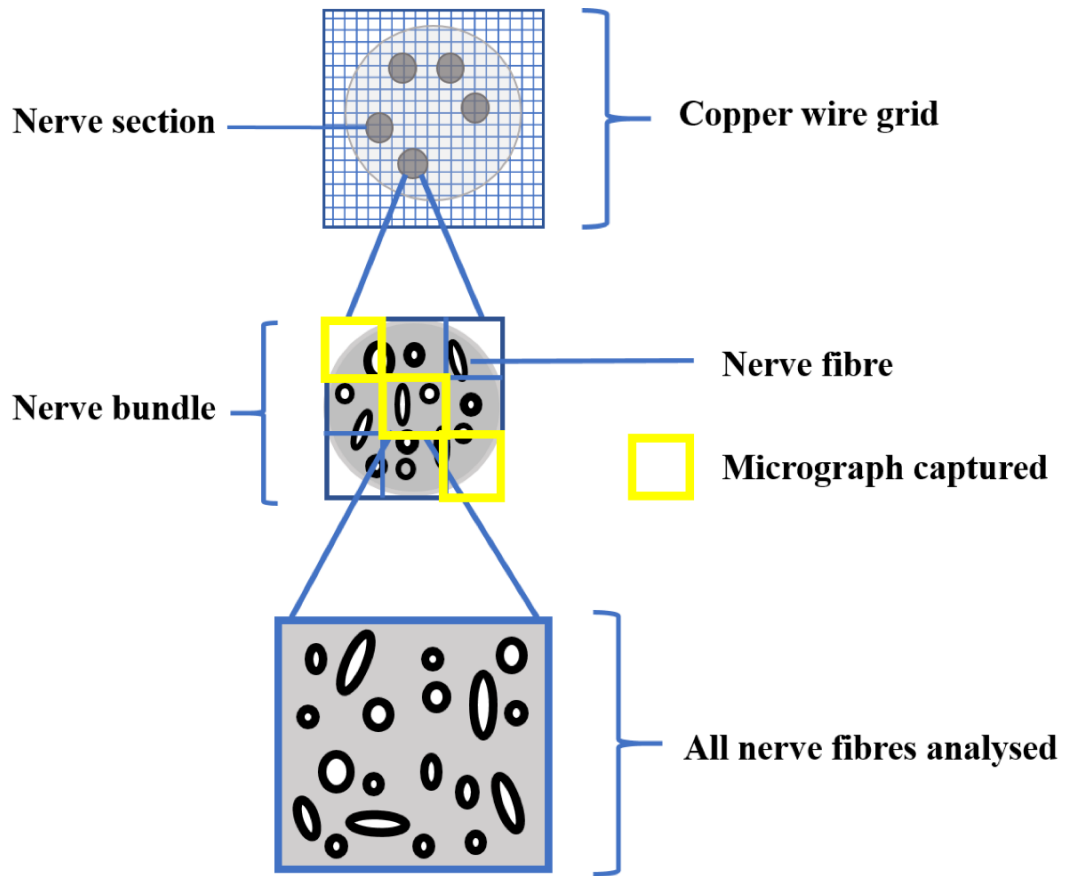
Figure 2.5 Representation of saphenous nerve imaging and analysis protocol.

Chapter 3: The Modulatory Effects of a Monoacylglyercol Lipase Inhibitor on MIA-Induced Joint Pain and Inflammation

Disclosures: Pilot data (n=5) for the first portion of the KML29 pain behaviour study was done with help from Nasser Abdullah, a former lab technician.

3.1 Background and hypotheses

The endocannabinoid system (ECS) ligands are synthesised on-demand under different pathophysiological conditions. For instance, anandamide (AEA) and 2-aracydonylglycerol (2-AG) are not found in healthy joints, but are upregulated in arthritic joints (Richardson *et al.,* 2008). Moreover, an increase in monoacylglycerol (MAGL) and fatty acid amide hydrolase (FAAH), the ECS ligand catabolic enzymes, were seen in arthritic joints when compared to normal healthy joints (Richardson *et al.,* 2008), indicating the existence of an active articular ECS. There is also evidence that CB_1Rs and CB_2Rs are expressed on neurones which innervate knee joints as well as the synovial membrane in rats (McDougall *et al.,* 2009; Schuelert *et al.,* 2010; McDougall *et al.,* 2011), where they are capable of modulating pain by reducing joint afferent firing (Schuelert *et al.,* 2010). More specifically, there is evidence provided by Schuelert *et al.* (2010), that in MIA-induced OA, there is tonic activation of the ECS locally in the joints of rodents. Wherein they showed that GW405833, a CB_2R agonist, was antinociceptive in normal control joints (Schuelert *et al.,* 2010). Thus, the ECS could be a practical target for combating OA-associated pain and inflammation.

Indirectly targeting, or modulating, the ECS is one potential way to successfully alleviate pain and inflammation, as opposed to direct action at the CBRs. The endocannabinoid ligands have beneficial effects on pain and inflammation in the joint, but they are rapidly degraded by efficient enzymatic hydrolysis mechanisms involving MAGL and FAAH, thereby shortening their duration of action (Guindon *et al.,* 2009). Inhibiting their degradation, by blocking MAGL or FAAH activity, would increase the tonic levels of 2-AG and AEA, respectively, and prolong their activity (Guindon *et al.,* 2009). Modulating the ECS using MAGL or FAAH inhibitors has shown great potential preclinically. When a FAAH inhibitor was administered locally into joints of OA animals, it improved joint pain, inflammation, and mechanonociception (Schuelert *et al.,* 2011; Krustev *et al.,* 2014). Furthermore, MAGL inhibitors, administered systemically, improved referred pain and hindlimb weight bearing deficits in the MIA model of OA (Burston *et al.,* 2016). Inhibition of MAGL reduced carrageenan-induced paw oedema and mechanical allodynia (Ignatowska-Jankowska *et al.,* 2014) as well as reduced mechanical allodynia in a sciatic nerve injury model (Ignatowska-Jankowska *et al.,* 2014). MAGL inhibition also reduced paw oedema in the formalin test of inflammatory pain (Guindon *et al.,* 2011).

Although the effects of MAGL inhibition have been assessed previously in an OA model, it's efficacy when harnessing the peripheral ECS at the site of the joint has not been investigated. The aim of this study was to assess the effectiveness of a MAGL inhibitor, when administered locally into an OA joint, at reducing OA-associated pain and joint inflammation.

Hypotheses evaluated in this study:

I.   **The MAGL inhibitor KML29, when administered locally into the joint, is antinociceptive in the MIA model of OA. The antinociceptive action of KML29 is mediated through cannabinoid receptors in the joint.**

II.   **Topical application of KML29 decreases joint inflammation in the acute phase of the MIA model.**

3.2   Action of locally administered KML29 on MIA-induced joint pain and involvement of the cannabinoid receptors

3.2.1 Methods

Male Wistar rats (332-377g) were deeply anaesthetised with isoflurane (2-4%; 100% oxygen at 1L/min) and MIA (3mg; 50µl saline) was injected i.artic. into the right knee joint. The MIA model was then followed for 14 days and rats were separated into two treatment groups, one group receiving i.artic. KML29 (700µg/50µl) and the other receiving i.artic. vehicle (50µl). On day 14, behavioural pain measurements were carried out using von Frey hair algesiometry and hindlimb incapacitance. Testing was conducted at 30, 60, 120, 180, 240 min following drug administration.

In a separate experimental cohort, male Wistar rats (227-276g) followed out to day 14 of the MIA model were organised into different treatment groups. Animals were treated locally by a s.c. injection around the knee with either the CB_1R antagonist, AM281 (75µg/50µl), the CB_2R antagonist, AM630 (75µl/50µl) or vehicle (50µl), 10 min

prior to i.artic. administration of KML29 (700µg). Behavioural pain measurements were performed at 30, 60, 120, 180, 240 min following KML29 administration.

3.2.2 Results

3.2.2.1 KML29 increased hindpaw withdrawal threshold

MIA induced OA pain at day 14 as evinced by the development of hindpaw secondary allodynia ($P<0.0001$; n=20; Figure 3.1A). Hindpaw withdrawal threshold decreased from 14.98 ± 0.08g at baseline (day 0) to 11.17 ± 0.70g on day 14. When KML29 was given i.artic. hindpaw withdrawal threshold significantly improved over the time course tested ($P<0.001$; n=8-10; Figure 3.1A). *Post hoc* analysis revealed significance at 60 min, where the withdrawal threshold improved to 13.19 ± 0.76g.

On day 14 of the MIA time course, both the CB_1R and CB_2R antagonists AM281 and AM630, respectively, significantly blocked the anti-nociceptive effect of KML29 on hindpaw withdrawal threshold ($P<0.0001$; n=6-10; Figure 3.2A1 & 3.2A2). *Post hoc* analysis revealed significance at 30 min and 120 min for AM281 (Figure 3.2A1) and 30 min and 180 min for AM630 (Figure 3.2A2). At 30 min, AM281 and AM630 were significantly different when compared to vehicle plus KML29 or vehicle alone treatment groups ($P<0.05$; n=6-10; Figure 3.2B), with *post hoc* analysis revealing AM281 as significant.

3.2.2.2 KML29 did not improve hindlimb weight bearing deficits

Hindlimb weight bearing deficits were observed 14 days post-MIA induction ($P<0.0001$; n=20; Figure 3.1B). Hindlimb weight bearing decreased from 49.94 ± 0.93 at baseline (day 0) to 43.33 ± 2.05 by day 14 of the model. Animals that received i.artic. KML29 did not have an improvement in hindlimb weight bearing, rather this treatment group was significantly decreased ($P<0.05$; n=8-10; Figure 3.1B), when compared to vehicle treated animals.

KML29 did not improve hindlimb incapacitance, so it would be expected that the CBR antagonists would not alter hindlimb weight bearing. The CB_1R antagonist, AM281, and the CB_2R antagonist, AM630, had no significant effect on hindlimb weight bearing ($P>0.05$; n=6-10; Figure 3.2C1 & 3.2C2). When compared at 30 mins, again there were no significant alterations on hindlimb weight bearing ($P>0.05$; n=6-10; Figure 3.2D).

3.3   Effects of locally administered KML29 on MIA-induced inflammation

3.3.1 Methods

Male Wistar rats (332-410g) underwent inflammation assessments, using IVM and LASCA, 24 hr after MIA (3mg; 50µl saline) was injected i.artic. into the right knee joint. The animals were anaesthetised and a surgical preparation was completed prior to obtaining inflammation measurements (detailed in Section 2.4.2.1). The trachea and right carotid artery were cannulated to provide an unrestricted airway and to monitor MAP, respectively. Circulating leukocytes were fluorescently stained by an i.v. injection of

rhodamine 6G (0.05%; 0.05ml saline) through the tail vein. The jugular vein was cannulated if i.v. access was not available through the tail vein.

3.3.1.1 IVM

The ipsilateral knee joint was exposed and three baseline videos of the joint microvasculature were recorded (1 min each). Next, a warmed (37°C) bolus of either KML29 (700µg) or vehicle (50µl), was applied topically over the exposed knee joint. Measurements were recorded at 5, 15, 30, 60, 120, 180 min post-drug administration. Leukocyte trafficking was quantified and averaged over the three videos obtained at each time point during the experiment. These values were compared to baseline values.

3.3.1.2 LASCA

A baseline LASCA recording (1 min) was taken directly following the baseline IVM recordings and all LASCA recordings followed immediately after IVM throughout the duration of the experiment. Again, experimental time points were 5, 15, 30, 60, 120, 180 post-drug administration. Mean perfusion was calculated and averaged over the 1 min recording at each time point, for a specific region of interest manually drawn over the knee joint. Once the dead scan value was subtracted from each recording, mean perfusion for each time point was used to compute vascular conductance. These values were used to normalise for any MAP differences between animals and were compared to baseline vascular conductance.

3.3.2 Results

3.3.2.1 KML29 decreased adherent leukocytes in day 1 MIA joints

Injection of MIA produced significant increases in both rolling (P<0.0001; n=6; Figure 3.3A) and adherent leukocytes (P<0.0001; n=6; Figure 3.3B) one day after induction. Rolling leukocytes increased from 5.64 ± 1.69 to 59.5 ± 3.36 and adherent leukocytes increased from 0.78 ± 0.13 to 3.61 ± 0.79. When compared to vehicle treated knee joints, KML29 (700µg) did not significantly decrease the number of rolling leukocytes (P>0.05; n=6; Figure 3.3A) in the joint microvasculature over 180 min. Conversely, KML29 did have a significant effect on adherent leukocytes, whereby it was able to decrease the number over the 180 min time course (P<0.0001; n=6; Figure 3.3B) when compared to vehicle treated animals. The largest decrease occurred at 30 min post-KML29 administration, where the KML29 treated group had 2.50 ± 0.51 adherent leukocytes compared to the vehicle treated group which had 7.15 ± 1.58.

3.3.2.2 KML29 did not affect knee joint hyperaemia

On day 1 MIA, knee joint hyperaemia was significantly increased when compared to naïve controls (P<0.0001; n=6; Figure 3.3C), where vascular conductance increased from 0.50 ± 0.06 to 3.75 ± 0.38. Topical administration of KML29 did not have a significant effect on knee joint blood flow (P>0.05; n=6; Figure 3.4C).

3.4   Chapter summary

3.4.1 KML29 administered locally into the joint blocks MIA-induced OA pain

The results presented in Section 3.2 indicate that KML29 may be a valid therapeutic for alleviating referred pain associated with OA. In established MIA joint pain, KML29 improved hindpaw withdrawal threshold, but was unsuccessful at altering hindlimb weight bearing deficits. The antinociceptive effects of KML29 seen in the von Frey algesiometry test were blocked by both CB_1R and CB_2R antagonists.

3.4.2 Local application of KML29 has modest antiinflammatory effects

Based on results from Section 3.3, KML29 applied topically to a day 1 MIA knee joint significantly decreased adherent leukocytes in the joint microvasculature, but had no effect on rolling leukocytes or knee joint hyperaemia. Thus, KML29 only has a moderate antiinflammatory effect, only affecting one inflammation outcome measure out of three.

Table 3.1: Chapter summary

	KML29 (MAGL inhibitor)
PAIN	**Decreased pain (mediated by CB_1R and CB_2R)**
Von Frey	Improved WT
DWB	No effect on WB
INFLAMMATION	
Rolling Leukocytes	No effect
Adherent Leukocytes	Decreased
Joint Perfusion	No effect

WB, weight bearing; WT, withdrawal threshold

A

B
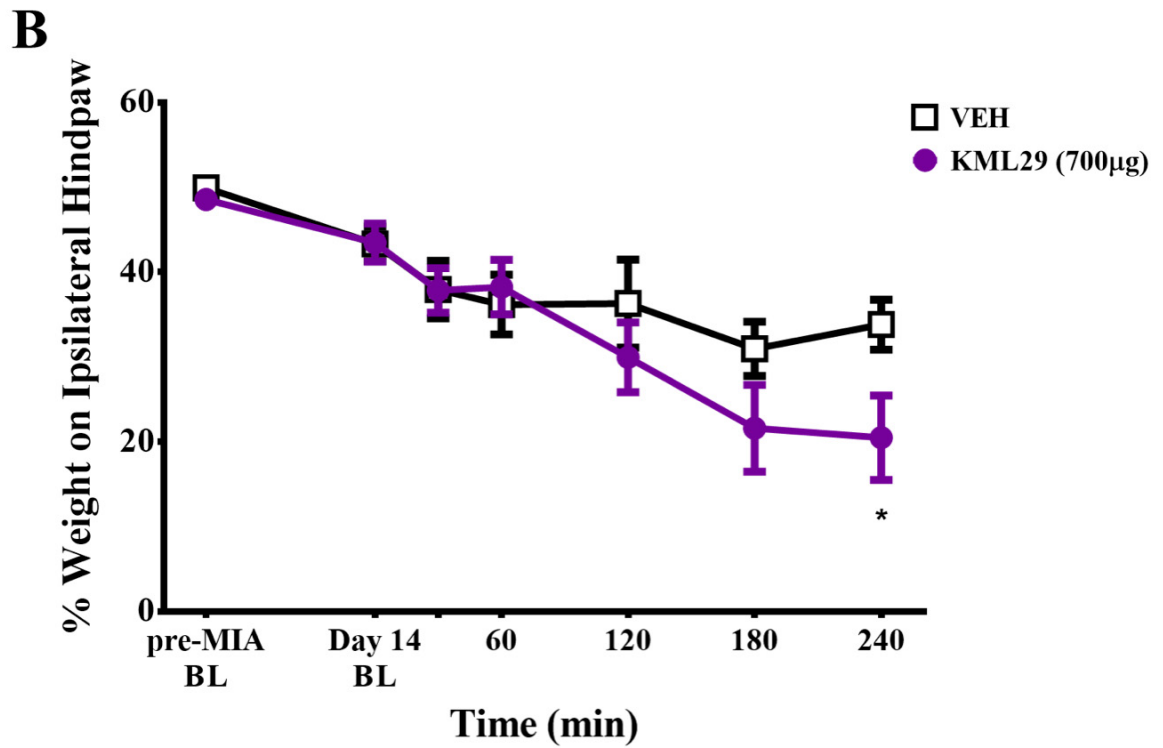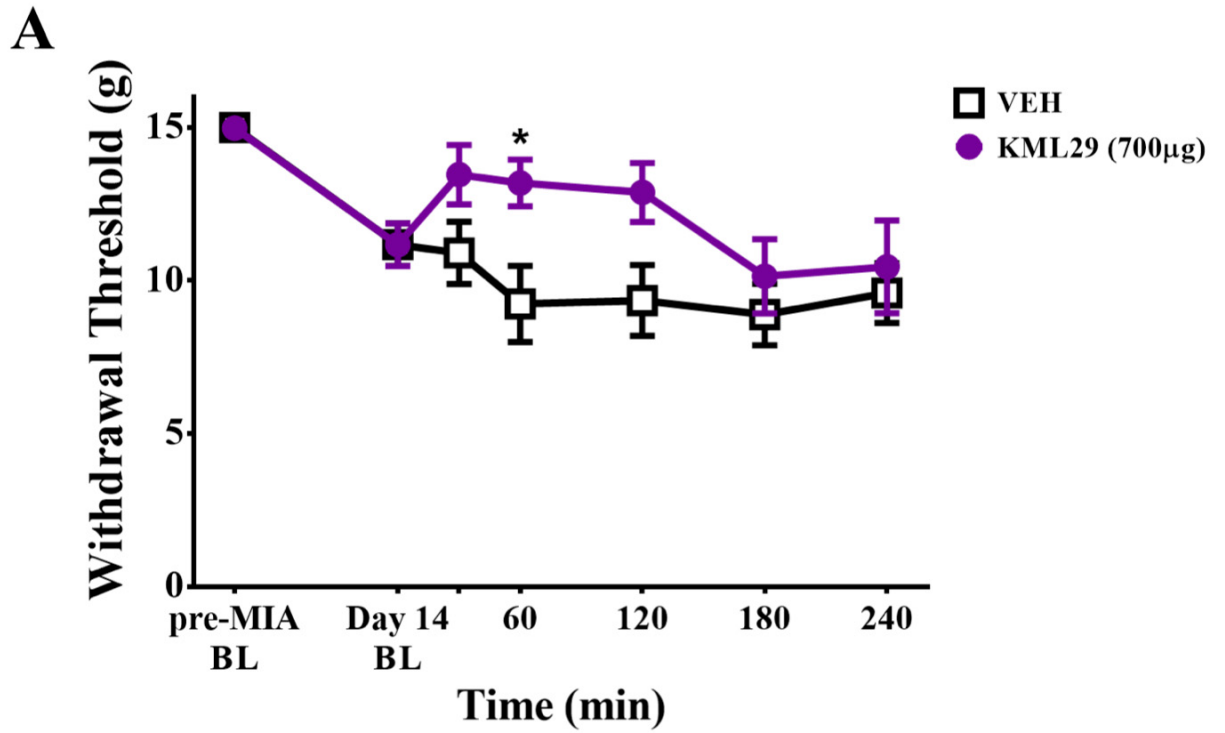
Figure 3.1 Effect of locally administered KML29 on behavioural pain in the MIA model of OA. Induction of MIA, via i.artic. injection, produced secondary allodynia and hindlimb weight bearing deficits by day 14 of the model (****$P<0.0001$; 1-way ANOVA with Dunnett *post hoc* test; n=20). Local administration (i.artic.) of KML29 (700μg) improved hindpaw withdrawal threshold **(A)** (***$P<0.001$; 2-way ANOVA with Bonferroni *post hoc* test; n=8-10), but increased hindlimb weight bearing deficits **(B)** over 240 min (*$P<0.05$; 2-way ANOVA with Bonferroni *post hoc* test; n=8-10). Data are mean values ± SEM. ANOVA, analysis of variance; BL, baseline; MIA, sodium monoiodoacetate; OA, osteoarthritis; VEH, vehicle.

A1

A2
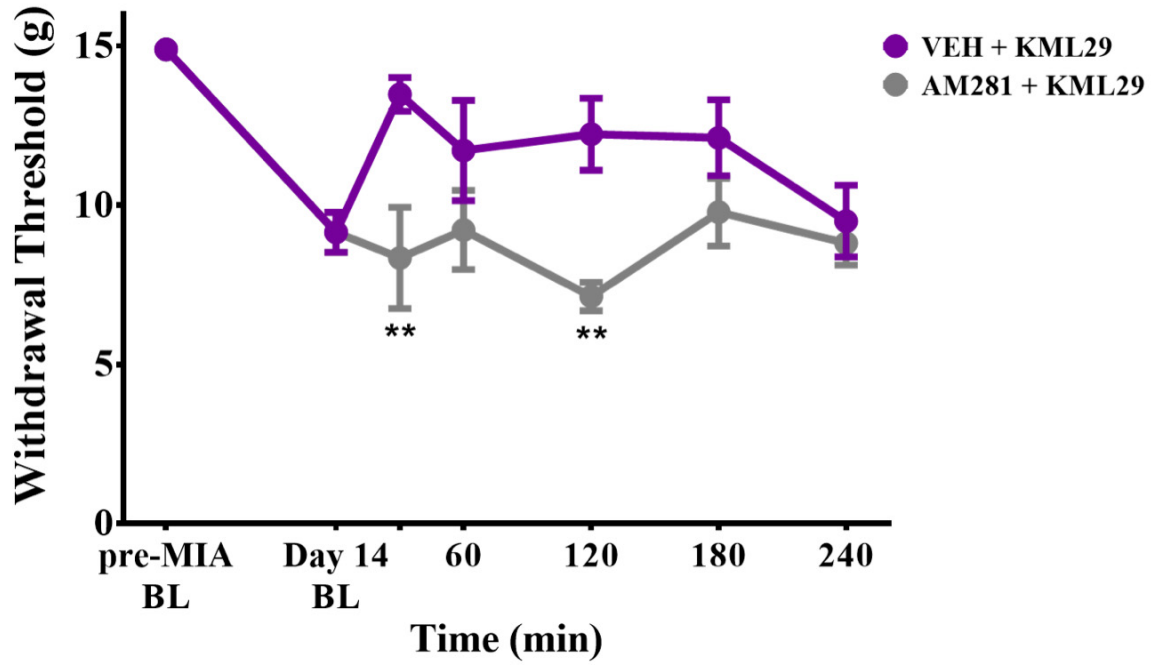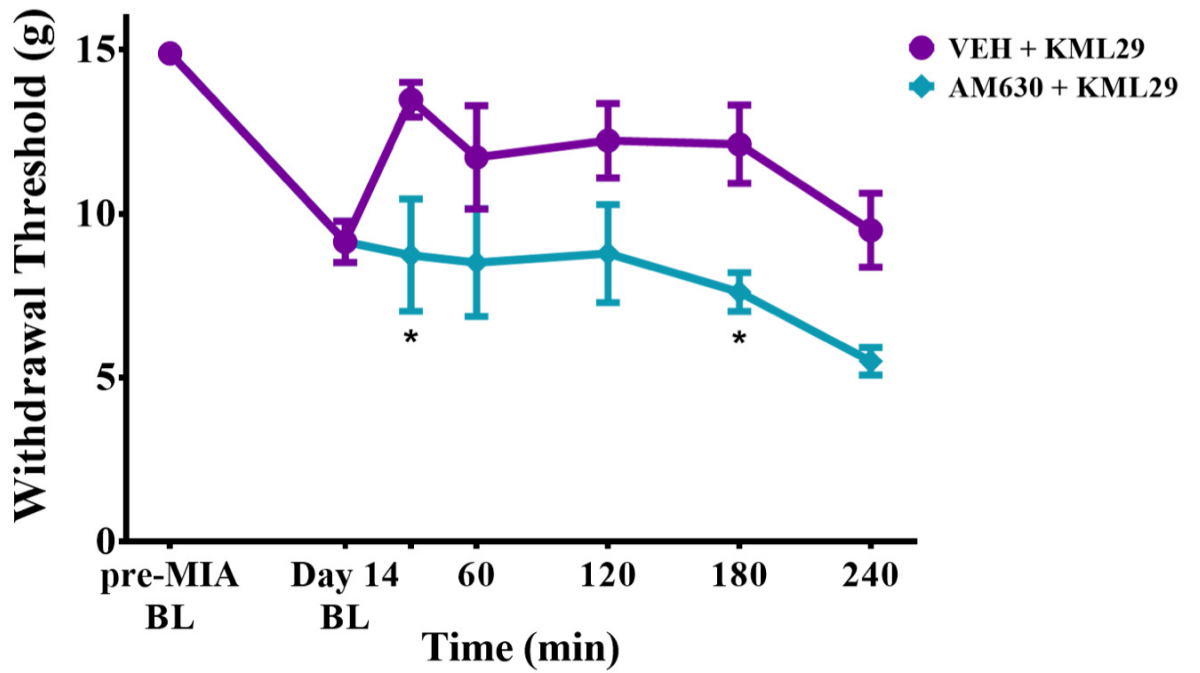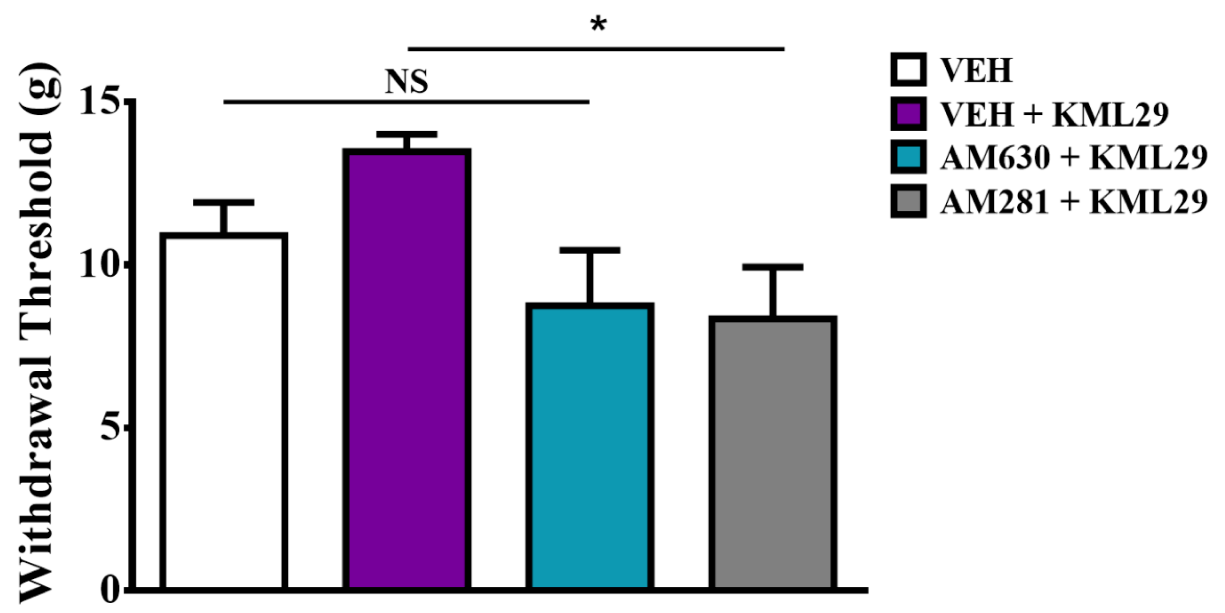
C1
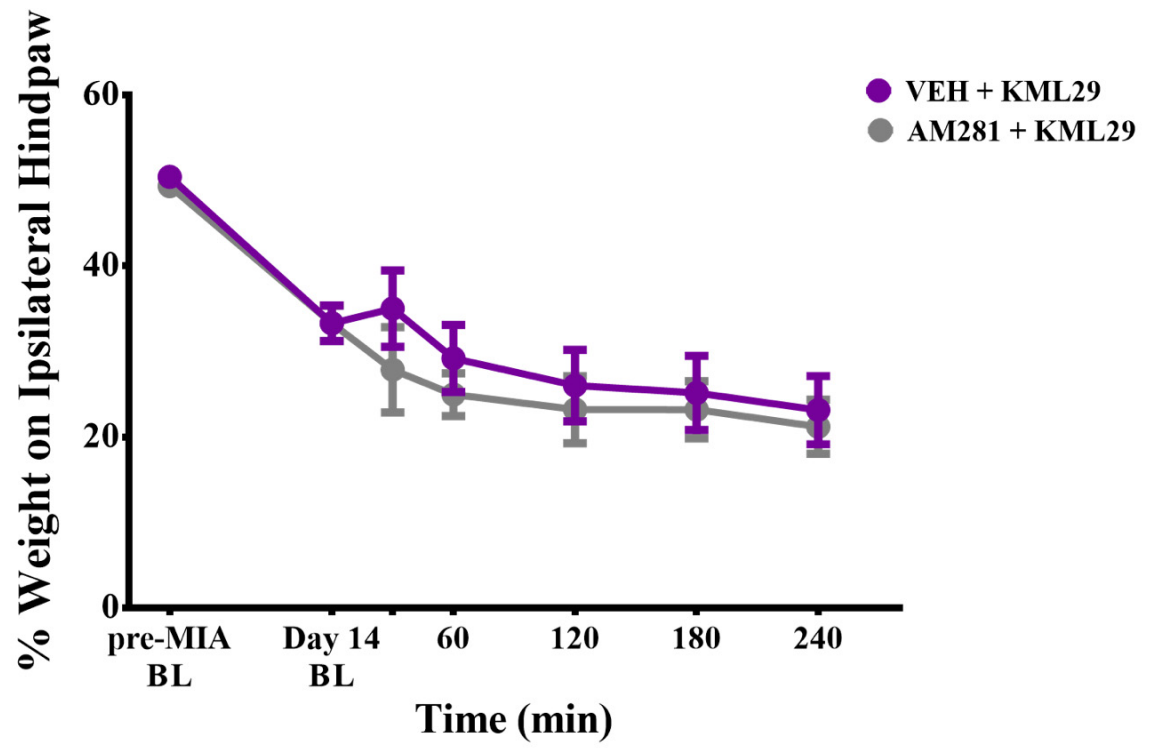
C2
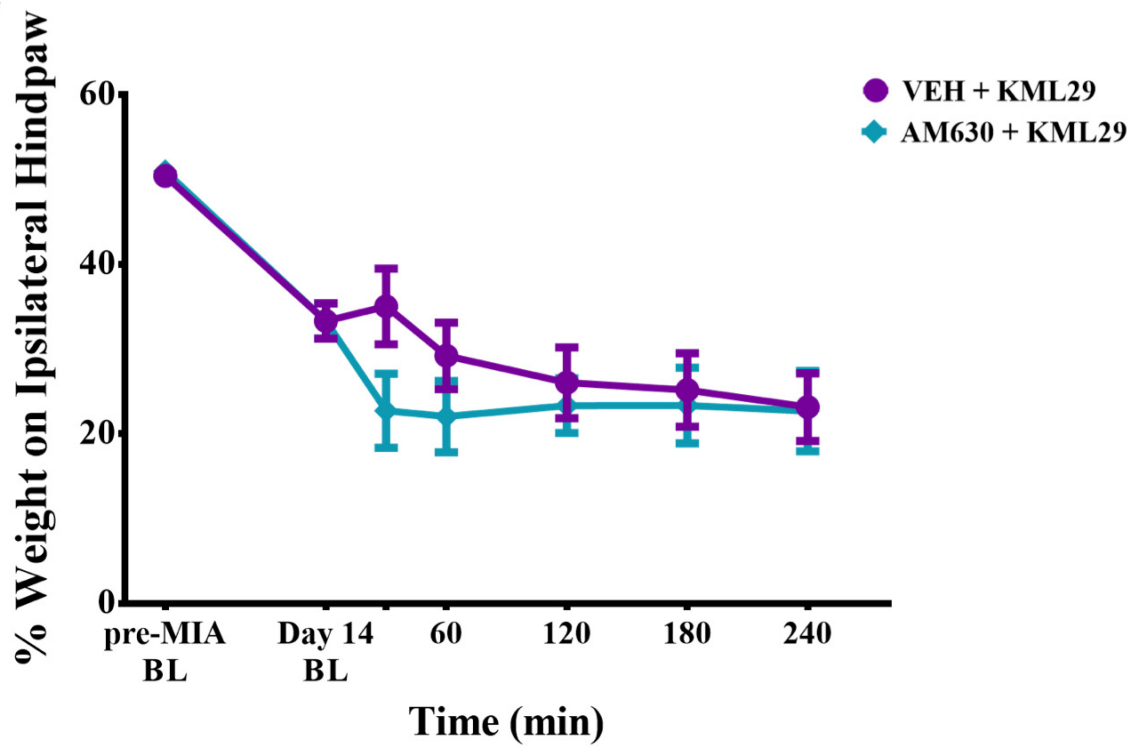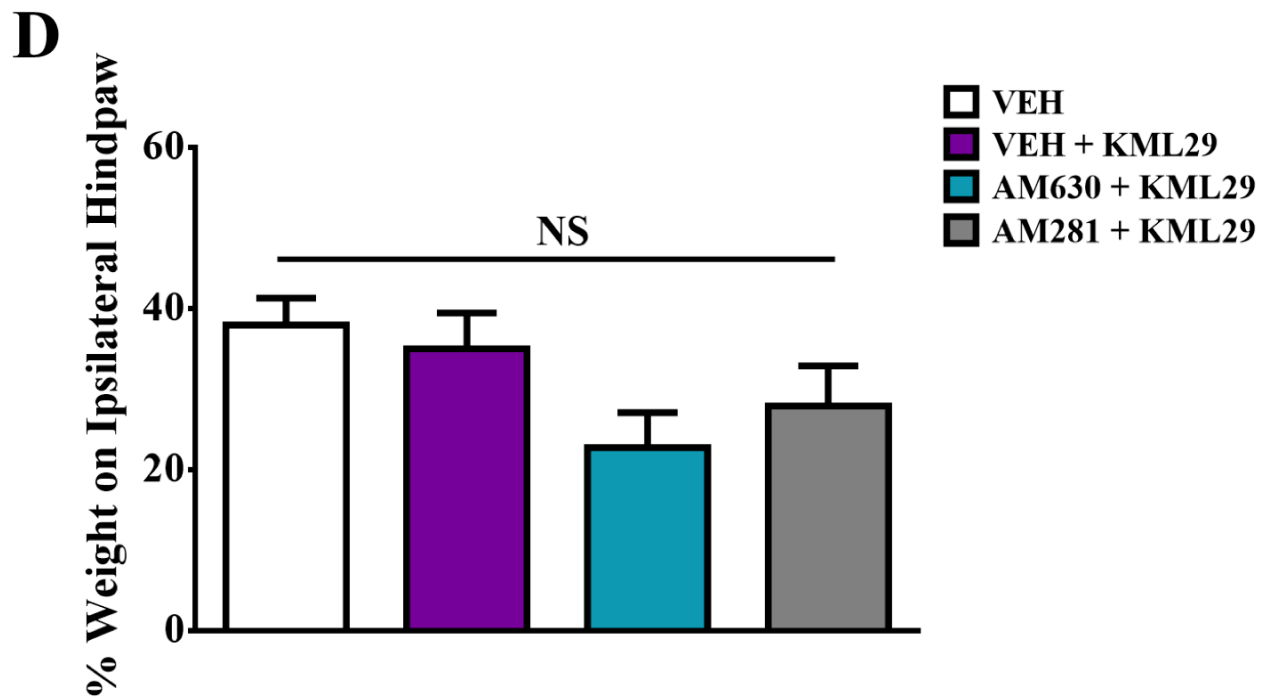
Figure 3.2 Contribution of the classical cannabinoid receptors to the antinociceptive action of KML29. The improvement in hindpaw withdrawal threshold by KML29 was blocked following administration of both the CB_1R antagonist, AM281 (75µg), **(A1)** and the CB_2R antagonist, AM630 (75µg), **(A2)** over 240 min (****$P<0.0001$; 2-way ANOVA with Bonferroni *post hoc* test; n=6-10). *Post hoc* analysis revealed significance at 30 min and 120 min for AM281 and significance at 30 min and 180 min for AM630. When both antagonists are compared to VEH + KML29 and VEH alone, at 30 min, only AM281 significantly blocks the effects of KML29 (*$P<0.05$; 1-way ANOVA with Dunnett *post hoc* test; n=6-10) **(B)**. Both the CB_1R antagonist **(C1)** and CB_2R antagonist **(C2)**, AM281 and AM630 respectively, did not alter hindlimb weight bearing over 4 hours ($P>0.05$; 2-way ANOVA with Bonferroni *post hoc* test; n=6-10). When comparing all groups at 30 min **(D)**, there were no significant differences between them ($P>0.05$; 1-way ANOVA with Dunnett *post hoc* test; n=6-10). Data are means ± SEM. ANOVA,

analysis of variance; BL, baseline; MIA, sodium monoiodoacetate; NS, not significant;

VEH, vehicle.

A

B

C
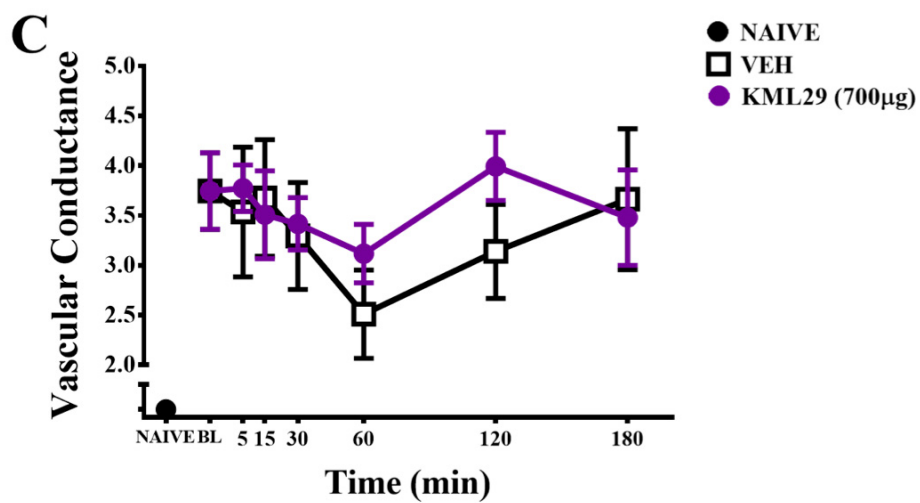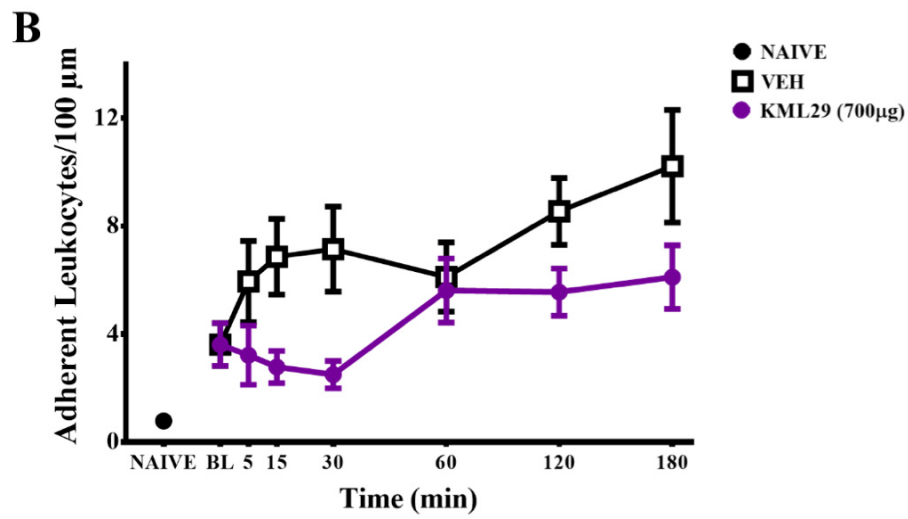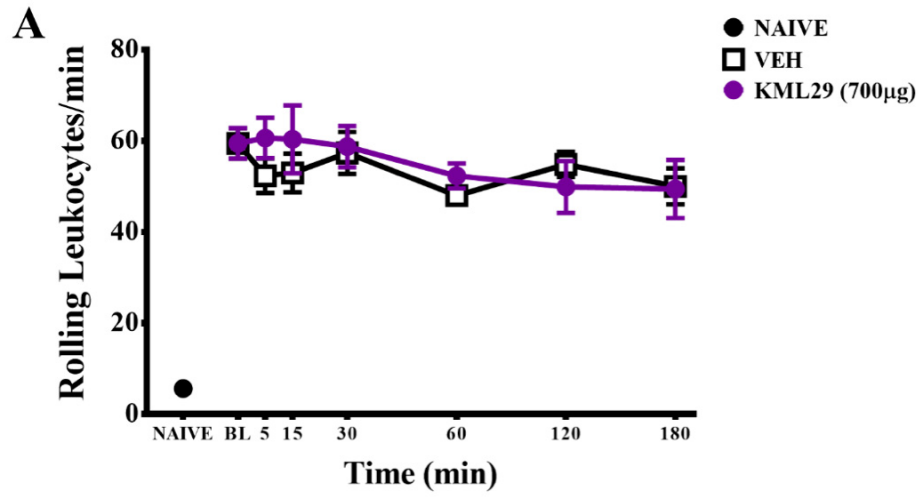
Figure 3.3 The effects of KML29 on day 1 MIA-induced inflammation. Injection of

MIA (i.artic.) significantly increased rolling **(A)** and adherent leukocytes **(B)**, and caused

synovial hyperaemia **(C)** when compared to naïve controls (****$P<0.0001$; student's t-

test; n=6-12) one day later. Topical administration of KML29 (700μg) did not alter

rolling leukocytes **(A)** ($P>0.05$; 2-way ANOVA with Bonferroni *post hoc* test; n=6), but

did decrease adherent leukocytes **(B)** over the 180 min time course (****$P<0.0001$; 2-

way ANOVA with Bonferroni *post hoc* test; n=6). Additionally, KML29 did not alter

synovial hyperaemia **(C)** ($P>0.05$; 2-way ANOVA with Bonferroni *post hoc* test; n=6)

when compared to vehicle. Data are means ± SEM. ANOVA, analysis of variance; BL,

baseline; MIA, sodium monoiodoacetate; VEH, vehicle.

Chapter 4: The Direct Effects of the CB2 Receptor Agonist, JWH133, on MIA-Induced Joint Pain and Inflammation

Disclosures: No disclosures for this chapter.

4.1 Background and hypotheses

The ECS is one of the body's important natural regulator of pain and inflammation. Cannabinoid receptors CB_1R and CB_2R are located throughout the body, with CB_1R mainly localised within the CNS and CB_2R historically distributed between different subsets of immune cells in the periphery (Svizenska *et al.,* 2008). In recent years however, CB_2Rs have been identified in the lumbar L4-L6 DRGs of rodents (Svizenska *et al.,* 2008; Schuelert *et al.,* 2010) as well as in the synovial membrane of sham and arthritic rat knee joints (Schuelert *et al.,* 2010). Both CB_1Rs and CB_2Rs are localised on nerves which innervate the rat knee joint (McDougall, 2009; Schuelert *et al.,* 2010, McDougall, 2011). Since CB_2Rs are not highly localised in the CNS, directly modulating CB_2Rs may allow for a highly targeted therapy devoid of centrally-mediated effects. Unlike CB_1R agonists, CB_2R agonists have not been shown to elicit any central effects (Hanus *et al.,* 1999; Malan *et al.,* 2001; Yao *et al.,* 2008). This is an important finding when considering adverse effects of developing novel therapeutics.

Directly activating CB_2Rs using synthetic agonists has been shown to decrease pain and inflammation *in vivo*. A study by Fukuda *et al.* (2014) administered JWH133, a CB_2R agonist, systemically to mice with inflammatory arthritis and found that it

decreased arthritis severity and immune cell infiltration. When administered in a model of neuropathic pain, JWH133 improved thermal and mechanical hypersensitivity (Vera *et al.,* 2013). In the MIA model of OA, again systemic administration of JWH133 improved behavioural pain outcomes, decreased serum proinflammatory mediators, and regulated central sensitisation (Burston *et al.,* 2013). In normal knee joints CB_2R agonists, JWH015 and JWH133, both caused a dose-dependent increase in synovial blood flow, but the vasodilator effect was absent in acute and chronic inflammatory models, kaolin-carrageenan and FCA, respectively (McDougall *et al.,* 2008). Paradoxically, a study carried out with a particular CB_2R agonist, GW405833, found that it was pronociceptive in OA joints (Schuelert *et al.,* 2010), delivering conflicting evidence of the involvement of CB_2Rs in OA joint pain. Furthermore, CB_1R agonists have been widely shown to produce analgesia in preclinical pain models (Vera *et al.,* 2013). Again, these compounds were administered systemically, which run the risk of producing centrally-mediated effects, or must be administered at non-psychoactive doses.

This study aimed to elucidate the role of CB_2R peripherally in an OA joint. Specifically using the synthetic CB_2R agonist, JWH133, locally to determine if directly activating CB_2Rs will block OA pain and reduce OA-associated inflammatory flares.

Hypotheses evaluated in this study:

I. **Peripherally administered JWH133 in the MIA model of OA is antinociceptive and this effect is mediated through classical cannabinoid receptors in the knee joint.**

II.   **Local administration of JWH133 reduces acute MIA-induced**

       inflammation.

4.2   Action of locally-administered JWH133 on MIA-induced joint pain and the contributions of the classical cannabinoid receptors

4.2.1 Methods

Male Wistar rats (381-491g) at 14 post-MIA (3mg; 50µl saline) induction were divided into treatment cohorts, with one receiving JWH133 (30µg/50µl) and the other receiving vehicle (50µl) i.artic into the joint. Behavioural pain assessments were conducted by using von Frey hair algesiometry and hindlimb incapacitance techniques at 30, 60, 120, 180, 240 min succeeding drug administration.

In a separate cohort, on day 14 of the MIA model, male Wistar rats (243-285g) were allocated into three treatment groups. The rats were given either the CB_1R antagonist, AM281 (75µg/50µl), the CB_2R antagonist, AM630 (75µg/50µl), or vehicle (50µl) by s.c. injection 10 min prior to the i.artic. administration of JWH133 (30µg). Behavioural pain outcomes were evaluated at 30, 60, 120, 180, 240 min after JWH133 administration.

4.2.2   Results

4.2.2.1   Local JWH133 blocks OA-associated referred pain

Injection of MIA caused a significant decrease in hindpaw withdrawal threshold ($P<0.001$; n=16; Figure 4.1A) by day 14 of the model. Hindpaw withdrawal threshold decreased from 14.79 ± 0.21g at day 0 baseline to 10.99 ± 0.87 on day 14 of the model. JWH133 delivered directly into the ipsilateral joints of animals 14 days post-MIA induction significantly improved hindpaw withdrawal threshold ($P<0.001$; n=8; Figure 4.1A). At 120 min post-drug administration, hindpaw withdrawal threshold increased to 13.20 ± 0.93g which was the largest improvement throughout the time course.

The antinociceptive action of JWH133 was blocked by the CB_2R antagonist, AM630 ($P<0.01$; n=6; Figure 4.2A1). *Post hoc* analysis showed significance at the 30 min time point (Figure 4.2B). However, the effects of JWH133 were not altered by the CB_1R antagonist AM281 ($P>0.05$; n=6; Figure 4.2A2).

4.2.2.2   Intraarticular JWH133 modifies hindlimb incapacitance

After 14 days post-MIA, hindlimb weight bearing deficits were apparent ($P<0.0001$; n=16; Figure 4.1B) when compared baseline. On day 0 hindlimb weight bearing was 49.99 ± 0.56 and decreased to 43.11 ± 1.14 by day 14. JWH133 significantly altered hindlimb weight bearing ($P<0.0001$; n=8; Figure 4.1B) when compared to vehicle treated animals. *Post hoc* analysis revealed significance at 30, 120, 180, and 240 min. The greatest improvement in weight bearing occurred at 30 min, where it increased to

45.35 ± 1.78. The largest difference between JWH133 treated animals (42.76 ± 1.86) and vehicle treated animals (29.26 ± 2.65) occurred at 180 min.

The group treated with the CB_1R antagonist, AM281, is significantly different when compared to the JWH133 treated group over the 240 min time course ($P<0.01$; n=6-8; Figure 4.2C1). *Post hoc* analysis showed the 180 min time point to be the only significant time point. The CB_2R antagonist, AM630, did not alter hindlimb weight bearing throughout the time course ($P>0.05$; n=6-8; Figure 4.2C2). The antinociceptive action of JWH133 seems to have lost effectiveness in this experimental cohort ($P>0.05$; n=6-8; Figure 4.2D), when compared to vehicle counterparts.

4.3   Effects of locally administered JWH133 on MIA-induced inflammation

4.3.1 Methods

Using IVM and LASCA, male Wistar rats (346-396g), underwent inflammation assessment 24 hr post-MIA (3mg; 50μl saline) induction. The animals were anaesthetised and surgical preparation was completed, as detailed in Section 2.4.2.1, prior to obtaining inflammation measurements. Circulating leukocytes were fluorescently stained by an i.v. injection of rhodamine-6G (0.05%; 0.05ml saline) through the tail vein.

4.3.1.1 IVM

Three baseline videos of the exposed knee joint microvasculature were recorded (1 min each). A warmed (37°C) bolus of either JWH133 (30μg) or vehicle (50μl), was

applied topically to the joint capsule and measurements were recorded at 5, 15, 30, 60, 120, 180 min post-drug administration. Leukocyte trafficking was quantified and averaged over the three videos obtained at each time point during the experiment. These values were compared to baseline values.

4.3.1.2 LASCA

All LASCA recordings followed immediately after each IVM recording throughout the duration of the experiment. Once the dead scan value was subtracted from each recording, mean perfusion was calculated at each time point. These values were then used to calculate vascular conductance and normalised for MAP differences between animals. All experimental time points and were then compared to the baseline vascular conductance.

4.3.2 Results

4.3.2.1 JWH133 is antiadherent but not antirolling in MIA knee joints

On day 1 post-MIA induction, rolling and adherent leukocytes were both significantly increased when compared to naïve animals (P<0.0001; n=6-12; Figure 4.3A & 4.3B). Rolling leukocytes increased from 5.64 ± 1.69 to 58.9 ± 2.88, and adherent leukocytes increased from 0.78 ± 0.13 to 3.86 ± 0.76. Topical application of JWH133 had no significant effect on rolling leukocytes when compared to vehicle treated counterparts (P>0.05; n=6; Figure 4.3A). However, JWH133 did significantly decrease adherent

leukocyte number (P<0.0001; n=6; Figure 4.3B) in the joint microvasculature when compared to the vehicle treated cohort. *Post hoc* analysis showed significance at 180 min, where JWH133 treated animals had 5.39 ± 1.24 adherent leukocytes and vehicle treated animals had 10.22 ± 2.09 adherent leukocytes.

4.3.2.2 JWH133 did not alter knee joint hyperaemia

Injection of MIA (i.artic.) caused a significant increase in synovial hyperaemia (P<0.0001; n=6-12; Figure 4.3C), whereby vascular conductance increased to 4.07 ± 0.41 compared to 0.50 ± 0.06 in naïve animals. JWH133 administered topically onto the exposed knee joint did not have a significant effect on vascular conductance (P>0.05; n=6; Figure 4.3C), when compared to vehicle treated joints.

4.4   Chapter summary

4.4.1 Locally applied JWH133 improves behavioural pain outcomes

The data presented in Section 4.2 suggests that blockade of CB_2Rs, locally in the joint, may be a beneficial therapy for treating OA-induced pain. JWH133 was able to significantly improve hindpaw secondary allodynia and hindlimb weight bearing deficits.

The analgesic effects of JWH133 on hindpaw secondary allodynia were blocked by the CB_2R antagonist, AM630, but not by the CB_1R antagonist, AM281. The hindlimb incapacitance results presented in Section 4.2.2.2 were difficult to interpret. The improvement in hindlimb weight bearing by JWH133 was not seen in this cohort of

animals, therefore it was not expected for the receptor antagonists to alter weight bearing deficits. However, surprisingly, the CB$_1$R antagonist treated group was significantly different from the vehicle plus JWH133 control group.

4.4.2 JWH133 has moderate antiinflammatory effects in day 1 MIA joints

On day 1 post-MIA, JWH133 decreased adherent leukocytes but had no effect on rolling leukocytes or arthritis-induced joint hyperaemia. Therefore, JWH133 may not be effective at relieving OA-associated inflammatory flares.

Table 4.1: Chapter summary

	JWH133 (CB$_2$R agonist)
PAIN	**Decreased pain (mediated by CB$_2$R)**
Von Frey	Improved WT
DWB	Improved WB
INFLAMMATION	
Rolling Leukocytes	No effect
Adherent Leukocytes	Decreased
Joint Perfusion	No effect

WB, weight bearing; WT, withdrawal threshold
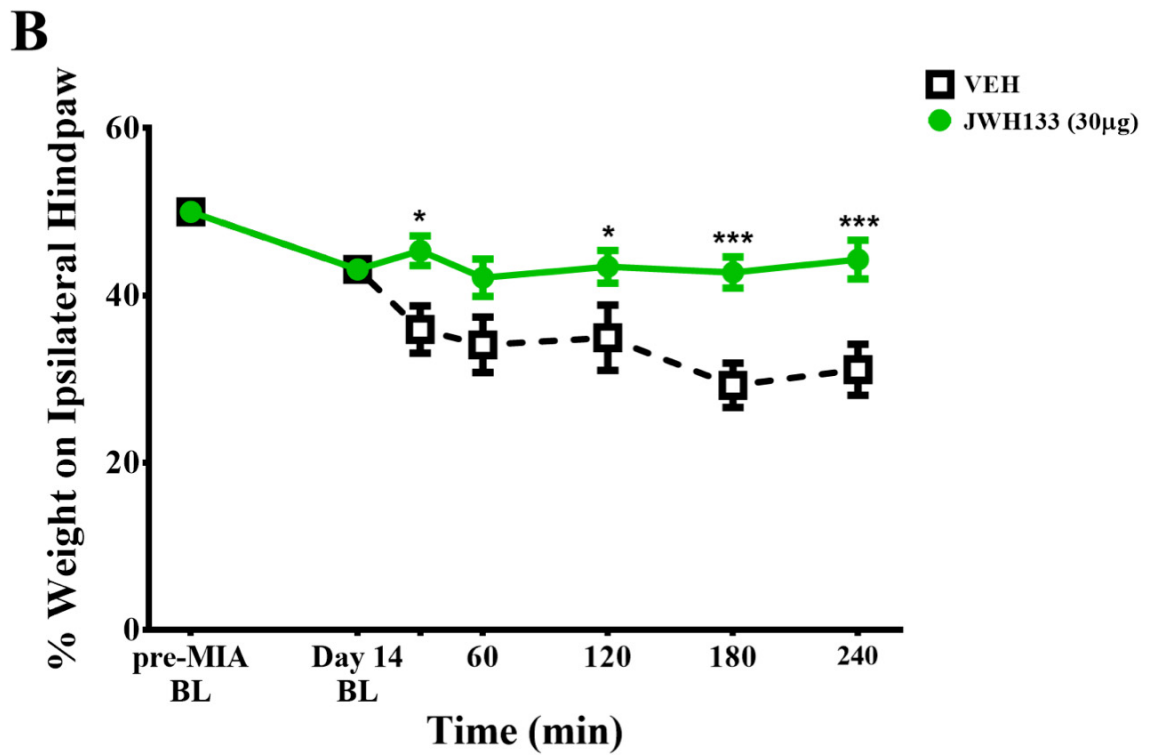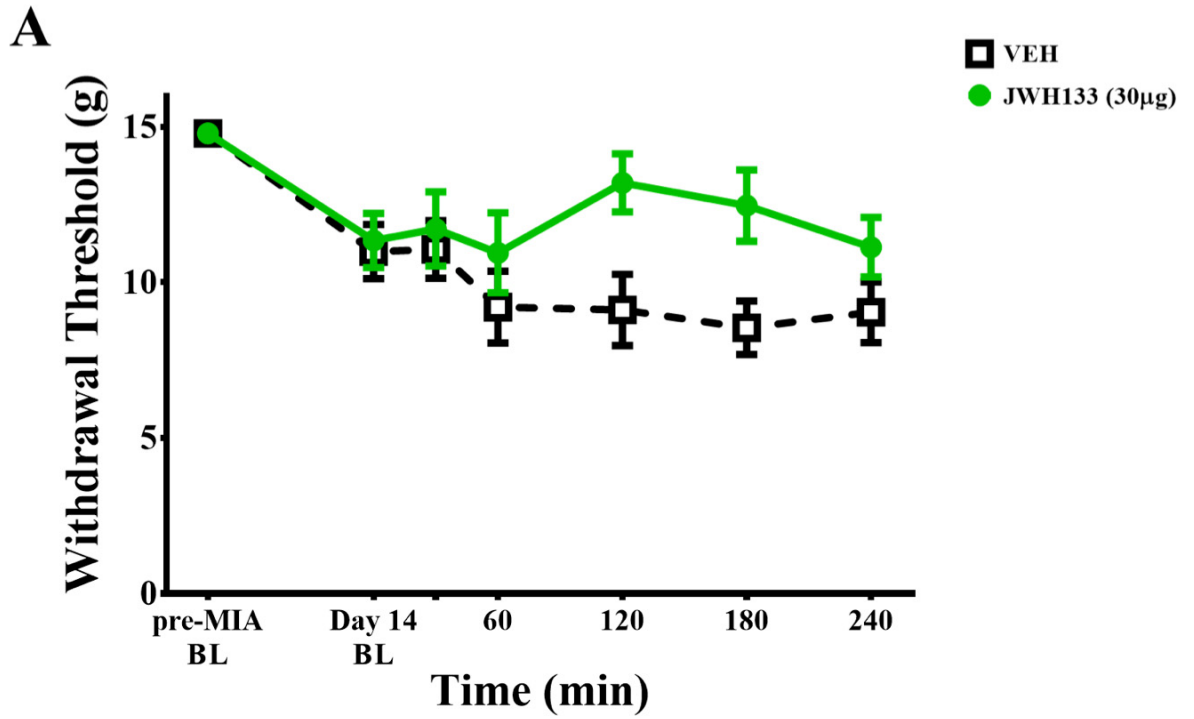
Figure 4.1 Action of locally administered JWH133 on behavioural pain measures in the MIA model of OA. Induction of MIA, via i.artic. injection, produced secondary allodynia and hindlimb weight bearing deficits by day 14 of the model (****$P<0.0001$; 1-way ANOVA with Dunnett *post hoc* test; n=16). Administration (i.artic.) of JWH133 (30µg) improved hindpaw withdrawal threshold **(A)** (***$P<0.001$; 2-way ANOVA with Bonferroni *post hoc* test; n=8), and also improved hindlimb weight bearing deficits **(B)** over 240 min (****$P<0.0001$; 2-way ANOVA with Bonferroni *post hoc* test; n=8). *Post hoc* analysis revealed significance at 30, 120, 180, and 240 min. Data are mean values ± SEM. ANOVA, analysis of variance; BL, baseline; MIA, sodium monoiodoacetate; OA, osteoarthritis; VEH, vehicle.

A1

VEH + JWH133
AM281 + JWH133

A2

VEH + JWH133
AM630 + JWH133
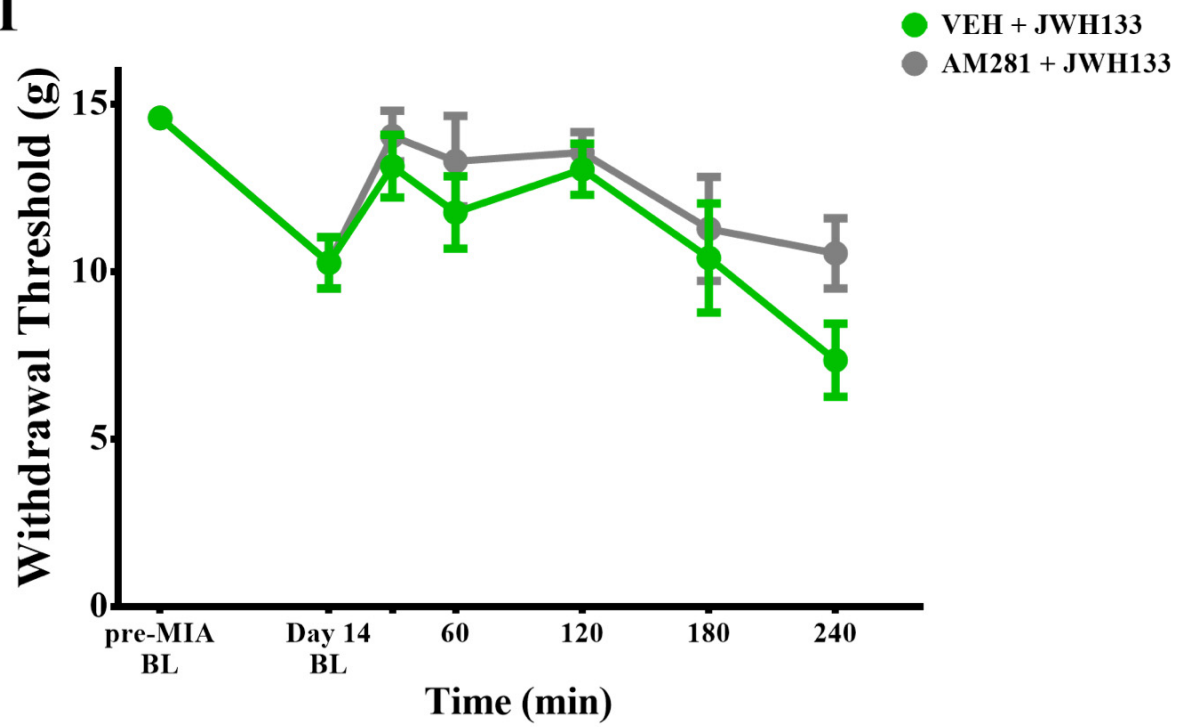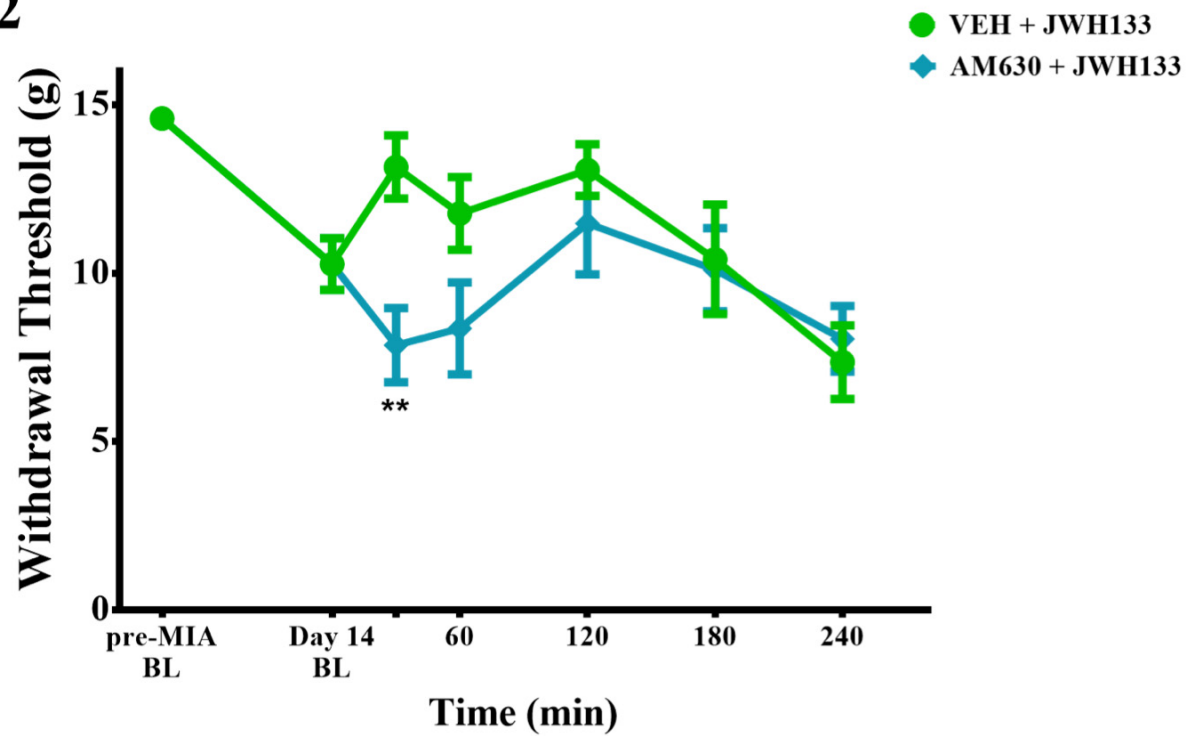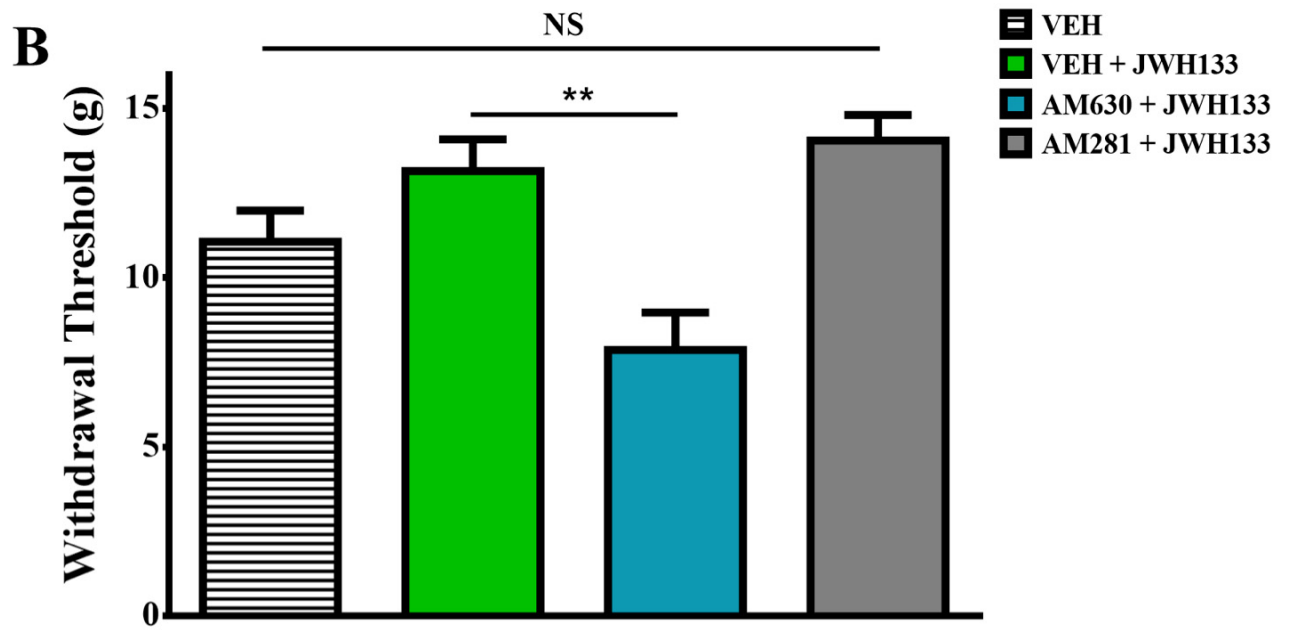
C1
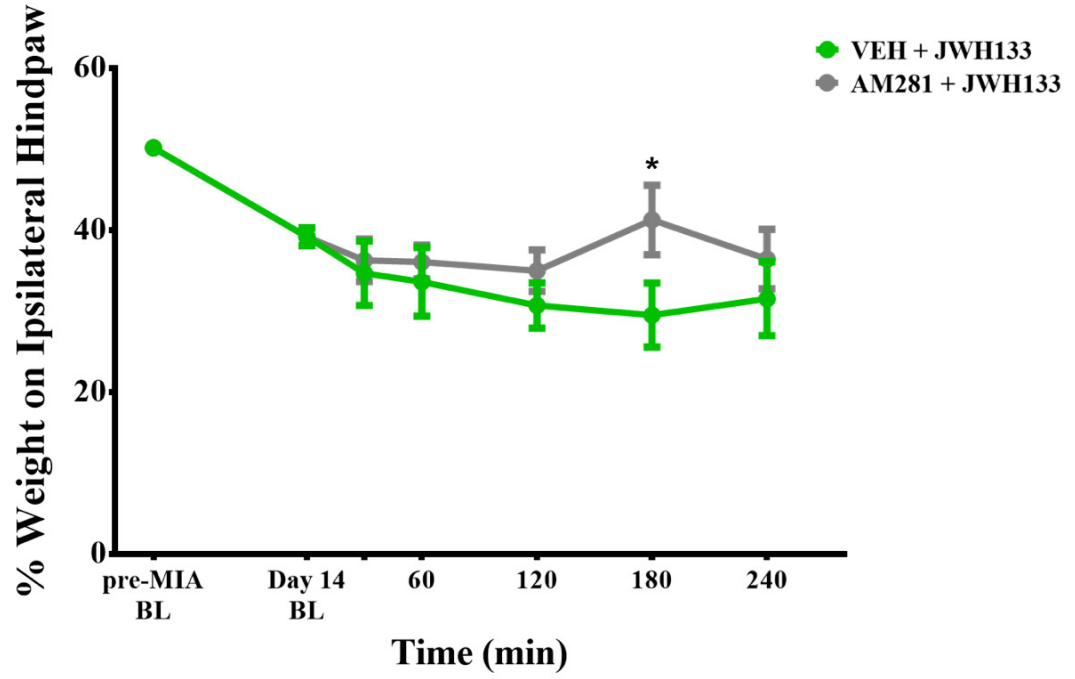
C2
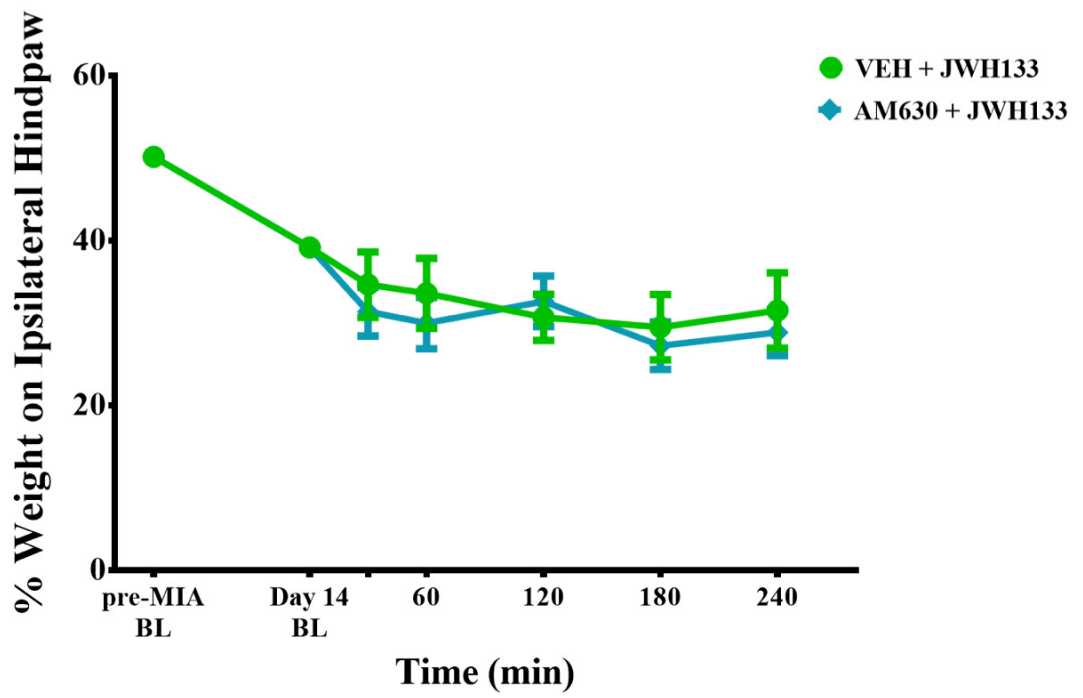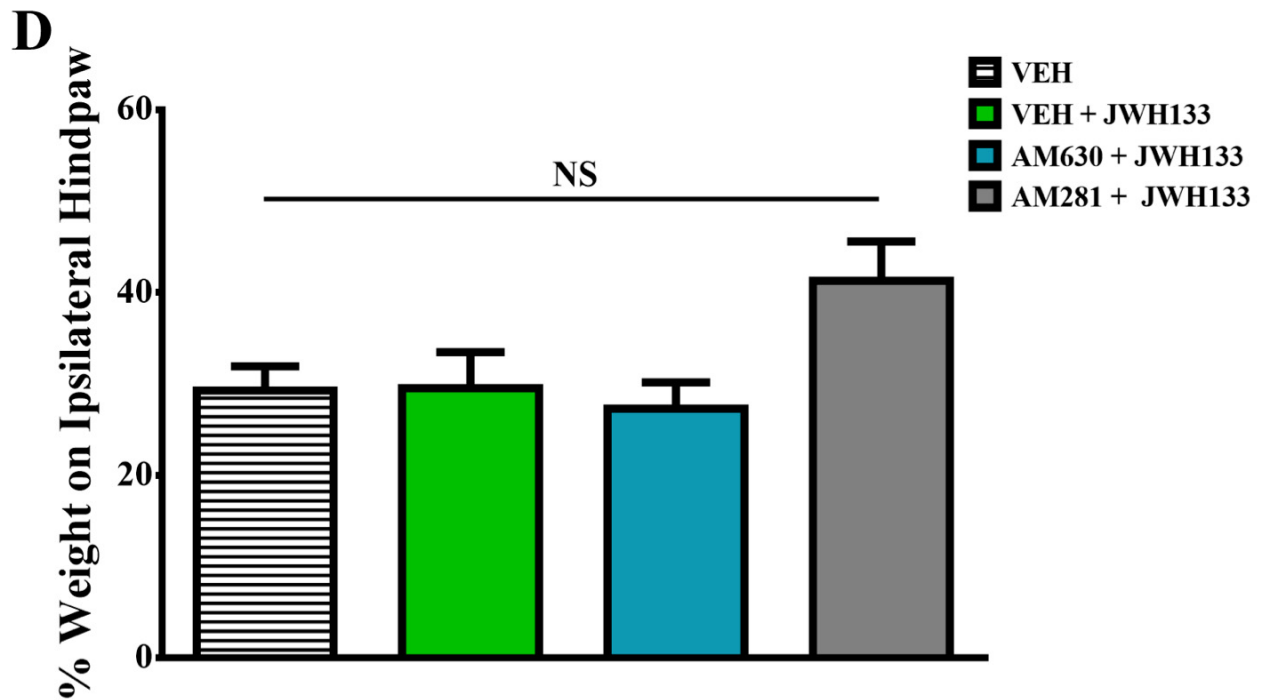
Figure 4.2 Contribution of the classical cannabinoid receptors to the antinociceptive effects of JWH133. The improvement in hindpaw withdrawal threshold by JWH133 was blocked following administration of the CB_2R antagonist AM630 (75µg) (**$P<0.01$; 2-way ANOVA with Bonferroni *post hoc* test; n=6-8) **(A2)**, but unaltered by the CB_1R antagonist AM281 (75µg) **(A1)** and over 240 min ($P>0.05$; 2-way ANOVA with Bonferroni *post hoc* test; n=6-8). *Post hoc* analysis revealed significance at 30 min. When compared to all other treatment groups, at 30 min, AM630 significantly blocks the effects of JWH133 (**$P<0.01$; 1-way ANOVA with Dunnett *post hoc* test; 6-8) **(B)**. The CB_1R antagonist, AM281, was significantly different from JWH133 treated animals over the 240 min time course (*$P<0.05$; 2-way ANOVA with Bonferroni *post hoc* test; n=6-8) **(C1)**. *Post hoc* analysis revealed the 180 min time point as significant. The CB_2R antagonist, AM630, did not alter hindlimb weight bearing ($P>0.05$; 2-way ANOVA with Bonferroni *post hoc* test; n=6-10) **(C2)**. When comparing all groups at 180 min **(D)**, there

were no significant differences between them (P>0.05; 1-way ANOVA with Dunnett *post hoc* test; n=6-10). Data are means ± SEM. ANOVA, analysis of variance; BL, baseline; MIA, sodium monoiodoacetate; NS, not significant; VEH, vehicle.
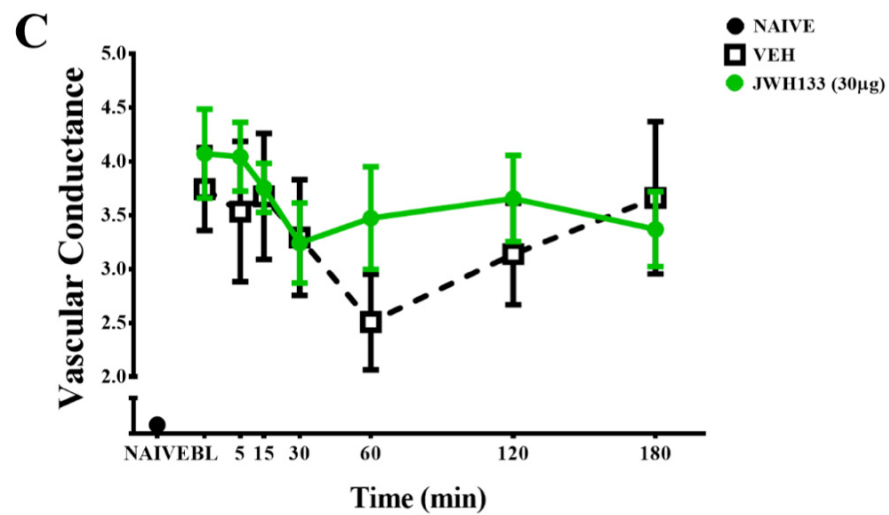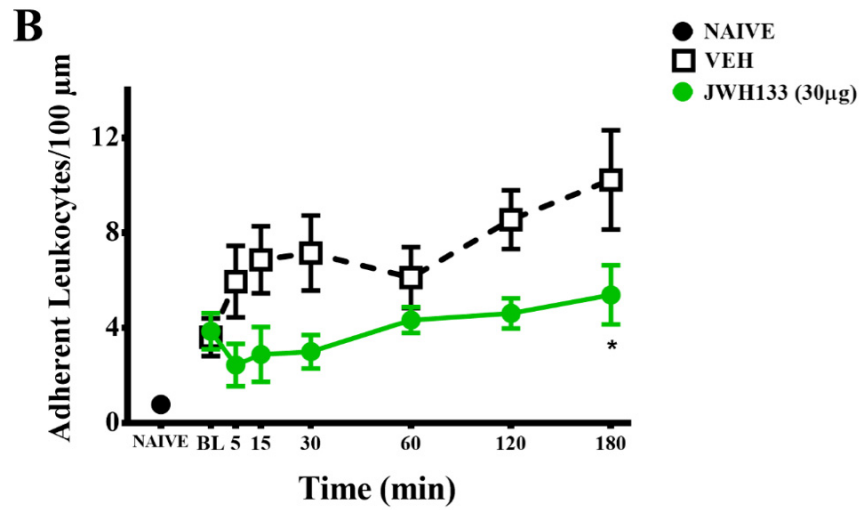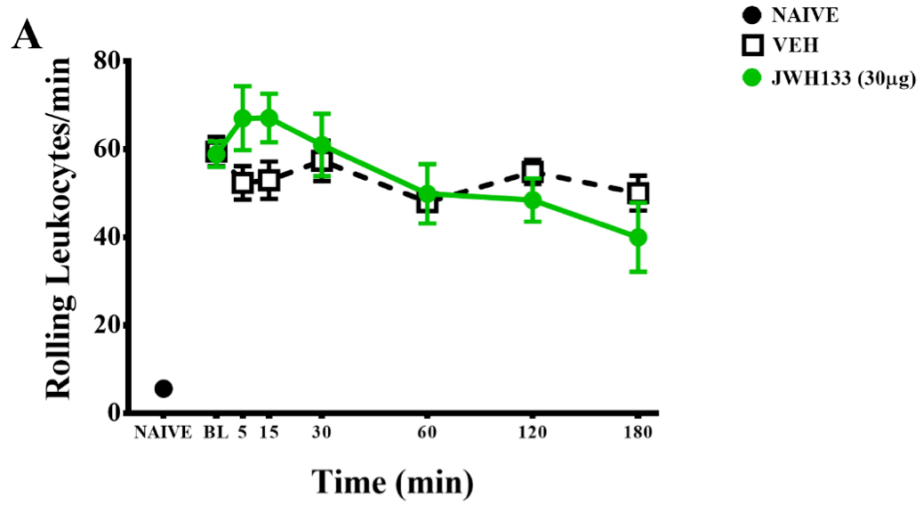
Figure 4.3 The action of JWH133 on day 1 MIA-induced inflammation. Injection of

MIA (i.artic.) significantly increased rolling **(A)** and adherent leukocytes **(B)**, and caused

synovial hyperaemia **(C)** when compared to naïve controls (****P<0.0001, *P<0.05;

student's t-test; n=6-12). Topical administration of JWH133 (30µg) did not alter rolling

leukocytes **(A)** (P>0.05; 2-way ANOVA with Bonferroni *post hoc* test; n=6), but did

decrease adherent leukocytes **(B)** over the 240 min time course (****P<0.0001; 2-way

ANOVA with Bonferroni *post hoc* test; n=6). *Post hoc* analysis revealed significance at

180 min. Additionally, JWH133 did not alter synovial hyperaemia **(C)** (P>0.05; 2-way

ANOVA with Bonferroni *post hoc* test; n=6) when compared to vehicle. Data are means

± SEM. ANOVA, analysis of variance; BL, baseline; MIA, sodium monoiodoacetate;

VEH, vehicle.

Chapter 5: The Effects of the Major Phytocannabinoid, Cannabidiol, on MIA-Induced Joint Pain and Inflammation

Disclosures: Data presented in this chapter, unless otherwise stated, have been published in Philpott *et al.,* 2017; PAIN. Furthermore, Milind Muley aided in the generation of naïve intravital microscopy (IVM) and laser speckle contrast analysis (LASCA) data.

5.1 Background and hypotheses

Historically, OA has been classified as a non-inflammatory arthritis and was thought of as simply wear and tear of the joints. Inflammation was considered a mere side effect of the joint damage occurring as OA develops, and not as a potential driver of the disease. It is now believed that inflammatory flares and low levels of chronic inflammation contribute to the degenerative changes that occur throughout the synovial joint, promoting OA disease progression (Gronblad *et al.,* 1988; Poole, 1999; Hill *et al.,* 2007; Guermazi *et al.,* 2011; Robinson *et al.,* 2016). These changes can lead to joint destruction (Krustev *et al.,* 2015), nerve damage, peripheral sensitisation, and generate nociceptive pain (McDougall *et al.,* 2009; Schuelert & McDougall, 2009; Krustev *et al.,* 2015). Chronic pain and disease progression in OA patients is under managed due to limited viable treatment options. Moreover, there is growing evidence suggesting that a subset of approximately 30% of OA patients suffer from neuropathic pain (Schomberg *et al.,* 2012; Ahmed *et al.,* 2014). The mixed nature of OA pain explains why commonly

prescribed pain therapies have limited effectiveness in a heterogeneous OA patient population.

The MIA model of experimental OA is a rapidly progressing and highly reproducible model of human OA. The pain and inflammatory components of this model have been thoroughly characterised (Bove *et al.,* 2003; Thakur *et al.,* 2012). The MIA model begins with an acute inflammatory phase that peaks at day 1 and decreases to low levels by day 7 (Bove *et al.,* 2003). The pain in this model is biphasic, where inflammation dictates pain in the first 7 days, but is then driven by joint damage, low levels of inflammation, and largely neuropathic processes by day 14 (Bove *et al.,* 2003; Thakur *et al.,* 2012). MIA also causes peripheral nerve damage as early as day 3, and has been reported as detectable up to day 35 (Ivanavicius *et al.,* 2007; Thakur *et al.,* 2012; McDougall *et al.,* 2017). These characteristics make this model ideal for testing potential antinociceptive and antiinflammatory agents, as well as agents that may be beneficial in slowing or reversing OA progression.

Cannabidiol is the main non-psychoactive component of the cannabis plant (Mechoulam & Gaoni, 1965). Currently, there is an oromucosal spray (1:1 ratio CBD: Δ^9-THC) available for the treatment of multiple sclerosis spasticity and pain. Other CBD and Δ^9-THC containing compounds are promising in human musculoskeletal diseases and pain conditions and the trend towards prescribing these therapies is increasing (Lynch & Campbell, 2011; Fitzcharles *et al.,* 2016). Akin to other cannabinoid compounds, CBD has a complex signalling mechanism where it can activate and mute classical endocannabinoid pathways as well as modulate atypical cannabinoid signalling pathways such as, TRP ion channels, serotonin receptors, and other orphaned GPCRs (*e.g.* GPR18,

GPR55) (Pertwee, 2005; Russo *et al.,* 2005; Demuth & Molleman, 2006). The above pathways are known to play an integral role in modulation of pain and inflammation (Guindon & Hohmann, 2009; Schumacher, 2010; Bardin, 2011; Witkamp & Meijerink, 2014).

CBD has been explored in several preclinical disease models, whereby systemic administration of CBD has produced favourable outcomes. In the carrageenan model of paw oedema, CBD had a dose-dependent effect on thermal hyperalgesia as well as decreased PGE2 plasma levels, COX activity, and nitric oxide production in the tissues of the inflamed paw (Costa *et al.,* 2004). Hammell *et al.* (2016) showed that CBD reduced joint swelling, synovial membrane thickening, proinflammatory molecule synthesis, and immune cell infiltration in the FCA model of inflammatory arthritis. Additionally, Malfait *et al.* (2000) demonstrated that CBD suppressed development of the collagen model of RA and decreased TNF-α and interferon-γ (IFN-γ) release. While the literature suggests a promising role for CBD in relieving joint inflammation and pain, the effectiveness of CBD in OA or CBD administered locally to the joint has yet to be investigated. This may be an important step towards the discovery of cannabinoid therapies which lack centrally-mediated side effects.

The aim of the present study was to assess the effects of locally administered CBD on joint pain in animals with end-stage OA. Since it has been established that inflammatory flares can contribute to the long-term development of OA joint pain (Robinson *et al.,* 2016), the action of CBD on acute OA-associated synovitis was assessed. Furthermore, a prophylactic regimen was carried out to test the effect of early CBD treatment on the progression of chronic OA pain and joint neuropathy.

Hypotheses assessed in this study:

I.   **Local administration of CBD is antinociceptive in established OA and this antinociceptive effect is mediated through cannabinoid receptors in the joint.**

II.   **Local administration of CBD decreases acute inflammation (day 1) induced by MIA and this antiinflammatory action is mediated through cannabinoid receptors in the joint.**

III.   **Prophylactic treatment with CBD during the early inflammatory phase of the MIA model (days 0-3) will prevent the subsequent development of OA pain and peripheral nerve damage.**

5.2 Examining antinociceptive properties of locally administered CBD on MIA-induced joint pain

5.2.1 Methods

Male Wistar rats (222-337g) were deeply anaesthetised with isoflurane (2-4%; 100% oxygen at 1L/min) and MIA (3mg; 50µl saline) was injected i.artic. into the right knee joint (as described in Section 2.2.1). On day 14, the rats were separated into cohorts and were treated locally with an i.artic. injection of either CBD (100, 200, or 300µg) or vehicle (50µl). Behavioural pain was assessed at 30, 60, 120, 180, 240 min following drug administration using von Frey hair algesiometry and hindlimb incapacitance.

To determine if CBD was restricted locally to the ipsilateral knee joint, in a separate cohort on day 14, 300μg of CBD was injected into the contralateral knee joint. Behavioural pain was then assessed in the ipsilateral joint over 240 min.

5.2.2 Results

5.2.2.1 CBD attenuates referred pain in day 14 MIA knee joints

Injection of MIA into the knee produced robust secondary allodynia in the ipsilateral hindpaw 14 days after injection when compared to day 0 naïve baseline ($P<0.0001$; n=24; Figure 5.1A). Hindpaw withdrawal threshold decreased from 15.0 ± 0.0g on day 0 to 8.57 ± 0.40g by day 14 of the model.

Compared to vehicle control, low and mid-range doses of CBD (100μg, 200μg) had no effect on withdrawal threshold ($P>0.05$; n=8; Figure 5.1A). A higher dose of CBD (300μg) significantly increased hindpaw withdrawal threshold over the time course tested ($P<0.0001$; n=8; Figure 5.1A), indicating a reduction in pain. *Post hoc* analysis revealed significance at 60 min, 120 min, and 180 min. As such, all subsequent experiments were completed using the 300μg dose of CBD. The greatest improvement in hindpaw withdrawal threshold was observed between 30 min and 120 min where the threshold remined between 14.0-14.9 ± 0.92-1.15g.

5.2.2.2 Local CBD improves hindlimb weight bearing deficits in OA joints

MIA (i.artic.) produced weight bearing deficits in the ipsilateral hindlimb 14 days after injection when compared to day 0 naïve baseline ($P<0.0001$; n=24; Figure 5.1B). Hindlimb weight bearing decreased from 50.0 ± 0.52 on day 0 to 39.3 ± 1.03 by day 14.

Similar to the results of the von Frey algesiometry low and mid-range doses of CBD (100µg, 200µg) had no effect on hindlimb incapacitance compared to vehicle control (P<0.0001; n=8; Figure 5.1B). The 300µg dose of CBD, on the other hand, significantly improved hindlimb weight bearing deficits over 240 min (P<0.0001; n=8; Figure 5.1B), with 180 min and 240 min being significant time points after *post hoc* analysis. The largest improvement in weight bearing deficits was at 180 min where the CBD treated group increased to 45.2 ± 4.24 compared to vehicle treated animals which remained at 29.3 ± 2.66.

5.2.2.3 *Effects of contralateral CBD on von Frey hair algesiometry and hindlimb incapacitance*

High dose CBD (300µg) injected into the contralateral knee joint had no effect on ipsilateral hindpaw withdrawal threshold and was significantly different when compared to CBD-treated ipsilateral joints (P<0.0001; n=8-9; Figure 5.2A), indicating that CBD was acting locally in the von Frey algesiometry test. *Post hoc* analysis revealed the 30 min, 60 min, and 120 min post-drug administration as significant. Conversely, in the hindlimb weight bearing test, contralateral CBD was not statistically different from the group treated with ipsilateral CBD (P>0.05; n=8-9; Figure 5.2B).

5.3   Contribution of classical and non-classical cannabinoid receptors to the anti-nociceptive effects of CBD

5.3.1   Methods

Male Wistar rats (341-409g) 14 days post-MIA induction (3mg; 50µl saline) were separated into four cohorts. Cohorts were treated locally (s.c.) with either vehicle (50µl), the CB$_1$R antagonist, AM281 (75µg/50µl), the CB$_2$R antagonist, AM630 (75µl/50µl), or the TRPV1 receptor antagonist, SB-366791 (30µg/50µl) 10 min prior to i.artic. administration of CBD. Behavioural pain measurements were conducted at 30, 60, 120, 180, 240 min following CBD administration.

5.3.2   Results

5.3.2.1   CBD-induced antinociception is blocked by TRPV1 antagonism

In day 14 post-MIA animals, over the 240 min time course the CB$_1$R and CB$_2$R antagonists, AM281 ($P>0.05$; n=6-8; Figure 5.3A) and AM630 ($P>0.05$; n=6-8; Figure 5.3A), as well as the TRPV1 antagonist SB-366791 ($P>0.05$; n=6-8; Figure 5.3A) had no significant effect on CBD-induced antinociception. Upon conducting *post hoc* analysis, SB-366791 was significantly different at 60 min ($P<0.05$; n=6-8; Figure 5.3A). When assessing the effects of the antagonists at the 60 min time point (peak effect of CBD) the CB$_1$R antagonist AM281 ($P>0.05$; n=6-8; Figure 5.3B) and CB$_2$R antagonist AM630 ($P>0.05$; n=6-8; Figure 5.3B) still had no significant effect on CBD-induced antinociception in the von Frey algesiometry pain test. However, administration of the

TRPV1 antagonist SB-366791 significantly inhibited the antinociceptive effects of CBD (P<0.05; n=6-8; Figure 5.3B).

5.3.2.2 *CBD improvement in weight bearing unaffected by receptor antagonism*

In day 14 post-MIA animals, the CB_1R and CB_2R antagonists, AM281 and AM630, as well as the TRPV1 antagonist SB-366791 had no significant effect on the CBD-induced improvement in hindlimb incapacitance over the 240 min time course tested (P<0.05; n=6-22; Figure 5.3C) or when the 180 min time point (peak effect of CBD in this pain test) was assessed (P<0.05; n=6-22; Figure 5.3D).

5.4 Assessing the antiinflammatory effects of locally administered CBD on MIA-induced joint inflammation

5.4.1 *Methods*

Male Wistar rats (292-414g) underwent inflammation assessments 24 hr post-MIA induction (3mg; 50µl saline). Prior to obtaining inflammation measurements, the animals were anaesthetised and surgical preparation was completed, as detailed in Section 2.4.2.1. Circulating leukocytes were fluorescently stained by an i.v. injection of rhodamine 6G.

5.4.1.1   IVM

The skin overlying the ipsilateral knee joint was removed and three baseline videos were recorded (1 min each). Following baseline recordings, a 50μl bolus of warmed (37°C) CBD (300μg) or vehicle was applied topically over the exposed knee joint capsule. The following time points post-CBD administration were recorded: 5, 15, 30, 60, 120, 180 min. Leukocyte rolling and adherence were then quantified and averaged between the three videos recorded at each time point and compared to baseline values.

5.4.1.2   LASCA

All LASCA recordings followed immediately after each IVM recording throughout the duration of the experiment at 5, 15, 30, 60, 120, 180 min. Once the dead scan value was subtracted from each recording, mean perfusion was calculated at each time point. These values were then used to calculate vascular conductance and normalised for MAP differences between animals. All experimental time points and were then compared to the baseline vascular conductance.

5.4.2   Results

5.4.2.1   CBD decreases leukocyte trafficking in the knee joint microvasculature

One day after i.artic. injection of MIA, rolling leukocytes ($P<0.0001$; n=6-12; Figure 5.4A) and adherent leukocytes ($P<0.0001$; n=6-12; Figure 5.4B) were significantly increased compared to naïve animals. MIA induction caused rolling

leukocytes to increase from 5.64 ± 1.69 (naïve values) to 72.08 ± 3.65 24 hr later. Additionally, adherent leukocytes increased from 0.78 ± 0.13 (naïve values) to 5.23 ± 0.50 on day 1 post-MIA.

Topical administration of CBD significantly decreased rolling and adherent leukocytes when compared to vehicle over the 180 min time course tested ($P<0.0001$; n=6; Figure 5.4A & 5.4B). *Post hoc* analysis showed that rolling leukocytes were significantly decreased at all time points tested, where the largest decrease in rolling leukocytes occurred at 60 min with the CBD treated group decreased to 22.5 ± 3.67 compared to vehicle treated animals at 48.0 ± 1.76. For adherent leukocytes, *post hoc* analysis revealed significance at 15, 30, 120, and 180 min. The largest decrease in adherent leukocytes occurred at 15 min where the number decreased to 0.98 ± 0.45. The largest difference between treatment groups occurred at 180 min where CBD treated animals had 2.34 ± 0.64 and vehicle treated had 10.2 ± 2.09 adherent leukocytes.

5.4.2.2 CBD did not alter knee joint perfusion

One day post-i.artic. injection of MIA, knee joint perfusion significantly increased from 0.50 ± 0.06 to 3.53 ± 0.22, when compared to naïve animals ($P<0.05$; n=6-12; Figure 5.4C).

When administered topically, CBD had no effect on ipsilateral knee joint hyperaemia ($P>0.05$; n=6; Figure 5.4C). Local CBD treatment lacked any systemic effect on MAP over the 180 min time course (CBD: 68.88 ± 2.38 mmHg; VEH: 70.7 ± 2.33 mmHg).

5.5 Contribution of classical and non-classical cannabinoid receptors to the anti-rolling and anti-adherence properties of CBD

5.5.1 Methods

Inflammation was assessed in male Wistar rats (334-409g) 24 hr post-MIA induction (3mg; 50µl saline). Prior to assessing inflammation, animals underwent a surgical preparation (detailed in Section 2.4.2.1).

Following baseline IVM and LASCA recordings, a warmed (37°C) 50µl bolus of either AM281 (75µg/50µl), AM630 (75µl/50µl), SB-366791 (30µg/50µl), or vehicle was applied topically over the exposed knee joint. After 10 mins, a 50µl bolus of CBD (300µg) or vehicle was applied topically over the exposed knee joint capsule. The following time points post-CBD administration were recorded: 5, 15, 30, 60, 120, 180 min. Leukocyte rolling and adherence were then quantified and averaged between the three videos recorded at each time point and compared to baseline values. The time points of LASCA recordings followed immediately after IVM at 5, 15, 30, 60, 120, 180 min. Mean perfusion values were used to calculate vascular conductance for each time point and compared to baseline values.

5.5.2 Results

5.5.2.1 Effects of receptor antagonism on leukocyte trafficking

Over the course of 180 min, the antirolling effect of CBD was blocked by both AM630 ($P<0.0001$; n=6; Figure 5.5A) and SB-366791 ($P<0.0001$; n=6; Figure 5.5A), but

was not blocked by AM281 (P>0.05; n=6; Figure 5.5A). *Post hoc* analysis showed that SB-366791 was significantly different at all time points tested and that AM630 was significantly different at all time points tested except 120 min. When assessing the antagonists at time of peak effect of CBD (30 min) the same results are shown for AM630 (P<0.0001; n=6; Figure 5.5B), SB-366791 (P<0.0001; n=6; Figure 5.5B), and AM281 (P>0.05; n=6; Figure 5.5B). Additionally, the antiadherence effect of CBD was blocked by SB-366791 (P<0.0001; n=6; Figure 5.5C), and by AM630 (P<0.0001; n=6; Figure 5.5C), and not effected by AM281 (P>0.05; n=6; Figure 5.5C) in day 1 MIA knee joints. After *post hoc* analysis, SB-366791 blocked the antiadherence effects significantly at all time points tested except 5 min. Again, when assessing at the 30 min time point, SB-366791 (P<0.0001; n=6; Figure 5.5D) blocked the antiadherence effect of CBD, but the cannabinoid antagonists AM630 (P>0.05; n=6; Figure 5.5D) and AM281 (P>0.05; n=6; Figure 5.5D) did not have any effect.

5.5.2.2 *Effects of receptor antagonism on knee joint perfusion*

Knee joint hyperaemia was significantly increased by SB-366791 (P<0.001; n=6; Figure 5.5E) and AM281 (P<0.05; n=6; Figure 5.5E), but was unaltered by AM630 (P>0.05; n=6; Figure 5.5E) over the course of 180 min. *Post hoc* analysis revealed that SB-366791 (P<0.01; n=6; Figure 5.5E) and AM281 (P<0.05; n=6; Figure 5.5E) augmented joint hyperaemia at 120 min. At the 30 min time point, joint hyperaemia was unaffected by any of the antagonists tested (P>0.05; n=6; Figure 5.5F).

5.6   Effects of prophylactic CBD on the development of MIA-induced joint pain and peripheral nerve damage

5.6.1 Methods

Results from the previous section showed that CBD (300µg) was capable of ablating the acute inflammatory phase (day 1) of the MIA model. Previous studies have shown a link between inflammatory flares and disease progression and development of joint pain. The aim of this portion of the study was to determine if blocking the inflammatory flare (over the first 3 days) could prevent the subsequent development of OA pain and peripheral nerve damage in the MIA model. For this study, male Wistar rats (282-338g) underwent baseline behavioural pain testing and then were divided into two separate treatment cohorts:
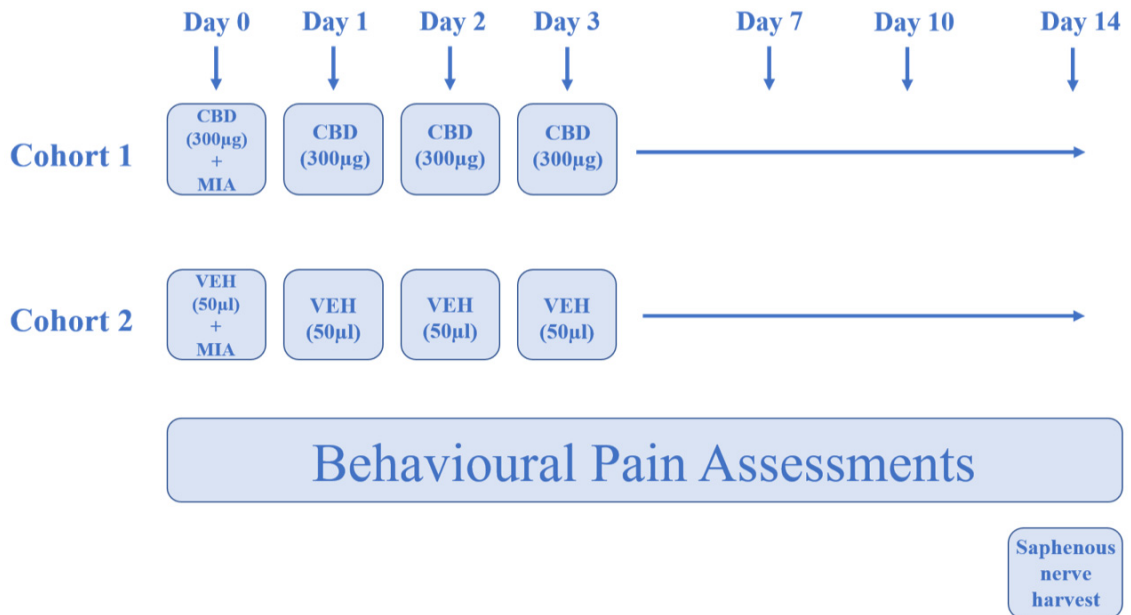
On day 0, animals were deeply anaesthetised (2-4% isoflurane; 100% oxygen at 1L/min) and CBD (300µg) or vehicle (50µl) was injected s.c. over the ipsilateral knee

joint. After 30 min, animals were anaesthetised again and MIA (3mg; 50µl saline) was injected i.artic. into the ipsilateral knee joint. The animals then received either treatment with CBD or vehicle for the subsequent three days of MIA development. Knee joint diameter was measured and pain testing was conducted on days 0, 1, 2, 3, 7, 10, 14 of MIA model development. At all time points, each rat underwent von Frey hair algesiometry testing and was then placed in the hindlimb incapacitance apparatus for 3 min. On day 14, after behavioural pain assessments were complete, all animals were sacrificed and a section of the saphenous nerve, proximal to the ipsilateral knee joint, was excised for histological analysis of nerve myelination.

5.6.2 Results

5.6.2.1 Early CBD treatment prevented the development of referred pain

Prophylactic treatment of MIA-injected knee joints (on days 0-3 of MIA) with CBD significantly prevented the development of MIA-induced secondary allodynia during the acute and chronic pain phase of OA model development (P<0.0001; n=8; Figure 5.6A) when compared to vehicle treated animals. *Post hoc* analysis revealed significance on days 2, 3, 7, and 14 of MIA development. CBD treatment prevented the complete MIA-associated decrease in withdrawal threshold from baseline 14.94 ± 0.06 on day 0 to 9.27 ± 1.05 on day 1, 7.73 ± 0.86 on day 2, and 7.34 ± 1.07 on day 3. The CBD treated group had withdrawal threshold levels of 12.6 ± 1.14 on day 1, 13.3 ± 1.05 on day 2, and 11.3 ± 1.15 on day 3. The CBD-induced antinociception remained out to

day 14 where the CBD group had a withdrawal threshold level of 13.6 ± 0.59 compared to the vehicle treated group level of 8.70 ± 1.19.

5.6.2.2 *Prophylactic CBD treatment did not alter hindlimb incapacitance*

In contrast with the results of von Frey hair algesiometry, early treatment with CBD had no effect on hindlimb incapacitance ($P>0.05$; n=8; Figure 5.6B), when compared to vehicle-treated animals.

5.6.2.3 *Knee joint diameter remained unaltered by CBD treatment*

Although CBD produced anti-inflammatory effects on day 1 MIA, early treatment with CBD had no effect on knee joint diameter ($P>0.05$; n=8; Figure 5.6C) when compared to vehicle treated counterparts.

5.6.2.4 *Prophylactic CBD prevented MIA-induced peripheral nerve damage*

Early treatment of OA joints with CBD during the inflammatory phase of MIA inhibited saphenous nerve demyelination on day 14, compared to vehicle treatment ($P<0.05$; n=6-8; Figure 5.7C).

5.7   Chapter Summary

5.7.1 Local application of CBD blocks MIA-induced OA pain

The results presented in section 5.2 suggest that CBD is able to alleviate OA joint pain. When applied locally to an MIA-injected knee joint on day 14, the highest dose of CBD (300µg) attenuated pain. However, the lower doses of CBD tested (100µg, 200µg) had no effect on pain behaviour.

The antinociceptive effect of CBD seen in the von Frey hair algesiometry test was blocked by administration of the TRPV1 antagonist, SB-366791, but not by the CB_1R or CB_2R antagonists AM281 and AM630, respectively. None of the antagonists tested blocked the antinociceptive effect of CBD seen in the dynamic weight bearing test.

To ensure that CBD was acting locally in the joint, 300µg was injected into the contralateral knee and pain testing was carried out on the ipsilateral joint. When administered in this manner, CBD did not improve ipsilateral secondary mechanical allodynia confirming that the antinociceptive effect of CBD was localised to the treated knee. The dynamic weight bearing data were inconclusive for this experiment.

5.7.2 Topical application of CBD decreases MIA-induced inflammation

On day 1 post-MIA injection, CBD applied topically to the knee joint significantly decreased leukocyte trafficking (rolling and adherence) and hyperaemia over the course of 180 min. The TRPV1 antagonist, SB-366791, was able to block the antiinflammatory effects of CBD on leukocyte trafficking. The CB_2R antagonist, AM630,

blocked the antirolling effects of CBD. The CB_1R antagonist, AM281, and the TRPV1

antagonists SB-366791 increase knee joint perfusion over the 180 min time course.

5.7.3   *Prophylactic administration of CBD prevents the development of MIA-induced joint pain and peripheral nerve damage*

The prophylactic treatment schedule of CBD (30 min prior to and for 3 days after

MIA injection) significantly prevented the development of secondary mechanical

allodynia and the demyelination of saphenous nerve fibres, but had no effect on the

development of weight bearing deficits or knee joint diameter by day 14.

Table 5.1: Chapter summary

	Cannabidiol (CBD)
PAIN: Day 14 MIA	**Dose-dependently decreased pain (mediated in part by TRPV1)**
Von Frey	Improved WT
DWB	Improved WB
INFLAMMATION: Day 1 MIA	**Decreased inflammation on day 1 MIA**
Rolling Leukocytes	Decreased (mediated in part by TRPV1 & CB_2R)
Adherent Leukocytes	Decreased (mediated in part by TRPV1)
Joint Perfusion	No effect (TRPV1 & CB_1R antagonists caused increase)
PROPHYLACTIC STUDY:	**Prevented development of pain and peripheral nerve damage**
Von Frey	Prevented decrease in WT
DWB	No change (mirrored VEH treated animals)
Knee joint diameter	No change (mirrored VEH treated animals)
Peripheral nerve damage (G-ratio)	CBD treated animals had lower G-ratio value

CBD, cannabidiol; WB, weight bearing; WT, withdrawal threshold

5.8   Figures
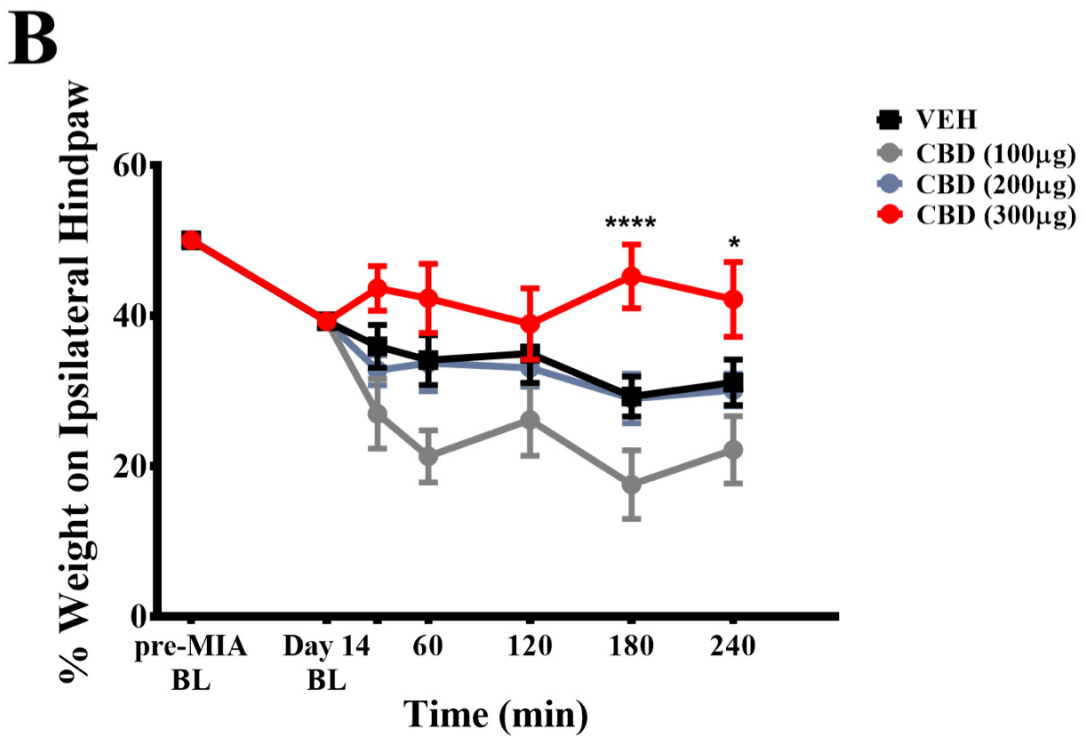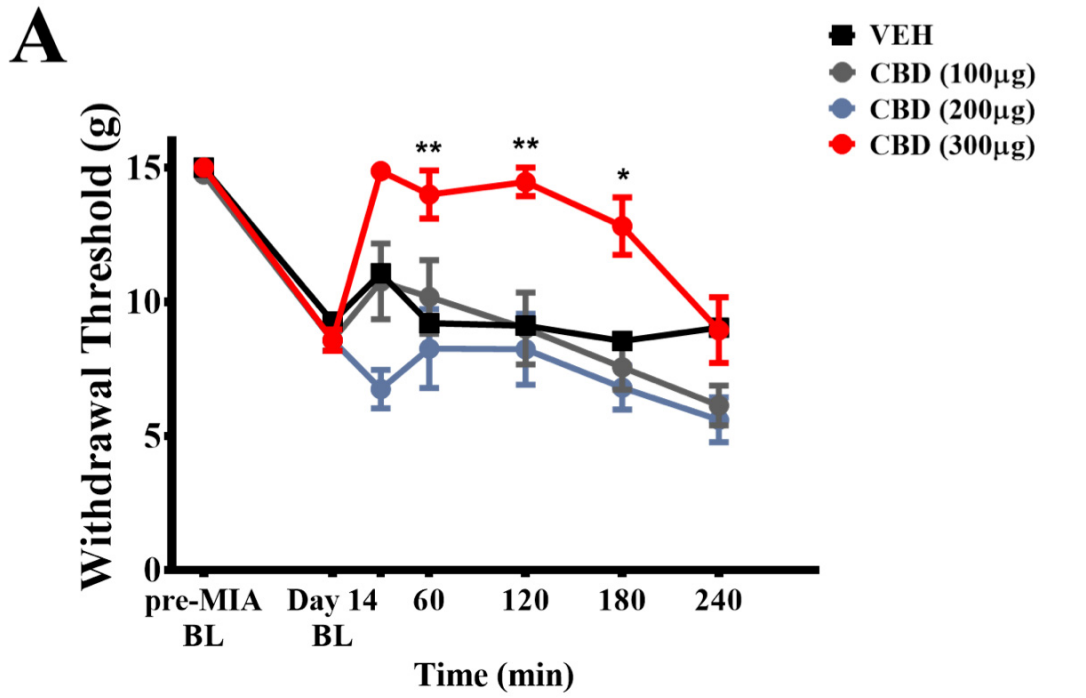
Figure 5.1 Dose-dependent effect of locally administered CBD on behavioural pain in OA. Injection of MIA (i.artic.) produced secondary allodynia and weight bearing deficits in the ipsilateral hindpaw and hindlimb 14 days post-induction (****P<0.0001; 1-way ANOVA with Dunnett *post hoc* test; n=24). Varying doses of CBD (100, 200, 300µg i.artic.) were administered at baseline. CBD improved hindpaw withdrawal threshold **(A)** and hindlimb weight bearing **(B)** in a dose-dependent manner, over 240 min (****P<0.0001; 2-way ANOVA with Bonferroni *post hoc* test; n=8). Data are mean values ± SEM. ANOVA, analysis of variance; BL, baseline, CBD; cannabidiol; MIA, sodium monoiodoacetate; OA, osteoarthritis; VEH, vehicle. (****P<0.0001; **P<0.01, *P<0.05). (Philpott *et al.,* 2017).

A

Withdrawal Threshold (g)

VEH
CBD (300μg)
CONTRA CBD (300μg)

**** *** ****

Time (min)

pre-MIA BL, Day 14 BL, 60, 120, 180, 240

B

% Weight on Ipsilateral Hindpaw

VEH
CBD (300μg)
CONTRA CBD (300μg)

Time (min)

pre-MIA BL, Day 14 BL, 60, 120, 180, 240
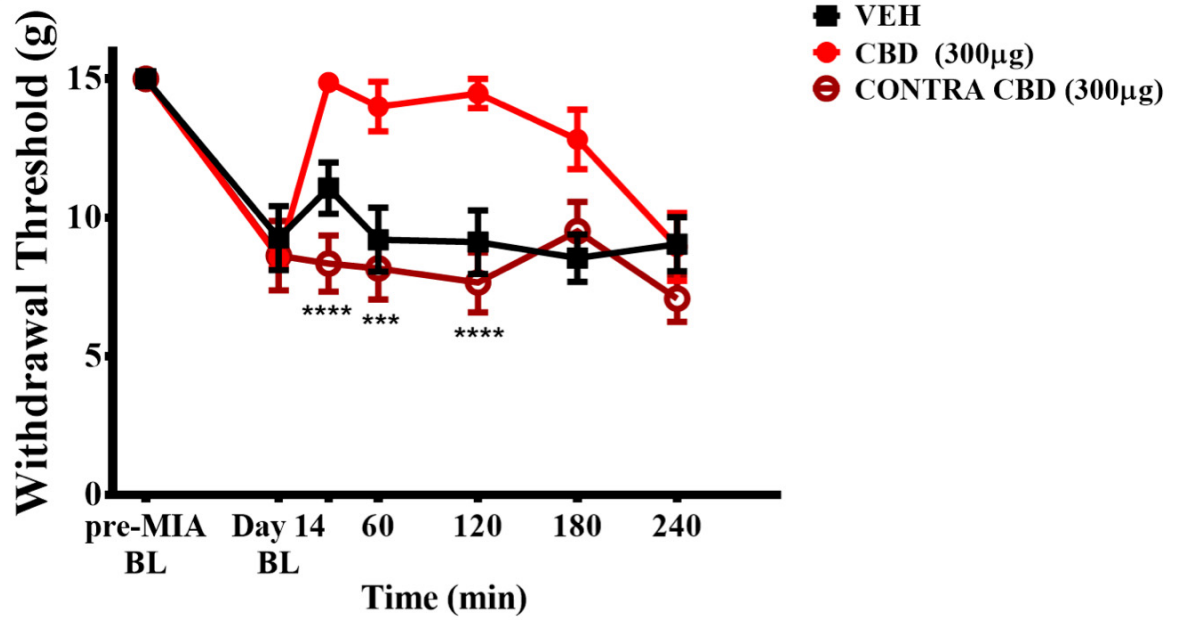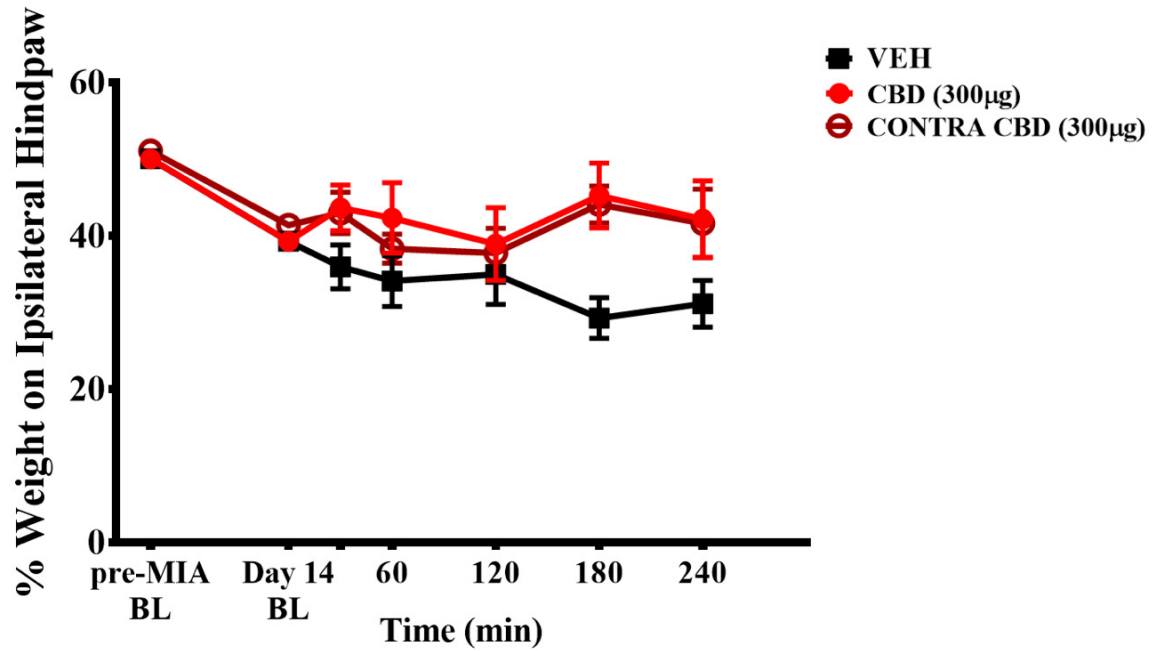
Figure 5.2 Effect of contralaterally-administered CBD on ipsilateral joint pain. The improvement in hindpaw withdrawal threshold with ipsilaterally-administered CBD was not observed in this experiment when CBD (300μg i.artic.) was administered into the contralateral knee joint **(A)** over 240 min. Contralateral CBD did not have a significantly effect on hindlimb weight bearing **(B)** when compared with ipsilaterally-administered CBD. (****$P<0.0001$; 2-way ANOVA with Bonferroni *post hoc* test; n=8-9). Data are mean values ± SEM. ANOVA, analysis of variance; BL, baseline; CBD, cannabidiol; CONTRA, contralateral; MIA, sodium monoiodoacetate; VEH, vehicle. (****$P<0.0001$; ***$P<0.001$). (Philpott *et al.,* 2017).

A1

A2

A3
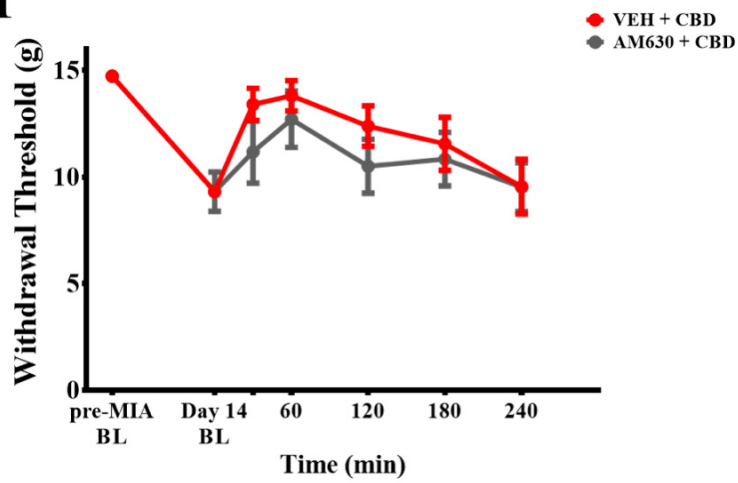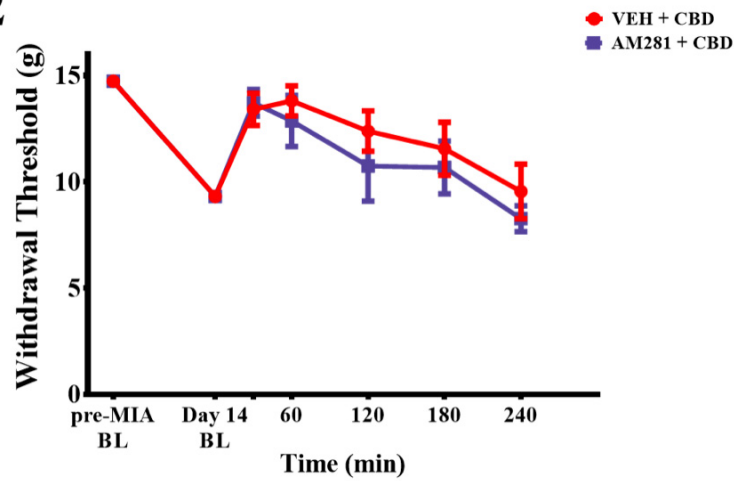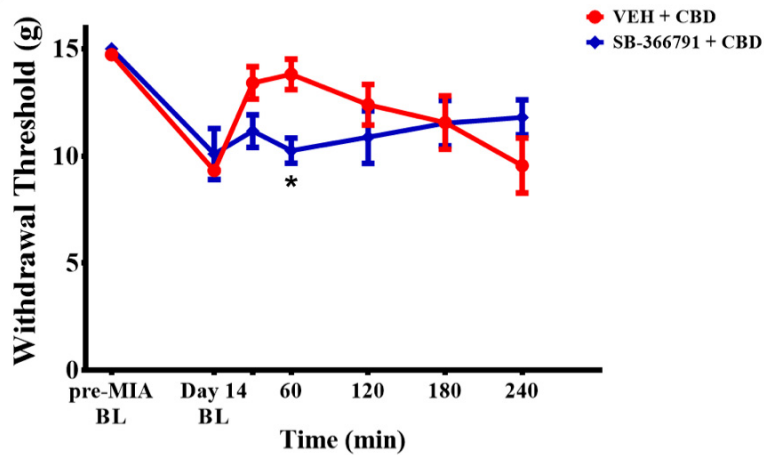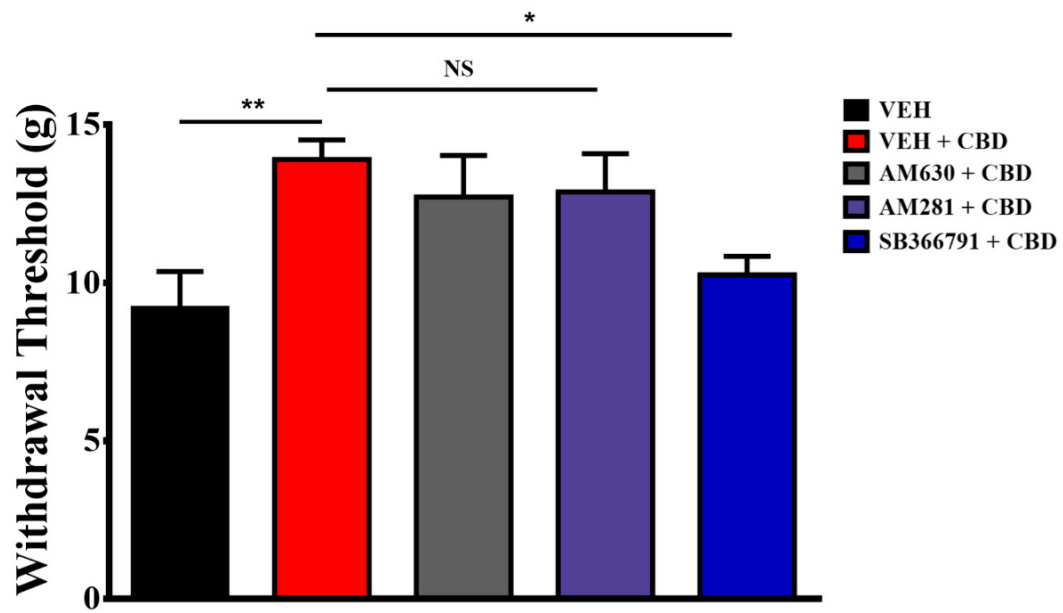
C1
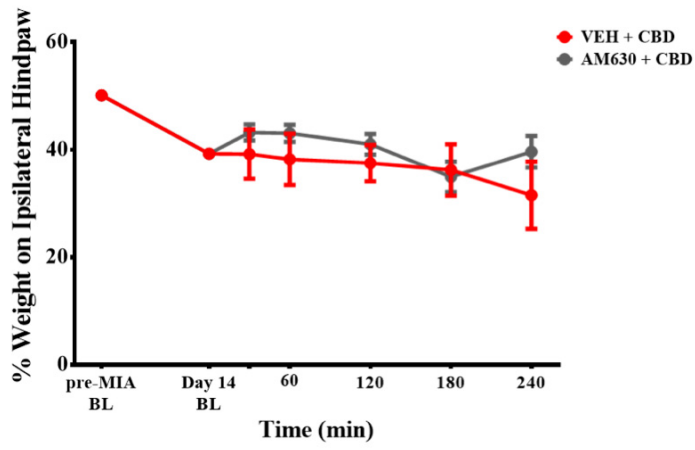
C2
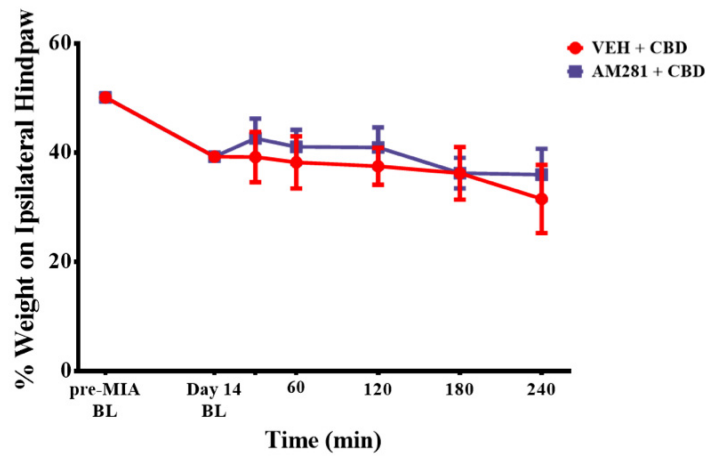
C3
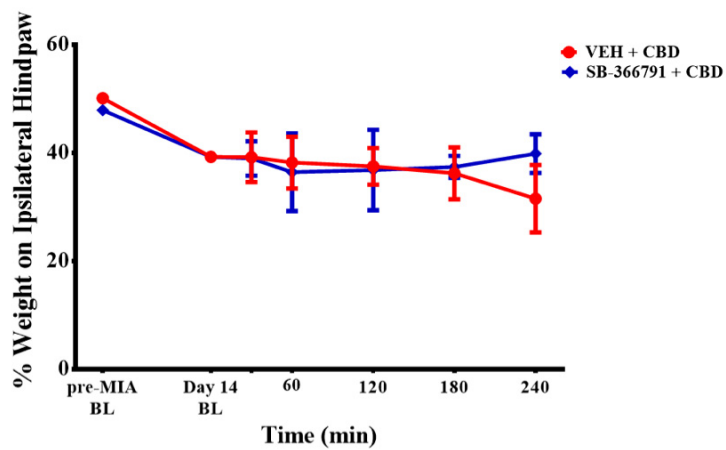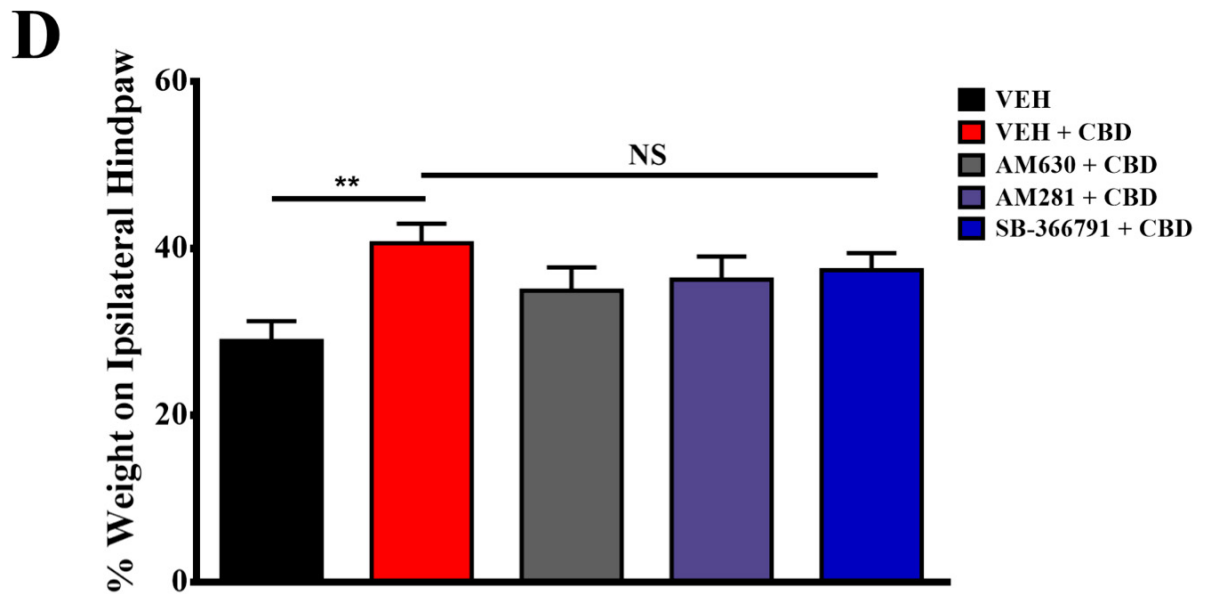
Figure 5.3 Contribution of classical cannabinoid and non-cannabinoid receptors to the antinociceptive action of CBD. Increases induced by CBD in both hindpaw withdrawal threshold **(A1-A3)** and hindlimb weight bearing **(C1-C3)** were unaltered following local administration of the CB_1R antagonist AM281 (75µg), the CB_2R antagonist AM630 (75µg), or the TRPV1 antagonist SB-366791 (30µg) over a 240 min time course ($P>0.05$; 2-way ANOVA with Bonferroni *post hoc* test; n=6-8). *Post hoc* analysis showed that SB-366791 significantly blocks the effects of CBD at 60 min. At 60 min, hindpaw withdrawal threshold **(B)** was reduced compared to control following administration of TRPV1 antagonist SB-366791, but hindlimb weight bearing **(D)** was unaltered (*$P<0.05$; 1-way ANOVA with Fisher's LSD *post hoc* test; n=6-8). Data are mean values ± SEM. ANOVA, analysis of variance; CBD, cannabidiol; MIA, sodium monoiodoacetate; VEH, vehicle. (****$P<0.0001$; ***$P<0.001$, **$P<0.01$, *$P<0.05$). (Philpott *et al.,* 2017).

A

Rolling Leukocytes/min

○ NAIVE
■ VEH
● CBD (300μg)

** *** **** **** **** ***

NAIVE BL 5 15 30 60 120 180
Time (min)

B

Adherent Leukocytes/100 μm

○ NAIVE
■ VEH
● CBD (300μg)

** * ** ***

NAIVE BL 5 15 30 60 120 180
Time (min)

C

Vascular Conductance

○ NAIVE
■ VEH
● CBD (300μg)

NAIVE BL 5 15 30 60 120 180
Time (min)
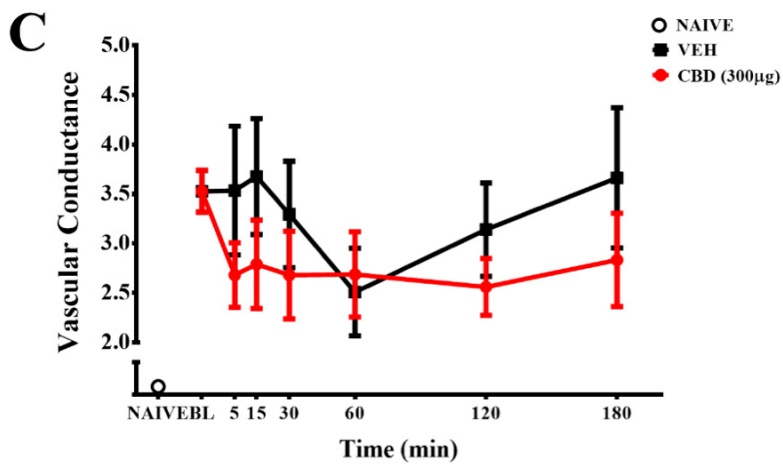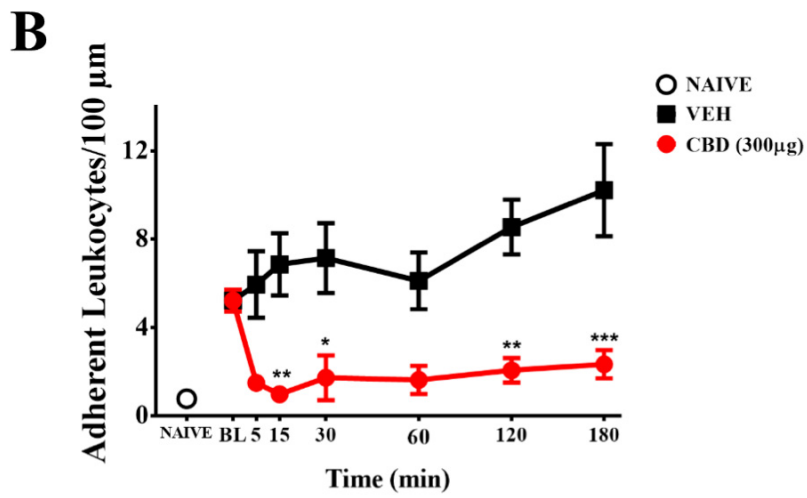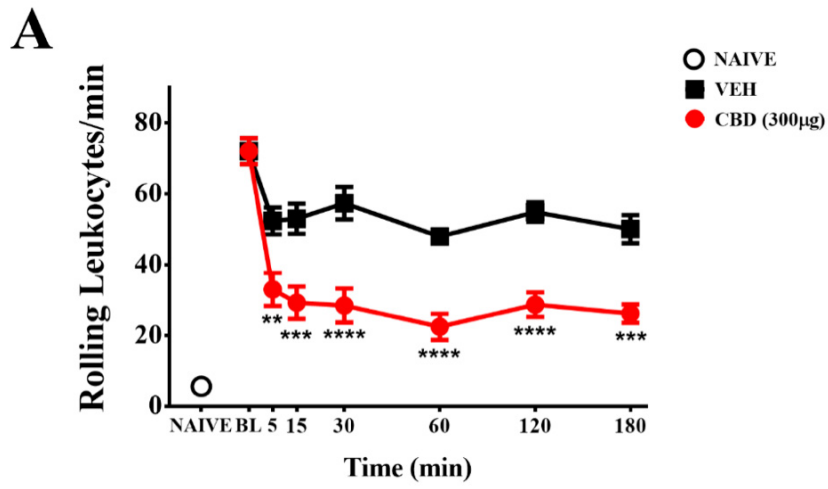
Figure 5.4 CBD has antiinflammatory properties on day 1 MIA-induced inflammation. Injection of MIA significantly increased rolling **(A)** and adherent **(B)** leukocytes, and caused synovial hyperaemia **(C)** when compared to naïve controls (****$P<0.0001$, *$P<0.05$; student's t-test; n=6-12). After topical administration of CBD (300µg), leukocyte rolling **(A)** and adherence **(B)** were significantly decreased when compared to vehicle. CBD however, did not alter synovial hyperaemia **(C)**. (****$P<0.0001$, ***$P<0.001$, **$P<0.01$, *$P<0.05$; 2-way ANOVA with Bonferroni *post hoc* test; n=6). Data are mean values ± SEM. ANOVA, analysis of variance; BL, baseline; CBD, cannabidiol; MIA, sodium monoiodoacetate; VEH, vehicle. (****$P<0.0001$; ***$P<0.001$, **$P<0.01$, *$P<0.05$). (Philpott *et al.,* 2017).

C1

Adherent Leukocytes/100 μm

○ NAIVE
● CBD (300μg)
● AM630 + CBD

Time (min)

C2

Adherent Leukocytes/100 μm

○ NAIVE
● CBD (300μg)
■ AM281 + CBD

Time (min)

C3

Adherent Leukocytes/100 μm

○ NAIVE
● CBD (300μg)
◆ SB366791 + CBD

Time (min)

E1

E2

E3
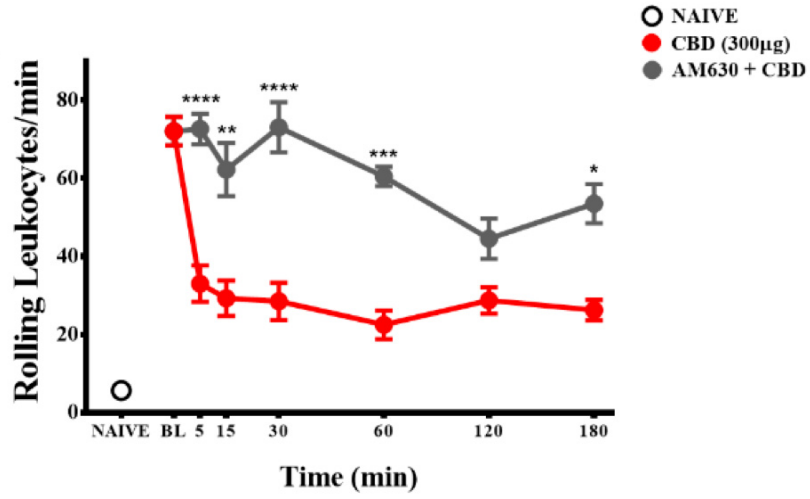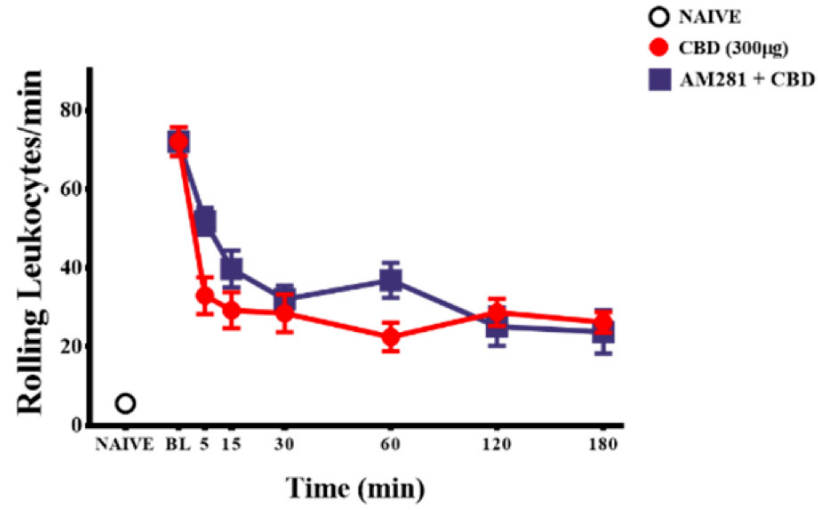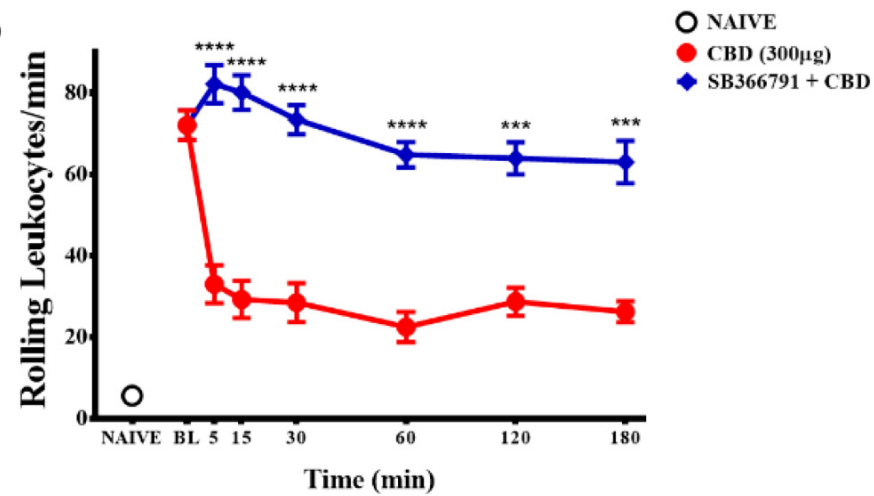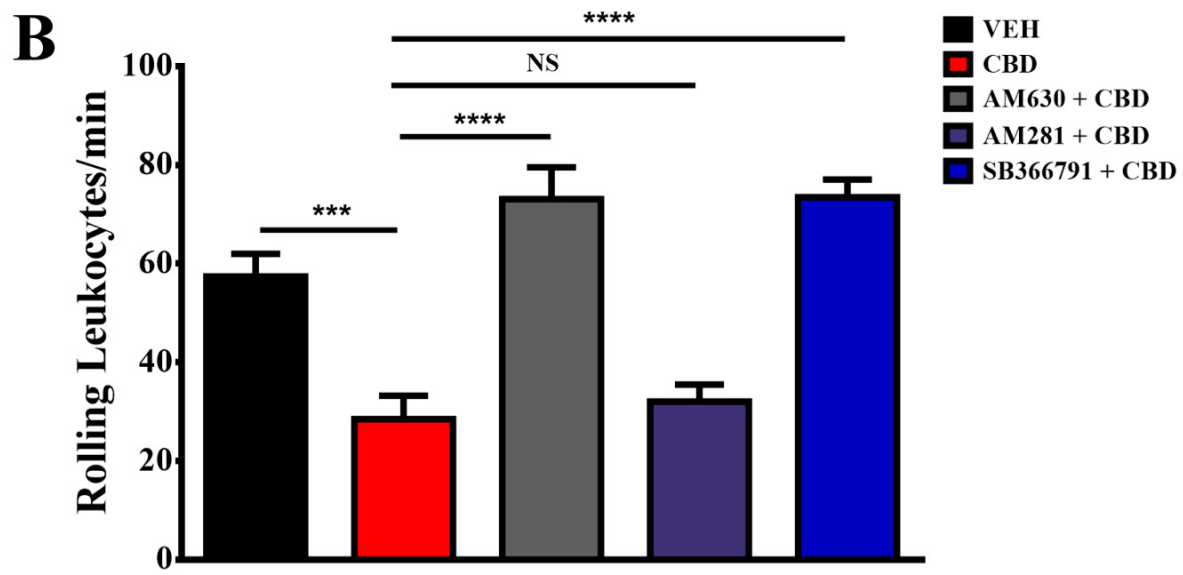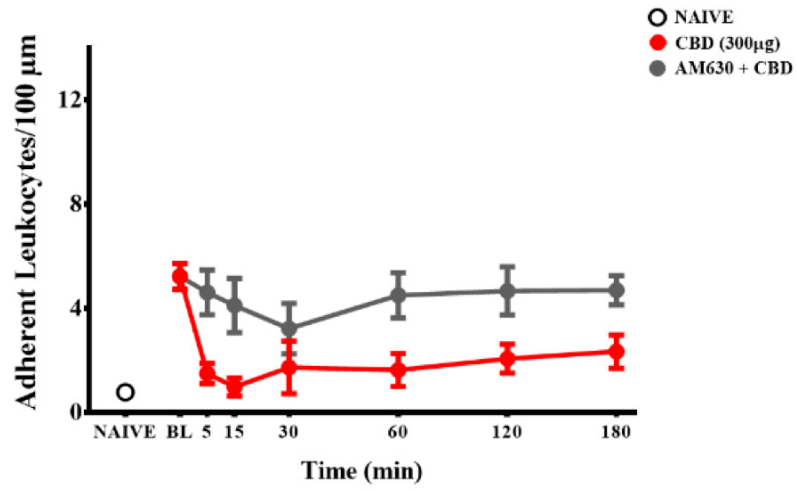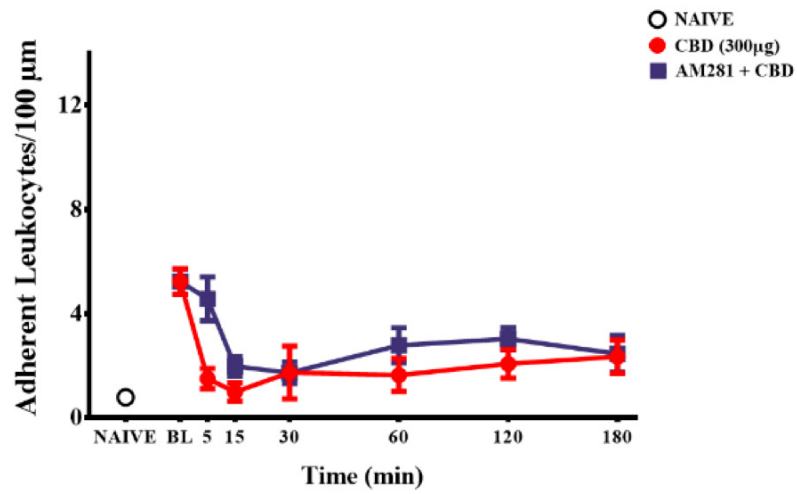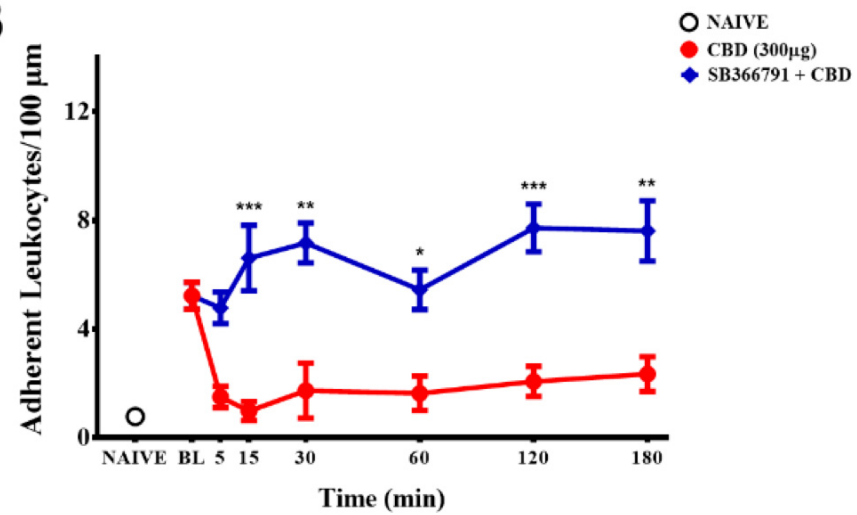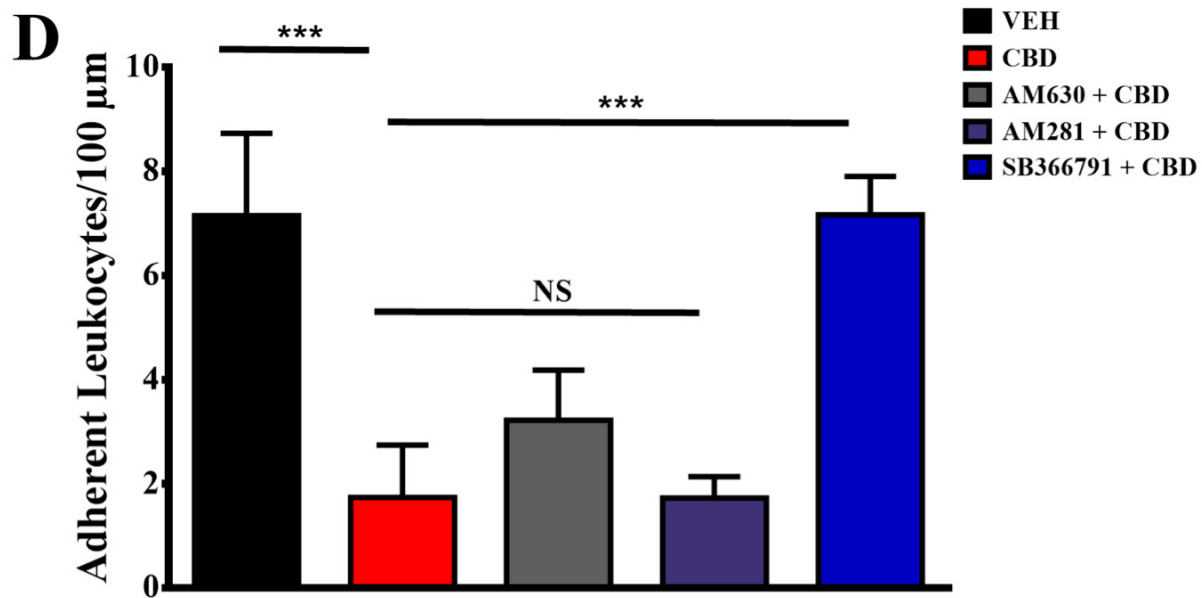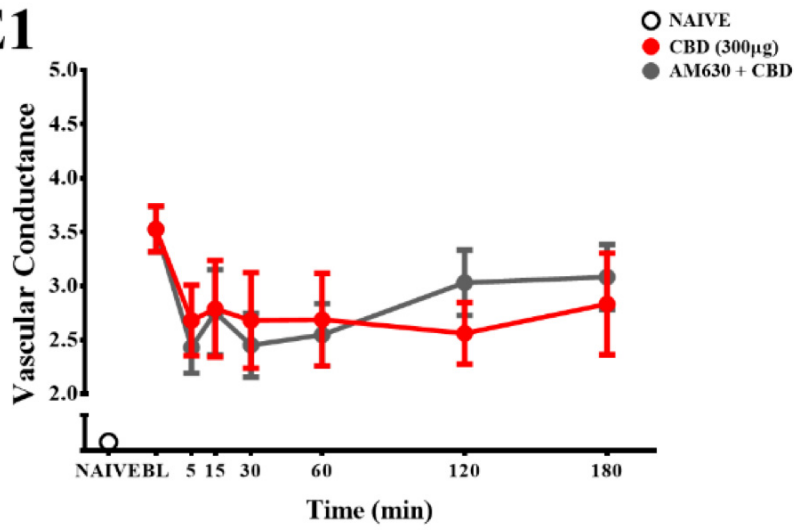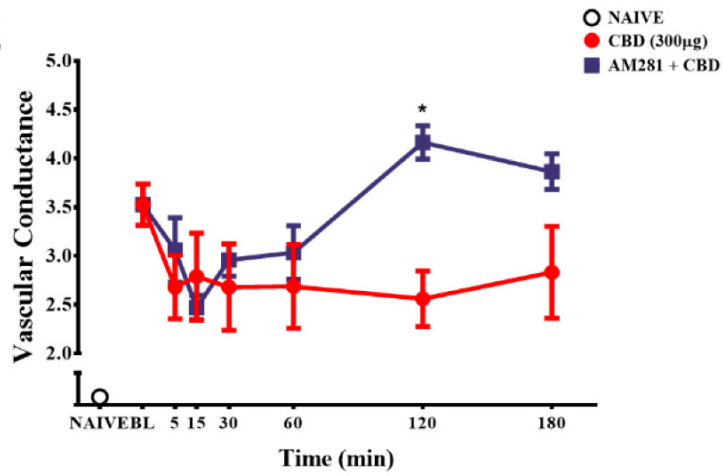
123
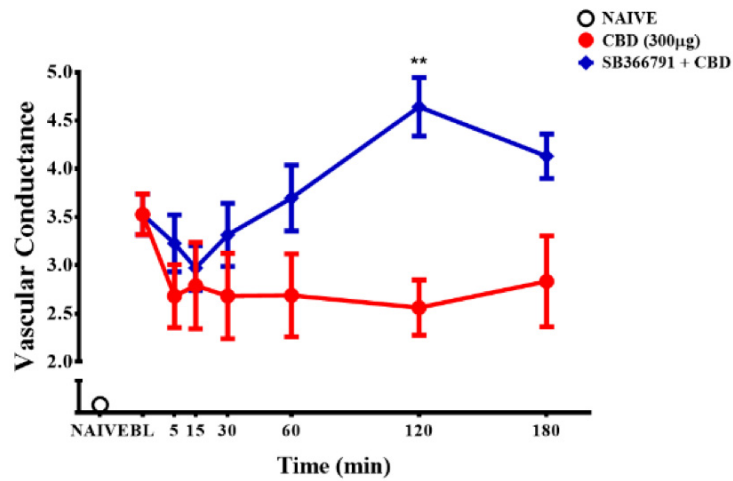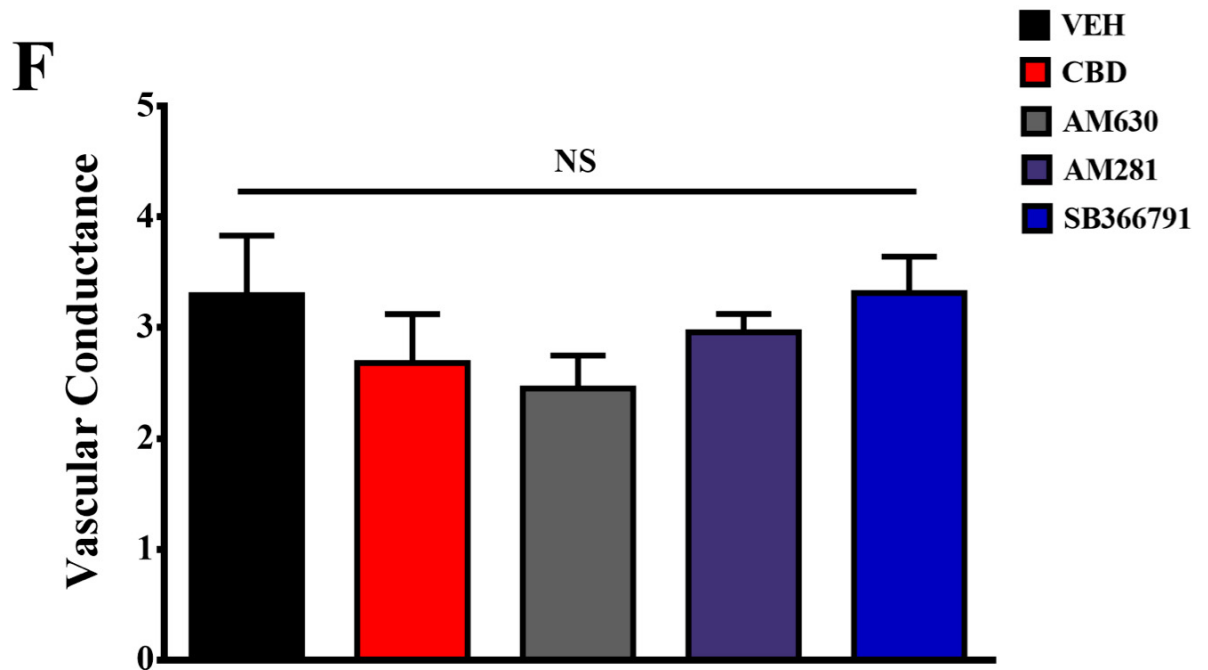
Figure 5.5 Contribution of classical cannabinoid and non-cannabinoid receptors to the antiinflammatory effects of CBD. The antirolling effect of CBD was blocked over the 180 min time course by the CB_2R antagonist AM630 and the TRPV1 receptor antagonist SB-366791, but not blocked by the CB_1R antagonist AM281 (****$P<0.0001$; 2-way ANOVA with Bonferroni *post hoc* test; n=6) **(A1-A3)**. Over the course of 180 min, the CB_2R antagonist AM630 and the TRPV1 receptor antagonist SB-366791 significantly blocked the antiadherence effect of CBD (****$P<0.0001$; 2-way ANOVA with Bonferroni *post hoc* test; n=6), but not blocked by CB_1R antagonist AM281 **(C1-C3)**. However, SB-366791 and AM281 caused a significant increase in vascular conductance when compared to CBD treated animals (***$P<0.001$, *$P<0.05$; 2-way ANOVA with Bonferroni *post hoc* test; n=6) **(E1-E3)**. The antirolling effect of CBD at 30 min was blocked by AM630 (75µg) and SB-366791 (30µg), but not by AM281 (75µg) **(B)**. The antiadherence effect of CBD in day 1 MIA joints was blocked by SB-

124

366791 only **(D)**. At the 30 min time point, vascular conductance was unaltered by any of the antagonists tested **(F)**. (****P<0.0001, ***P<0.001; 1-way ANOVA with Fisher's LSD *post hoc* test; n=6). Data are mean values ± SEM. ANOVA, analysis of variance; BL, baseline; CBD, cannabidiol; LSD, least significant difference; MIA, sodium monoiodoacetate; NS, not significant; VEH, vehicle. (****P<0.0001; ***P<0.001, **P<0.01, *P<0.05). (Philpott *et al.,* 2017).
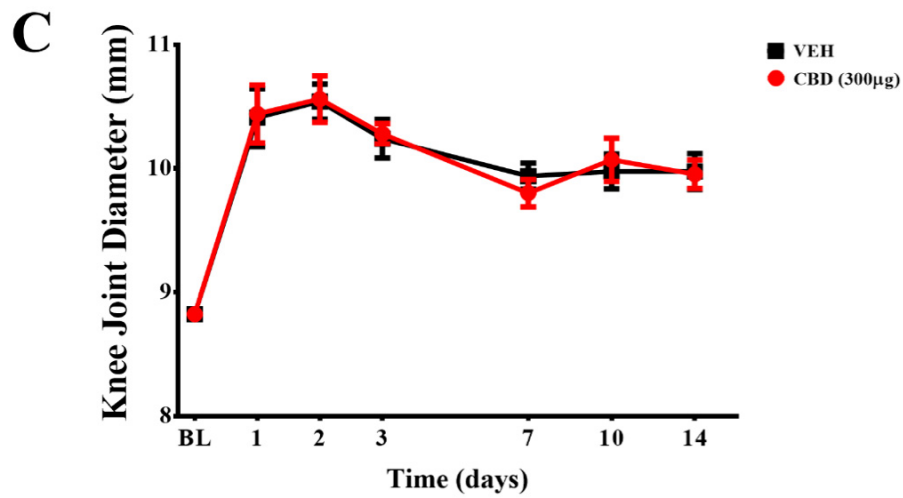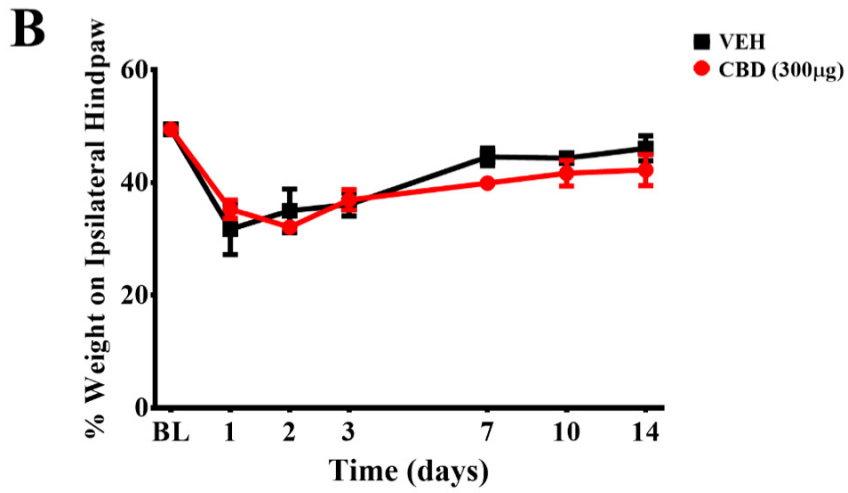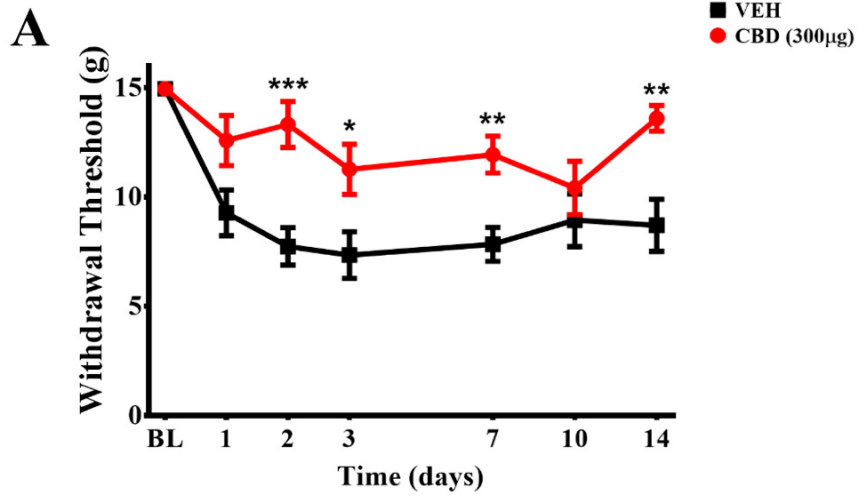
Figure 5.6 Early administration of CBD administration prevents pain development over 14 days post-MIA injection. Prophylactically treating MIA knee joints with CBD (300μg; s.c. on days 0-3) significantly improved hindpaw withdrawal threshold over the 14-day development of the OA model when compared to vehicle treated animals **(A)** (****$P<0.0001$; 2-way ANOVA with Bonferroni *post hoc* test; n=8). Early treatment with CBD had no significant effect on hindlimb weight bearing **(B)** or knee joint diameter throughout MIA development ($P>0.05$; 2-way ANOVA with Bonferroni *post hoc* test; n=8). Data are mean values ± SEM. ANOVA, analysis of variance; BL, baseline; CBD, cannabidiol; MIA, sodium monoiodoacetate; OA, osteoarthritis; VEH, vehicle. (****$P<0.0001$; ***$P<0.001$, **$P<0.01$, *$P<0.05$). (Philpott *et al.,* 2017).

A VEH

B CBD

C

G-ratio

VEH
CBD (300μg)

*
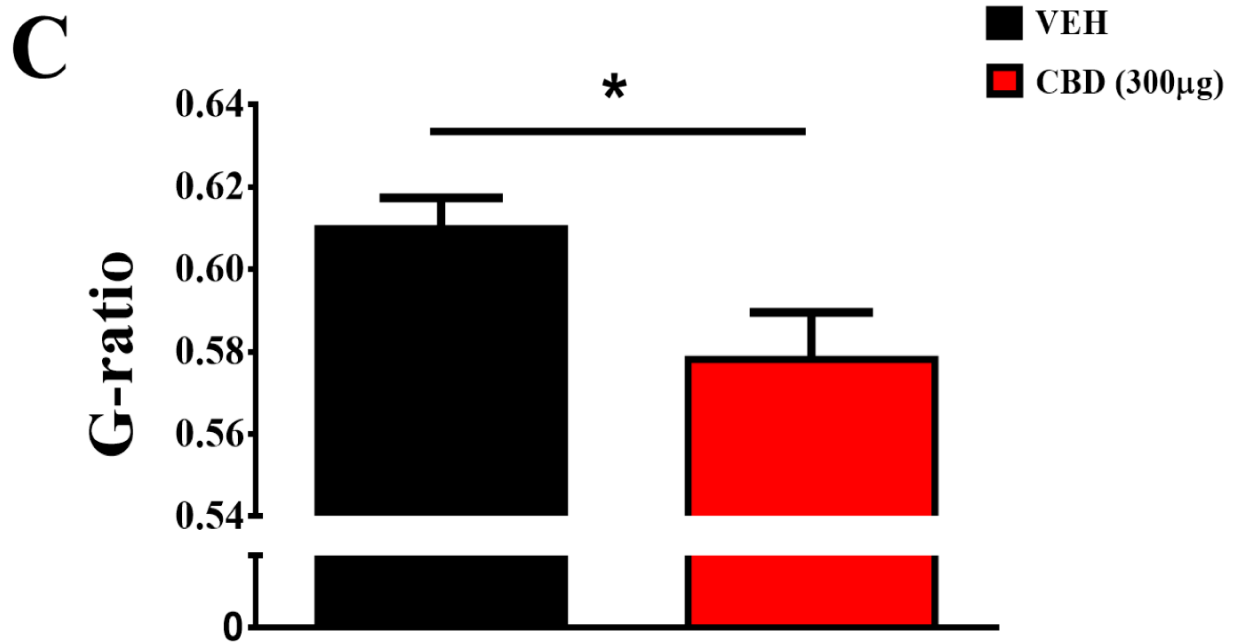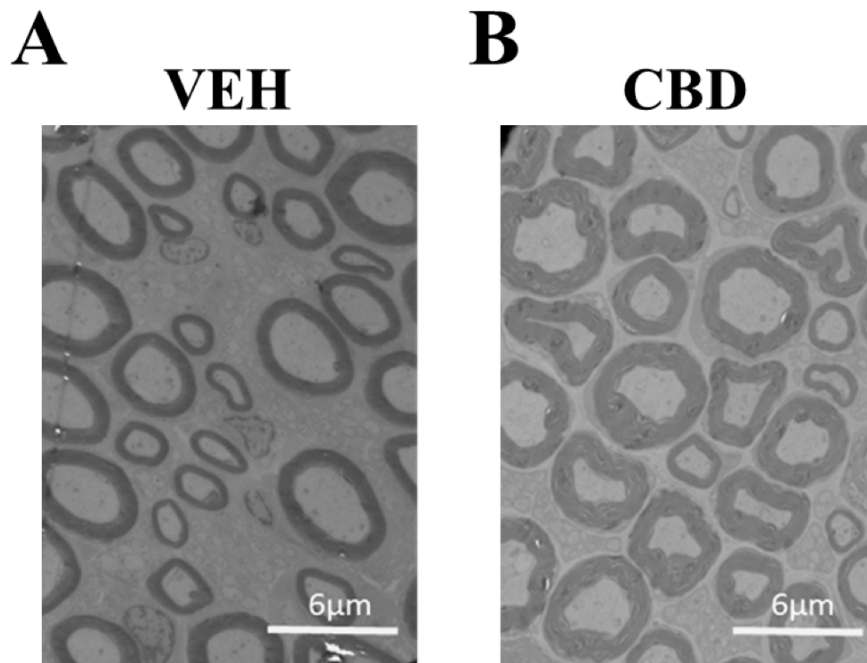
Figure 5.7 Early treatment with CBD reduces knee joint nerve demyelination in MIA-induced OA. Representative electron micrographs of saphenous nerve sections taken on day 14 from MIA knee joints treated with vehicle **(A)** or CBD (300μg; s.c. on days 0-3) **(B)**. Quantification of G-ratio calculations showing that MIA-induced axonal demyelination is prevented by CBD treatment **(C)**. Scale bar is 6μm. (*$P<0.05$; student's t-test; n=6-8). Data are means ± SEM. CBD, cannabidiol; MIA, sodium monoiodoacetate; OA, osteoarthritis; VEH, vehicle. (Philpott *et al.,* 2017).

Chapter 6: Discussion

Pain and joint damage are poorly managed in many OA patients because of the complex nature of the disease. Injection of MIA into the knee joint of rats produces a robust monoarthritis that recapitulates many aspects of human OA; these include joint pain, inflammation, and peripheral nerve damage. The ECS has been implicated as a beneficial therapeutic in regulating pain and inflammation in many pathological states and an active ECS has been identified in arthritic joints. The results presented in this project validate the role of inflammation in OA pathogenesis and pain, and highlight a positive role of the ECS. This study used three distinct approaches of targeting the ECS (endocannabinoid, synthetocannabinoid, and phytocannabinoid) to produce beneficial effects on OA-associated inflammation and pain.

6.1 Effects of using a MAGL inhibitor to modulate the ECS in MIA-induced pain and inflammation

On day 14 of the MIA model, local application of KML29 improved hindpaw withdrawal threshold; these results corroborate other studies focused on the role of inhibiting MAGL for the treatment of pain (Ghosh *et al.,* 2013; Hernandez-Torres *et al.,* 2014; Ignatowska-Jankowska *et al.,* 2014; Burston *et al.,* 2016). The significant improvement in paw withdrawal threshold by KML29 is indicative of a reduction in secondary allodynia or referred pain. Conversely, KML29 did not improve hindlimb incapacitance, meaning it was not effective at altering non-evoked pain. Our findings suggest that KML29 has varied actions on different aspects of the pain pathway and may

specifically be acting to combat MIA-induced central sensitisation. This study is the first to assess the antinociceptive effects of a MAGL inhibitor administered locally in to the joint. Other studies conducted previously have shown promising results using systemic administration of MAGL inhibitors (Ghosh *et al.,* 2013; Hernandez-Torres *et al.,* 2014; Ignatowska-Jankowska *et al.,* 2014; Burston *et al.,* 2016). A study using MJN110 (MAGL inhibitor) systemically, demonstrated a reduction in referred pain, as well as an improvement in weight bearing deficits, in the MIA model of OA (Burston *et al.,* 2016). These pain-attenuating effects were blocked by both CB_1R and CB_2R antagonists (Burston *et al.,* 2016), corroborating the results presented here and elsewhere (Ghosh *et al.,* 2013). The antinociceptive effect of KML29 has also been demonstrated in the carrageenan-induced model of paw oedema as well as in the sciatic nerve chronic constriction model of neuropathic pain (Ignatowska-Jankowska *et al.,* 2014). These antiinflammatory and antinociceptive actions were shown to be mitigated by both CB_1R and CB_2R antagonism (Ignatowska-Jankowska *et al.,* 2014). There exists a variety of MAGL inhibiting compounds that have been investigated to date. These compounds have produced results in several models of pain and inflammation (Ghosh *et al.,* 2013; Hernandez-Torres *et al.,* 2014; Ignatowska-Jankowska *et al.,* 2014; Burston *et al.,* 2016) that both corroborate and contrast the results presented in this study. Most of the studies mentioned here used systemic administration of a MAGL inhibitor in a variety of pain paradigms; however, in our study KML29 was administered locally in a specific model of OA, which could explain why mixed results were obtained regarding the antinociceptive effects of KML29. A limitation of many MAGL inhibitors is that tolerance develops rapidly when administered chronically at high doses (Ghosh *et al.,* 2013; Ignatowska-

Jankowska *et al.,* 2014; Burston *et al.,* 2016). Additionally, these compounds have been shown to block MAGL activity with different affinities in different species (*e.g.* rat versus mouse) (Chang *et al.,* 2012). Ghosh *et al.* (2013) showed that JZL184 produced antinociceptive and antiinflammatory actions, and these effects diminished after repeated treatment with high systemic doses. Conversely, repeated low dose injections had sustained efficacy (Ghosh *et al.,* 2013). Additionally, in the MIA model of OA, tolerance developed with repeated high dose administration of MJN110 over 7 days, whereas repeated low doses produced sustained antinociception without tolerance (Burston *et al.,* 2016). These MAGL inhibitors fall under the classification of irreversible inhibitors, which is likely the reason they cause tolerance. In the hopes of avoiding the development of tolerance, a reversible MAGL inhibitor (compound 21), which does not permanently block MAGL, was developed (Hernandez-Torres *et al.,* 2014). Compound 21 given systemically in a mouse model of MS (experimental autoimmune encephalomyelitis: EAE), ameliorated disease severity while avoiding cannabinoid-associated side effects (Hernandez-Torres *et al.,* 2014). Additionally, spinal histology showed that compound 21 decreased leukocyte infiltration, microglial activation, prevented axonal damage, and partially restored myelin morphology (Hernandez-Torres *et al.,* 2014). Whether compound 21 could improve OA pain and neuropathy warrants further inquiry.

The results presented here show that topical application of KML29 had modest antiinflammatory effects in OA knee joints. Leukocyte adherence was significantly decreased, however KML29 did not alter leukocyte rolling or knee joint hyperaemia. In other studies using the MIA model of OA, repeated dosing of MJN110 did not alter synovial thickening scores, or cartilage damage (Burston *et al.,* 2016). These findings

suggest that inhibiting MAGL may not be the most effective way of combatting OA inflammation or disease progression.

Since there are many pathways involved in cannabinoid signalling, combination therapies have become an attractive treatment strategy. Inhibition of another endocannabinoid catabolic enzyme FAAH, has shown great preclinical potential in reducing arthritis pain (Schuelert *et al.,* 2011; Krustev *et al.,* 2014) as well as inflammation (Krustev *et al.,* 2014). FAAH inhibitors have, however, failed to alleviate OA pain in clinical trials despite achieving >96% systemic blockade of FAAH activity (Huggins *et al.,* 2012). There are a number of reasons cited by Huggins *et al.* as to why the FAAH inhibitor (PF-04457845) failed in this study. The study incorporated a heterogeneous population of OA patients with no division of pain phenotypes. It is conceivable that FAAH inhibition is more beneficial for certain types of pain (*e.g.* inflammatory pain) compared to other phenotypes (Huggins *et al.* 2012). Additionally, PF-04457845 is an irreversible inhibitor that almost completely ablated FAAH activity. This could cause a profound accumulation of AEA which would increase the risk of producing off-target effects (Gauldie *et al.,* 2001; Huggins *et al.,* 2012). Over accumulation of AEA has been shown to activate nociceptive afferents innervating the rat knee joint (Gauldie *et al.,* 2001), and as previously discussed, can form proinflammatory and proalgesic PG via COX-2 metabolism (Di Marzo, 2008; Yates & Barker, 2009). MAGL and FAAH inhibition may involve overlapping signalling pathways and, therefore, a combination of the two could perhaps provide the most beneficial outcome. Studies using a dual FAAH/MAGL inhibitor (JZL195) have demonstrated pain reductions preclinically in an inflammatory pain model (Anderson *et al.,* 2014) and in a

neuropathic pain model (Adamson-Barnes *et al.,* 2016). The combination therapies proved more efficacious than the enzyme inhibitors on their own and did so without centrally-mediated effects or tolerance (Anderson *et al.,* 2014; Adamson-Barnes *et al.,* 2016). Furthermore, another group administered a dual FAAH/TRPV1 inhibitor in the MIA model of OA and demonstrated greater antinociceptive effects compared to each inhibitor alone (Malek *et al.,* 2015). CB_1R and CB_2R have been shown to be co-localised with TRPV1 in the joint (Schuelert *et al.,* 2010) and therefore targeting both MAGL and TRPV1 may also prove more efficacious.

6.2   Effects of CB$_2$R agonism in MIA-induced pain and inflammation

Fourteen days post-MIA induction, locally administered JWH133 significantly improved hindpaw withdrawal threshold and hindlimb weight bearing deficits. These findings corroborate recent findings by Burston *et al.* (2013) who found that chronic administration of JWH133 blocked the development of MIA-induced secondary allodynia and hindlimb weight bearing deficits for 21 days. Additionally, chronic administration of JWH133 attenuated spinal astrogliosis in the MIA model (Burston *et al.,* 2013). Since activation of microglia and astrocytes in the CNS causes the release of an array of immune modulating molecules which can contribute to the maintenance of central sensitisation (Costigan *et al.,* 2009), the finding by Burtson and colleagues (2013) suggests a role for CB_2R in regulating sensitisation in the MIA model of OA.

The antinociceptive effect of JWH133 on von Frey hair-determined referred pain was blocked by a CB_2R antagonist, but not a CB_1R antagonist, confirming that JWH133

was selective for the CB_2R. However, JWH133 had no effect on dynamic incapacitance. The CB_2R antagonist did not affect hindlimb weight bearing, but co-administration of JWH133 with the CB_1R antagonist caused a significant improvement in weight bearing near the end of the time course (at 180 min). These mixed results could be due to potential technical errors during the experiment such as injection technique, dosage, timing, or due to potential off-target effects of AM281. Another CB_1R antagonist, AM251, has been shown to have inverse agonist activity and off-target effects on GPR55 (Kapur *et al.,* 2009), and μ-opioid receptors (Seely *et al.,* 2012). Although AM281 has not been shown to have these same sort of off-target effects, this has not been specifically assessed in joints and may explain some of the conflicting results seen in this study.

On day 1 of the MIA model, topically administered JWH133 did not alter rolling leukocytes or knee joint hyperaemia. However, JWH133 significantly decreased adherent leukocytes in the knee joint. A study by Xu *et al.* (2007) demonstrated that JWH133 inhibited leukocyte trafficking in the inflamed retina by blocking P-selectin, which is largely responsible for leukocyte capture and initiation of rolling; therefore, it would be feasible that JWH133 could also have significant antirolling effects in the knee joint, which was not the case in this study.

Since CB_2Rs have been shown to be largely localised on immune cells and within the rat knee joint (McDougall *et al.,* 2008) it is surprising that the antiinflammatory effects of JWH133 observed here were not more pronounced. However, there have been a number of paradoxical findings concerning the effects of CB_2R agonists on pain and inflammation. A study conducted by McDougall *et al.* (2008) demonstrated that JWH133 caused an increase in knee joint blood flow in normal knees, but failed to illicit any

changes in articular blood flow in both acute and chronically inflamed knee joints. Another study also showed paradoxical effects of a CB_2R agonist between normal and OA joints where administration of the agonist caused a reduction in joint afferent mechanosensitivity in normal joints, but was pronociceptive in OA knee joints (Schuelert *et al.,* 2010). Conversely, in the same study the CB_2R agonist was able to produce improvements in hindlimb weight bearing in OA knee joints, indicative of a reduction in non-evoked pain (Schuelert *et al.,* 2010). Other studies have shown efficacy of CB_2R agonists in models of acute inflammatory pain (Nackley *et al.,* 2003; Whiteside *et al.,* 2005), therefore the pharmacological action of CB_2R agonists may vary between different pathophysiological conditions. Additionally, there is evidence that CB_2R activation can modulate TRPV1 sensitivity (Anand *et al.,* 2008), and may be acting as a weak partial agonist at the TRPV1 receptor. Activation of TRPV1 can lead to the secondary release of inflammatory neuropeptides which could further sensitise joint nociceptors as well as increase synovial blood flow (McDougall *et al.,* 2008). These complex findings suggest that CB_2R may play a role in OA inflammation and pain; however, better pharmacological tools and assessment in multiple animal models are required to verify this possibility.

6.3   Effects of a phytocannabinoid on MIA-induced pain and inflammation

On day 14 of the MIA model, 300µg of CBD improved behavioural pain measures. Hindpaw withdrawal threshold was increased and hindlimb weight bearing deficits improved, both indicative of less pain. Contralateral administration of CBD did not have any effect on ipsilateral hindpaw secondary allodynia confirming that the effect

of CBD was localised to the site of administration for this pain test. These experiments suggest that CBD is acting solely in the periphery and localised to the joint.

Although CBD has been shown to act as a full antagonist at CB_1R (Thomas *et al.,* 2007) and an inverse agonist at CB_2R (Thomas *et al.,* 2007), the action of CBD has not been investigated locally within the joint. Both CB_1R and CB_2R antagonists failed to block the CBD-mediated improvements in hindpaw withdrawal threshold and weight bearing. The action of CBD has also been shown to be mediated through various TRP ion channels (Bisogno *et al.,* 2001; De Petrocellis *et al.,* 2011; Iannotti *et al.,* 2013), GPR55 (Ryberg *et al.,* 2007), GPR18 (McHugh *et al.,* 2012), and serotonin receptors (e.g. 5-HT_{1A}) (Russo *et al.,* 2005; Resstel *et al.,* 2009). In this study, the TRPV1 antagonist, SB-366791, successfully attenuated the effects of CBD on secondary allodynia in the MIA model of OA. A TRPV1 antagonist was chosen for this study because of the known involvement of TRPV1 ion channels in MIA-induced peripheral sensitisation (Kelly *et al.,* 2015). This mechanism of action of CBD has been previously reported both in *in vitro* (Bisogno *et al.,* 2001) and *in vivo* (Costa *et al.,* 2004; Comelli *et al.,* 2008) experiments. A study using human embryonic kidney cells, as well as cell membranes from rodent brains, showed that TRPV1 antagonism by capsazepine blocked the Ca^{2+}-increasing and subsequent desensitising effects of CBD (Bisogno *et al.,* 2001). *In vivo*, antagonism of TRPV1 attenuated the pain-relieving effect of CBD in a model of neuropathic pain (chronic constriction injury) (Costa *et al.,* 2004) and the carrageenan model of paw oedema (Comelli *et al.,* 2008). It is possible that the action of CBD on TRPV1 could be occurring by an indirect mechanism. CBD has the ability to inhibit the reuptake of AEA, as well as the catabolic action of FAAH (Bisogno *et al.,* 2001), which

would ultimately lead to an elevation of AEA levels in the joint. These abnormally high levels of AEA could lead to the activation and subsequent desensitisation of TRPV1 (Bisogno *et al.,* 2001).

One day after i.artic. injection of MIA, there was an increase in leukocyte trafficking and in knee joint blood flow. Topically administered CBD significantly reduced these early inflammatory changes in MIA-injected knee joints by decreasing leukocyte trafficking, but did not alter knee joint blood flow. An *in vitro* study by Zygmunt *et al.* (1999) demonstrated that accumulation of AEA can induce vasodilation by activating vanilloid receptors on sensory nerves and causing subsequent release of CGRP. This process may explain why CBD was not able to decrease synovial hyperaemia here. Potent antiinflammatory action of CBD, however, has been previously described in the literature. A study by Malfait *et al.* (2000) showed that systemic administration of CBD decreased serum cytokine levels and suppressed disease severity in the collagen-induced model of RA. In the carrageenan model of plantar oedema, oral CBD was antiinflammatory and antihyperalgesic (Costa *et al.,* 2004). Furthermore, CBD administered via a transdermal gel, applied to the backs of rats, reduced immune cell infiltration, synthesis of proinflammatory biomarkers, synovial membrane thickening, and joint swelling in the FCA model of inflammatory arthritis (Hammell *et al.,* 2016). The data presented in this study corroborate that CBD has potent antiinflammatory action, but demonstrate for the first time that local application of CBD has the ability to reduce OA-associated acute inflammatory flares. These findings suggest a promising therapeutic which could help patients by preventing or slowing disease progression and pain by treating early inflammatory flares.

The antirolling effect of CBD on leukocytes within the MIA knee joints was blocked by AM630 (CB$_2$R antagonist) suggesting that CB$_2$Rs may be involved in inhibiting leukocyte trafficking. A study by Zhao *et al.* (2010) demonstrated that activation of CB$_2$Rs can inhibit the expression of P-selectin, which is an adhesion molecule involved in leukocyte capture and rolling. Further investigation into whether CBD blocks P-selectin activity in the joint via a CB$_2$R mechanism is required to test this molecular pathway. Additionally, the role of CBD on other adhesion molecules present in the joint should also be explored. A study conducted by Ramer *et al.* (2012) showed that CBD prevented lung cancer cell invasion via an ICAM1-dependent mechanism. The inhibitory effect of CBD on both aspects of leukocyte trafficking, rolling and adherence, were blocked by the TRPV1 antagonist SB-366791. The antiinflammatory effects of CBD observed here could be due to desensitisation of TRPV1 ion channels (Iannotti *et al.,* 2013). Opening of TRPV1 ion channels has been shown to cause release of inflammatory neuropeptides in the periphery, which in turn promote neurogenic inflammation and can enhance knee joint leukocyte trafficking (Varga *et al.,* 2005; Krustev *et al.,* 2017). Thus, CBD may be blocking this classic neurogenic inflammatory pathway by inactivating TRPV1.

6.4   Effects of prophylactic CBD on the development of OA pain and nerve damage

One of our central hypotheses is that early blockade of MIA-induced acute inflammatory flares by CBD would prevent the development of chronic pain and peripheral nerve damage. Prophylactic treatment with CBD before induction, and on days

1-3 following MIA prevented the development of MIA-induced secondary allodynia throughout the 14 days, but did not influence hindlimb weight bearing or knee joint diameter. These results suggest that CBD attenuates the central sensitisation associated with MIA-induced OA. Previous studies demonstrate that MIA induces peripheral nerve damage (Thakur *et al.,* 2012; McDougall *et al.,* 2017), whereby nerve demyelination was confirmed by an increase in G-ratio compared to saline control animals (McDougall *et al.,* 2017). Early treatment with CBD prevented the loss of nerve myelin 14 days post-MIA, suggesting that by ablating the acute inflammatory flares in the model the joint was protected from subsequent nerve damage. Furthermore, the G-ratio data would be strongly supported by future studies qualitatively examining the nerve sections by using an ultrastructure grading system designed to grade peripheral neuropathy within the sections (Kaptanoglu *et al.,* 2002; Tun *et al.,* 2009; Dagtekin *et al.,* 2011). Additionally, these data would be further supported by measuring the expression of biomarkers for peripheral nerve damage such as activating transcription factor-3 (ATF-3) (Thakur *et al.,* 2012; McDougall *et al.,* 2017).

The findings presented here support the idea that CBD treatment may be a beneficial therapeutic for the subset of OA patients who experience neuropathic symptoms and who are refractory to prescribed first and second line analgesics (*i.e.* NSAIDs and opioids). Along with CBD, other phytocannabinoid compounds have been shown to be neuroprotective in demyelinating diseases such as multiple sclerosis. Cannabinol (CBN) and Δ^9-THC have both been implicated in slowing the progression in a preclinical model of amyotrophic lateral sclerosis (ALS) and promoting the survival of neurones (Weydt *et al.,* 2005; Iuvone *et al.,* 2009). Furthermore, CBD improved motor

coordination and clinical recovery scores in a preclinical model of MS (EAE), by having

a neuroprotective effect (Pryce *et al.,* 2015). It has been postulated that CBD confers

neuroprotective properties through several mechanisms, which are both cannabinoid-

dependent and cannabinoid-independent (Campos *et al.,* 2016). CBD-mediated

neuroprotection has been explored in preclinical models of MS (Pryce *et al.,* 2015),

Alzheimer's disease (Iuvone *et al.,* 2004; Esposito *et al.,* 2011; Scuderi *et al.,* 2014),

hypoxic brain injury (Alvarez *et al.,* 2008; Castillo *et al.,* 2010; Pazos *et al.,* 2013), and

the paclitaxel model of neuropathic pain (Ward *et al.,* 2014). Mechanisms underlying the

neuroprotective effects of CBD are thought to involve multiple targets such as attenuation

of microglial activation, decrease in proinflammatory mediators, and reduction in

oxidative stress (Campos *et al.,* 2016). These have all been assessed centrally, but may

play a similar role in neuroprotection of peripheral nerves. The potential mechanisms in

which CBD generates neuroprotective action should be explored in OA-associated

peripheral nerve injury.

The study presented in Chapter 5 demonstrates for the first time that CBD is an

effective antinociceptive and antiinflammatory agent when administered locally around

the joint. CBD is a non-psychoactive phytocannabinoid and has a more desirable side

effect profile compared to other cannabinoids and commonly prescribed analgesics.

Preclinically, when CBD was administered systemically there were no signs of adverse

events in the animals (Malfait *et al.,* 2000; Hammell *et al.,* 2016), whereby exploratory

behaviour was not altered, indicating limited motor deficits and a lack of psychoactivity

(Hammell *et al.,* 2016). Relief of OA symptoms by local CBD, without centrally-

mediated events, would be a valuable therapeutic option which would be desirable for patients.

6.5   Summary

The results presented and discussed here provide evidence that manipulating the ECS locally could be an important and beneficial therapeutic for the treatment of pain and inflammation in both established OA, as well as during the development or early progression of the disease.

6.6   Limitations

6.6.1 Animal models of OA

There is no existing animal model which can recapitulate the entirety of any human disease state or is devoid of limitations. In this study, the MIA model of OA was used for all experimental protocols because our main questions were the effects of various cannabinoid treatments on OA pain, OA-associated inflammation, and peripheral nerve damage, all of which have been well-characterised in this model (Bove *et al.,* 2003; Thakur *et al.,* 2012; McDougall *et al.,* 2017).

Although the MIA model has been well-identified as producing a pain phenotype very similar to that seen in OA patients, the joint damage produced by this model recapitulates only some aspects of human OA. The model produces joint damage by triggering rapid chondrocyte death, which is not the pathway or timeline that joint

degeneration occurs in human disease. Therefore, the MIA model is not ideal for assessing structural knee joint histopathology. Ideally, the efficacy of any compound would be tested in a variety of OA models to attempt to encompass the entire pathology of the disease to tease out in which aspects of OA the compound is most effective.

Another important consideration when using animal models are the differences in joint loading and gait in animals (quadrupeds) compared to humans (bipeds) which contributes to differences in joint pain and joint degeneration (O'Brien *et al.,* 2017).

6.6.2 *Measuring pain in animals*

There has been some speculation as to whether or not hindlimb incapacitance is a robust indicator of non-evoked pain. If weight bearing deficits are due solely to spontaneous pain in the joint or if they arise from abnormal joint biomechanics (*e.g.* instability, altered gait) remains to be teased out. It is recommended that these assessments be paired with other pain tests to strengthen any findings. In this study, hindlimb incapacitance was paired with hindpaw von Frey hair algesiometry in an attempt to assess multiple aspects of the pain pathway, both peripherally and centrally.

Von Frey hair algesiometry in the clinic is typically done by applying the filaments directly to the injured area or the immediate surrounding areas to assess tactile allodynia and pain diffusion. In our studies, the filaments were applied to the plantar surface of the hindpaw which gives a measurement of referred pain. The animals are also standing on their paws while the testing is performed, which may add a mechanical loading aspect to the pain we are measuring, and would be different if the animal was lying down. Additionally, the undulating surface on which the animals stand (*i.e.* mesh

flooring) has been shown to influence von Frey hair responses, and a smoother floor may give more consistent results (Pitcher *et al.,* 1999). Naïve baseline as well as vehicle control cohort measurements were taken to mitigate some of these potential limitations.

Pain sensation is largely subjective and can be influenced by sex, age, and psychosocial aspects. Chronic pain patients are typically female (Berkley, 1997) and middle-aged (Gagliese & Melzack, 1997). However, historically, young male animals have been used for experimental assessments. The incorporation of cohorts including both sexes, as well as a larger age range, may help with translatability of our findings to the human pain experience. The psychosocial aspects of pain often experienced by chronic pain patients include anxiety or depression, sleep disturbances, decreased social interaction, and appetite suppression, are difficult to quantify in animals (Mogil *et al.,* 2009). Attempts to assess these affective aspects of pain in animals have been done using conditioned place preference (CPP) assays, (Qu *et al.,* 2011) elevated plus maze, as well as assessing facial characteristics of pain (Sotocinal *et al.,* 2011). Due to time constraints, these behavioural read-outs of pain affect were not performed in this project.

6.6.3 *Measuring endocannabinoid levels in the rat knee joint*

While it has been demonstrated that the ECS is upregulated in arthritic joints compared to healthy joints (Richardson *et al.,* 2008), and is a viable target for modulating pain and inflammation locally, it was beyond the scope of this project to assess the expression of endocannabinoids and their receptors within the joint. Although, a MAGL inhibitor was used to augment the endogenous levels of 2-AG, we did not directly measure 2-AG or MAGL levels within the joint to determine if the drug was exerting its

desired effect. These compounds are highly lipophilic and labile, making them difficult to measure. Additionally, the rat knee joint contains only 15-20µl of synovial fluid which is inadequate for carrying out these types of measurements.

6.6.4 Inflammation induced from surgical preparation

Prior to the inflammation assessments, the skin surrounding the knee joint was excised and the capsule exposed which could produce surgery-induced inflammation in these animals. Therefore, a caveat when interpreting the IVM and LASCA is that an acute underlying inflammation may be influencing the vascular read-outs. Nevertheless, naïve controls were used as a comparison in these studies to try to mitigate any effect of skin excision.

6.6.5 Rhodamine 6G staining of leukocytes

A limitation of using rhodamine 6G in our IVM protocol is that it is a non-specific leukocyte stain. This means that it is not possible to distinguish between different types of leukocytes. Additionally, it is not known whether the rolling and adherent leukocytes have a proinflammatory or antiinflammatory phenotype.

6.6.6 Tissue-laser interactions

The LASCA experiments are limited by tissue-laser interactions. The depth of tissue penetration of the 785nm laser is approximately 1500-1800µm through skin. We

mitigate this by removing the skin and exposing the knee joint capsule. The joint vasculature is fairly superficial in the rat knee so we are confident that we are monitoring synovial blood flow. In oedematous tissue, the water content increases which can alter the scattering pattern and absorbance properties of the laser photons. We avoid these possible limitations by using naïve controls and comparing perfusion with baseline scans (*i.e.* prior to drug administration). A dead scan is also recorded at the end of the experiments which acts as a biological zero for each animal and accounts for any changes in tissue optical properties. A final limitation is that the data produced by the LASCA are assigned arbitrary perfusion units which are not standardised and can therefore only describe relative changes in blood flow.

6.7   Future directions

6.7.1 Can cannabinoids alter arthritic joint damage?

It has been well-established that the ECS is present in arthritic joints and is active, but the involvement of the ECS in the progression of arthritis has not been investigated in great detail. It would be interesting to assess the effects of the cannabinoid compounds tested in this project on a possible protective effect on joint pathology. This would preferably be carried out in a model of OA that better recapitulates osteoarthritic joint pathology such as a surgically-induced model or naturally-occurring model. Several groups have attempted to elucidate the important physiological role the ECS plays in bone metabolism. The ECS is a main regulator of bone mass, bone loss, and overall bone cell function (Idris & Ralston, 2010). Bone and synovial cells express CB_1R, CB_2R, and

GPR55, and 2-AG and AEA are produced within the bone microenvironment (Idris *et al.,* 2005; Tam *et al.,* 2006; Tam *et al.,* 2007; Idris & Ralston, 2010). A complete ECS, was also found in osteoblasts, osteoclasts, bone marrow stromal cells, and macrophages (Tam *et al.,* 2006; Tam *et al.,* 2007; Whyte *et al.,* 2009). *In vitro* studies identified CB_1R and CB_2R expression on chondrocytes; endocannabinoids (AEA) and synthetic compounds (WIN-55,212) were shown to be protective against joint degeneration by having direct effects on chondrocyte metabolism, which results in a reduction of proteoglycan breakdown and cartilage protection (Mbvundula *et al.,* 2005). Other *in vitro* studies demonstrated that synovial cells from mice with collagen-induced arthritis, produced large numbers of TNF-α (Malfait *et al.,* 2000). In culture, when these synovial cells were treated with CBD, they produced less TNF-α (Malfait *et al.,* 2000). Furthermore, CBD treatment suppressed the clinical signs of inflammatory arthritis and the hindpaws of these mice were protected from joint destruction (Malfait *et al.,* 2000).

6.7.2   Could combination therapy using MAGL and COX2 inhibitors effectively block OA pain and inflammation?

As discussed previously, in the endocannabinoid ligand biosynthesis and degradation pathways, AEA and 2-AG can be oxygenated via a COX-2 pathway which leads to the formation of proinflammatory and pain inducing PG derivatives. Increases in 2-AG accumulation by blocking MAGL could cause shunting of these ligands down the COX-2 pathway, which could counteract the beneficial effects of endocannabinoids. Therefore, to potentially achieve greater alleviation of pain and inflammation selective

MAGL inhibitors may need to be administered in combination with selective COX-2 blockers. It would be interesting to see if the actions of KML29 would be more efficacious when paired with a COX-2 inhibitor, such as celecoxib, in the MIA model of OA.

Another potential benefit of combining these two therapeutic approaches is the decrease in adverse gastrointestinal effects perpetrated by COX-2 inhibitors. Two studies conducted using the diclofenac-induced model of gastric haemorrhages in mice showed that two different MAGL inhibitors were gastroprotective in a dose-dependent manner (Kinsey *et al.,* 2013; Ignatowska-Jankowska *et al.,* 2014) suggesting that a combination approach using MAGL and COX-2 inhibitors may circumvent the adverse gastrointestinal effects seen with COX inhibitors alone.

6.7.3   *Can cannabinoids and opioids synergistically alleviate OA pain?*

Opioids are typically a second line therapy for OA patients, and are highly potent and effective analgesics, but their use is limited because of some major negative side effects (*e.g.* tolerance, cardiorespiratory depression, constipation, risk of abuse). In recent years there has been increasing interest in providing a combination therapy with opioids to allow for their use at lower doses or even subclinical doses to treat pain effectively.

Opioids and cannabinoids have been shown to be coupled to similar intracellular signalling pathways which ultimately lead to a decrease in cyclic adenosine monophosphate production (Pugh *et al.,* 1994; Welch *et al.,* 1995; Welch & Eads, 1999). Additionally, some studies demonstrated that cannabinoids can increase the synthesis of

endogenous opioids (Smith *et al.,* 1998; Cichewicz *et al.,* 1999). Animal models have shown synergy between morphine and Δ^9-THC, whereby Δ^9-THC was postulated to enhance the effects of morphine via kappa and delta opioid receptors (Pugh *et al.,* 1996). Abrams *et al.* (2011) conducted the first human study which demonstrated that inhaled cannabis safely augments the analgesic effects of opioids which would allow for opioid sparing.

More specifically, the effects of opioids in combination with the non-psychoactive phytocannabinoid, CBD, has not been widely explored preclinically. Neelakantan *et al.* (2015) were the first group to study the effects of morphine and CBD on behavioural pain in mice. The combination therapy, administered systemically, demonstrated synergism in one pain assay and subadditive effects in a different assay, suggesting that successful synergy may lead to safer treatment strategies (Neelakantan *et al.,* 2015). These preclinical and clinical findings highlight a potential strategy for developing combination therapies to treat pain symptoms and avoid the undesirable adverse effects associated with high doses or long-term use of opioids. It would therefore be interesting to assess a potential synergy between CBD and an opioid compound in the context of OA pain and inflammation.

6.7.4   Can terpenoids help cannabinoids become more effective therapeutics?

"Some plants are better drugs than the natural products isolated from them" (Mechoulam & Ben-Shabat, 1999; Russo, 2011). Cannabinoids are not the only bioactive compounds found in the cannabis plant. Terpenoids, or terpenes, are essential oils that are very prominent in the plant, with over 200 being identified. While terpenoids are

responsible for the aroma of cannabis, they are also pharmacologically diverse and can impart biological responses (Russo, 2011). Terpenoids are lipophilic, act on neuronal ion channels, GPCRs, neurotransmitter receptors, second messenger systems, enzymes, and interact with cell membranes (Bowles, 2003; Buchbauer, 2010; Russo, 2011). These actions are similar to those of cannabinoid compounds within the ECS, therefore it has been suggested that there may be synergistic interactions between terpenoids and cannabinoids. Due to their shared and complementary actions, it is hypothesised that terpenoids will improve the therapeutic index of cannabis extracts (Russo, 2011). Terpenes have received less attention than the phytocannabinoids but have been shown to have important analgesic and antiinflammatory properties preclinically (Gertsch *et al.,* 2008). However, the most studied areas of application for terpenoid-cannabinoid synergy are for dermatological, psychological, and addiction-relief purposes (Russo, 2011). Assessing the entourage effects of terpenoids and cannabinoids in the MIA model of OA could provide evidence which allows for patients to become properly informed about the correct choice of cannabis strains to be used for the treatment of different pain conditions.

6.8   Conclusions

The results presented in this study show that locally administered phytocannabinoids, endocannabinoids, and synthetocannabinoids have robust antinociceptive and antiinflammatory effects in the MIA model of OA. These results add to the emerging body of preclinical evidence which highlights the utility of using cannabinoids to treat musculoskeletal disorders. As such, cannabinoid compounds are

promising therapeutics which have the ability to reduce joint inflammation, peripheral

neuropathy, and the pain associated with OA.

References

Abrams, D. I., Couey, P., Shade, S. B., Kelly, M. E., & Benowitz, N. L. (2011). Cannabinoid-opioid interaction in chronic pain. *Clin Pharmacol Ther, 90*(6): 844–51.

Adamson-Barnes, N. S., Mitchell, V. A., Kazantzis, N. P., & Vaughan, C. W. (2016). Actions of the dual FAAH/MAGL inhibitor JZL195 in a murine neuropathic pain model. *Br J Pharmacol, 173*(1): 77–87.

Aggarwal, S. K., Carter, G. T., Sullivan, M. D., ZumBrunnen, C., Morrill, R., & Mayer, J. D. (2009). Characteristics of patients with chronic pain accessing treatment with medical cannabis in Washington State. *J Opioid Manag, 5*(5): 257–86.

Agur, A. M. R. & Dalley, A. F. (2013). *Grant's Atlas of Anatomy*. Philadelphia, Pennsylvania: Wolters Kluwer, pp. 357–476.

Ahmed, M., Bjurholm, A., Kreicbergs, A., & Schultzberg, M. (1993). Sensory and autonomic innervation of the facet joint in the rat lumbar spine. *Spine, 18*(14): 2121–6.

Ahmed, S., Magan, T., Vargas, M., Harrison, A., & Sofat, N. (2014). Use of the painDETECT tool in rheumatoid arthritis suggests neuropathic and sensitization components in pain reporting. *J Pain Res, 7*: 579–588.

Aigner, T., Rose, J., Martin, J., & Buckwalter, J. (2004). Aging theories of primary osteoarthritis: From epidemiology to molecular biology. *Rejuven Res, 7*(2): 134–145.

Aigner, T., Soder, S., Gebhard, P. M., Mcalinden, A., & Haag, J. (2007). Mechanisms of disease: Role of chondrocytes in the pathogenesis of osteoarthritis—structure, chaos and senescence. *Nat Clin Prac Rheumatol, 3*(7): 391–399.

Alvarez, F. J., Lafuente, H., Rey-Santano, C. M., Mielgo, V. E., Gastiasoro, E., Rueda, M., Pertwee, R. G., Castillo, A. I., Romero, J., & Martinez-Orgado, J. (2008). Neuroprotective effects of the nonpsychoactive cannabinoid cannabidiol in hypoxic-ischemic newborn piglets. *Pediatr Res, 64*(6): 653-8.

Anand, U., Otto, W. R., Sanchez-Herrara, D., Facer, P., Yiangou, Y., Korchev, Y., Birch, R., Benham, C., Bountra, C., Chessell, I. P., & Anand, P. (2008). Cannabinoid receptor CB2 localisation and agonist-mediated inhibition of capsaicin responses in human sensory neurons. *Pain, 138*(3): 667–80.

Anderson, W. B., Gould, M. J., Torrees, R. D., Mitchell, V. A., & Vaughan, C. W. (2014). Actions of the dual FAAH/MAGL inhibitor JZL195 in a murine inflammatory pain model. *Neuropharmacology, 81*: 224–30.

Andruski, B., McCafferty, D. M., Ignacy, T., Millen, B., & McDougall, J. J. (2008). Leukocyte trafficking and pain behavioural responses to a hydrogen sulfide donor in acute monoarthritis. *Am J Physiol Regul Integr Comp Physiol, 295*(3): R814–20.

Arendt-Nielsen, L., Nie, H., Laursen, M. B., Laursen, B. S., Madeleine, P., Simonsen, O. H., & Graven-Nielsen, T. (2010). Sensitization in patients with painful knee osteoarthritis. *Pain, 149*(3): 573–81.

Arendt-Nielsen L. (2017). Pain sensation in osteoarthritis. *Clin Exp Rheumatol, 35*(S107): S68–S74.

Arevalo-Martin, A., Vela, J., Molin-Holgado, E., Borrell, J., & Guaza, C. (2003). Therapeutic action of cannabinoids in a murine model of multiple sclerosis. *J Neurosci, 7*(23): 2511–2516.

Ayhan, E., Kesmezacar, H., & Akgun, I. (2014). Intraarticular injections (corticosteroid, hyaluronic acid, platelet rich plasma) for the knee osteoarthritis. *World J Orthop, 5*(3): 351–361.

Baatz, H., Steinbauer, M., Harris, A. G., & Krombach, F. (1995). Kinetics of white blood cell staining by intravascular administration of rhodamine 6G. *Int J Microcirc, 15*(2): 197–206.

Baker, C. L. & McDougall, J. J. (2004). The cannabinomimetic arachidonyl-2-chloroethylamide (ACEA) acts on capsaicin-sensitive TRPV1 receptors but not cannabinoid receptors in rat joints. *Br J Pharmacol, 142*(8): 1361–7.

Baker, K., Grainger, A., Niu, J., Clancy, M., Guermazi, A., Crema, M., Hughes, L., Buckwalter, J., Wooley, A., Nevitt, M., & Felson, D. T. (2010). Relation of synovitis to knee pain using contrast-enhanced MRIs. *Ann Rheum Dis, 69*(10): 1779–83.

Bardin, L. (2011). The complex role of serotonin and 5-HT receptors in chronic pain. *Behav Pharmacol, 22*(5-6): 390–404.

Battista, N., Tommaso, M. D., Bari, M., and Maccarrone, M. (2012). The endocannabinoid system: An overview. *Front Behav Neurosci, 6*: 9.

Benito, M., Veale, D., FitzGerald, O., van den Berg, W. & Bresnihan, B. (2005). Synovial tissue inflammation in early and late osteoarthritis. *Ann Rheum Dis* 64: 1263–1267.

Berkley, K. J. (1997). Sex differences in pain. *Behav Brain Sci, 20*: 371–380.

Bierma-Zeinstra, S. & Verhagen, A. P. (2011). Osteoarthritis subpopulations and implications for clinical trial design. *Arthritis Res Ther, 13*(2): 213.

Bisogno, T., Hanus L., De Petrocellis, L., Tchilibon, S., Ponde, D. E., Brandi, I., Moriella, A. S., Davis, J. B., Mechoulam, R., & Di Marzo, V. (2001). Molecular targets for cannabidiol and its synthetic analogues: effect on vanilloid VR1 receptors and on the cellular uptake and enzymatic hydrolysis of anandamide. *Br J Pharmacol, 134*(4): 845–52.

Boas, D. A., & Dunn, A. K. (2010). Laser speckle contrast imaging in biomedical optics. *J Biomed Opt, 15*(1): 011109.

Bondeson, J., Blom, A., Wainwright, S., Hughes, C., Caterson, B., & van den Berg, W. (2010). The role of synovial macrophages and macrophage-produced mediators in driving inflammatory and destructive responses in osteoarthritis. *Arthritis Rheum, 62*: 647–657.

Booth, J., Moseley, G. L., Schiltenwolf, M., Cashin, A., Davies, M., & Hubscher, M. (2017). Exercise for chronic musculoskeletal pain: a biopsychosocial approach. *Musculoskeletal Care,* 1–9.

Bove, S. E., Calcaterra, S. L., Brooker, R. M., Huber, C. M., Guzman, R. E., Juneau, P. L., Schrier, D. J., & Kilgore, K. S. (2003). Weight bearing as measure of disease progression and efficacy of anti-inflammatory compounds in a model of monosodium iodoacetate-induced osteoarthritis. *Osteoarthr Cartil, 11*(11): 821–830.

Bowles, E. J. The Chemistry of Aromatherapeutic Oils. 3rd ed. Crow's Nest, NSW: Allen & Unwin; 2003.

Brackmann, U. (1986). Lambdachrome laser dyes. *Goettingen Lambda Phys GmbH, 1.*

Bradshaw, H. B., Lee, S. H., & McHugh, D. (2009). Orphan endogenous lipids and orphan GPCRs: A good match. *Prostaglandins Other Lipid Mediat, 89*(3-4):131–134.

Brooks, P. M. (2006). The burden of musculoskeletal disease--a global perspective. *Clin Rheumatol, 25*(6): 778–781.

Buchbauer, G. Biological activities of essential oils. In: Baser K. H. C., Buchbauer, G., eds. Handbook of Essential Oils: Science, Technology, and Applications. Boca Raton, FL: CRC Press; 2010. pp. 235–280.

Buma, P., Elmans, L., Van Den Berg, W. B., & Schrama, L. H. (2000). Neurovascular plasticity in the knee joint of an arthritic mouse model. *Anat Rec, 260*(1): 51–61.

Burston, J. J., Sagar, D. R., Shao, P., Bai, M., King, E., Brailsford, L., Turner, J. M., Hathway, G. J., Bennett, A. J., Walsh, D. A., Kendall, D. A., Lichtman, A., & Chapman, V. (2013). Cannabinoid CB2 receptors regulate central sensitization and pain responses associated with osteoarthritis of the knee joint. *PLoS One, 8*(11): e80440.

Burston, J. J., Mapp, P.I., Sarmad, S., Barrett, D. A., Niphakis, M. J., Cravatt, B. F., Walsh, D. A., & Chapman, V. (2016). Robust anti- nociceptive effects of monoacylglycerol lipase inhibition in a model of osteoarthritis pain. *Br J Pharmacol, 173*(21): 3134–3144.

Campos, A. C., Fogaca, M. V., Sonego, A. B., & Guimaraes, F. S. (2016). Cannabidiol, neuroprotection and neuropsychiatric disorders. *Pharmacol Res, 112*: 119–127.

Castillo, A., Tolon, M. R., Fernandez-Ruiz, J., Romero, J., & Martinez-Orgado, J. (2010). The neuroprotective effect of cannabidiol in an in vitro model of newborn hypoxic-ischemic brain damage in mice is mediated by CB(2) and adenosine receptors. *Neurobiol Dis, 37*(2): 434–40.

Catre, M. G., & Salo, P. T. (1999). Quantitative analysis of the sympathetic innervation of the rat knee joint. *J Anat, 194(2)*: 233–9.

Cedraschi, C., Delezay, S., Marty, M., Berenbaum, F., Bouhassira, D., Henrotin, Y., Laroche, F., & Perrot, S. (2013). Let's Talk about OA pain: a qualitative analysis of the perceptions of people suffering from OA. Towards the development of a specific pain OA-related questionnaire, the Osteoarthritis Symptom Inventory Scale (OASIS). *PLoS One, 8*(11): e79988.

Chang, J. W., Niphakis, M. J., Lum, K. M., Cognetta, A. B., Wang, C., Matthews, M. L., Niessen, S., Buczynski, M. W., Parsons, L. H., & Cravatt, B. F. (2012). Highly selective inhibitors of monoacylglycerol lipase bearing a reactive group that is bioisosteric with endocannabinoid substrates. *Chem Biol, 19*(5): 579–88.

Chaplan, S. R., Bach, F. W., Pogrel, J. W., Chung, J. M., & Yaksh, T. L. (1994). Quantitative assessment of tactile allodynia in the rat paw. *J Neurosci Methods, 53*(1): 55–63.

Cichewicz, D. L., Martin, Z. L., Smith, F. L. & Welch, S. P. (1999). Enhancement mu opioid antinociception by oral delta9–tetrahydrocannabinol: dose–response analysis and receptor identification. *J Pharmacol Exp Ther, 289*: 859–867.

Clapper, J. R., Moreno-Sanz, G., Russo, R., Guijarro, A., Vacondio, F., Duranti, A., Tontini, A., Sanchini, S, Sciolino, N. R., Spradley, J. M., Hohmann, A. F., Calignano, A., Mor, M., & Piomelli, D. (2010). Anandamide suppresses pain initiation through a peripheral endocannabinoid mechanism. *Nat Neurosci, 13*(10): 1265–1270.

Combe, R., Bramwell, S., & Field, M. J. (2004). The monosodium iodoacetate model of osteoarthritis: a model of chronic nociceptive pain in rats? *Neurosci Lett, 370*(2-3): 236-40.

Comelli, F., Giagoni, G., Bettoni, I., Colleoni, M., & Costa, B. (2008). Antihyperalgesic effect of a cannabis sativa extract in a rat model of neuropathic pain: mechanisms involved. *Phytother Res, 22*(8): 1017–24.

Cormier, J., Cone, K., Lanpher, J., Kinens, A., Henderson, T., Liaw, L., Bilsky, E. J., King, T., Rosen, C. J., & Stevenson, G. W. (2017). Exercise reverses pain-related weight asymmetry and differentially modulates trabecular bone microarchitecture in a rat model of osteoarthritis. *Life Sci, 180*: 51–59.

Costa, B., Colleoni, M., Conti, S., Parolaro, D., Franke, C., Trovato, A. E., & Giagnoni, G. (2004). Oral anti-inflammatory activity of cannabidiol, a non-psychoactive constituent of cannabis, in acute carrageenan-induced inflammation in the rat paw. *Naunyn Schmiedebergs Arch Pharmacol, 369(*3): 294–299.

Costa, B. & Comelli, F. Pain. In: Pertwee, R. G. (2014), Handbook of Cannabis. Oxford, UK: Oxford University Press; pp. 473–486.

Costigan, M., Scholz, J., & Woolf, C. J. (2009). Neuropathic pain: a maladaptive response of the nervous system to damage. *Annu Rev Neurosci, 32*: 1–32.

Crichton, B. & Green, M. (2002). GP and patient perspectives on treatment with non-steroidal anti-inflammatory drugs for the treatment of pain in osteoarthritis. *Curr Med Res Opin, 18*(2): 92–6.

Dagtekin, A., Comelekoglu, U., Bagdatoglu, O., Yilmaz, N., Dagtekin, O., Koseoglu, A., Vayisoglu, Y., Karatas, D., Korkutan, S., Avci, E., Bagdatoglu, C., & Talas, D. (2011). Comparison of the effects of different electrocautery applications to peripheral nerves: an experimental study. *Acta Neurochirurgica, 153*(10): 2031–2039.

Dawson, W. R. (1934). Studies in the Egyptian Medical Texts: III (Continued). *J Egypt Arch*, 41–46.

Dean, G., Hoyland, J., Denton, J., Donn, R., & Freemont, A. (1993). Mast cells in the synovium and synovial fluid in osteoarthritis. *Br J Rheumatol, 32*: 671–675.

de Lange-Brokaar, B. J., Ioan-Facsinay, A., van Osch, G. J., Zuurmond, A. M., Schoones, J., Toes, R. E., Huizinga, T. W., & Kloppenburg, M. (2012). Synovial inflammation, immune cells and their cytokines in osteoarthritis: a review. *Osteoarthr Cartil, 20*(12):1484–1499.

Demuth, D. G., & Molleman, A. (2006). Cannabinoid signalling. *Life Sci, 78*(6): 549–563.

De Petrocellis, L., Ligresti, A., Moriello, A. S., Allara, M., Bisogno, T., Petrosino, S., Stott, C. G., & Di Marzo, V. (2011). Effects of cannabinoid and cannabinoid-enriched cannabis extracts on TRP channels and endocannabinoid metabolic enzymes. *Br J Pharmacol, 163*(7): 1479-1494.

Deutsch, D. G., & Chin, S. A. (1993). Enzymatic synthesis and degradation of anandamide, a cannabinoid receptor agonist. *Biochem Pharmacol, 46*(5): 791–796.

Devane, W. A., Hanus, L., Breuer, A., Pertwee, R. G., Stevenson, L. A., Griffin, G., Gibson, D., Mandelbaum, A., Etinger, A., & Mechoulam, R. (1992). Isolation and structure of a brain constituent that binds to the cannabinoid receptor. *Science, 258*(5090): 1946–1949.

Devor, M. & Seltzer, Z. Pathophysiology of damaged nerves in relation to chronic pain. In: Wall, P. D., Melzack, R. eds. Textbook of Pain. Churchill Livingstone, Edinburgh; 1999, pp. 129–164.

Di Marzo, V. (2008). Endocannabinoids: Synthesis and degradation. *Rev Physiol Biochem Pharmacol, 160*: 1–24.

Dimitroulas, T., Duarte, R. V., Behura, A., Kitas, G. D., & Raphael, J. H. (2014). Neuropathic pain in osteoarthritis: a review of pathophysiological mechanisms and implications for treatment. *Semin Arthritis Rheum, 44*(2): 145–154.

Ding, L., Heying, E., Nicholson, N., Stroud, N. J., Homandberg, G. A., Buckwalter, J. A., Guo, D., & Martin, J. A. (2010). Mechanical impact induces cartilage degradation via mitogen activated protein kinases. *Osteoarthr Cartil, 18*(11): 1509–1517.

Djourhi, L., Koutsikou, S., Fang, X., McMullan, S., & Lawson, S. N. (2006). Spontaneous pain, both neuropathic and inflammatory, is related to frequency of spontaneous firing in intact C-fiber nociceptors. *J Neurosci, 26*(4): 1281–1292.

Dray, A. (2008). New horizons in pharmacologic treatment for rheumatic disease pain. *Rheum Dis Clin North Am, 34*(2): 481–505.

Esposito, G., Scuderi, C., Valenza, M., Togna, G. I., Latina, V., De Filippis, D., Cipriano, M., Carratu, M. R., Iuvone, T., & Steardo, L. (2011). Cannabidiol reduces Aβ-induced neuroinflammation and promotes hippocampal neurogenesis through PPARγ involvement. *PLoS One, 6*(12): e28668.

Fagan, S.G. & Campbell, V. A. (2014). The influence of cannabinoids on generic traits of neurodegeneration. *Br J Pharmacol, 171*(6): 1347–1360.

Farahat, M. N., Yanni, G., Poston, R., & Panayi, G. S. (1993). Cytokine expression in synovial membranes of patients with rheumatoid arthritis and osteoarthritis. *Ann Rheum Dis*, *52*(12): 870–875.

Felson, D. T. & Chaisson, C. E. (1997). Understanding he relationship between body weight and osteoarthritis. *Baillieres Clin Rheumatol, 11*(4): 671–681.

Felson, D., McLaughlin, S., Goggins, J., LaValley, M., Gale, M., Totterman, S., Li, W., Hill, C., & Gale, D. (2003). Bone marrow edema and its relation to progression of knee osteoarthritis. *Ann Intern Med, 139*(5): 330–336.

Felson, D. T. (2004). Risk factors for osteoarthritis: understanding joint vulnerability. *Clin Orthrop Relat Res,* (427 Suppl): S16–S21.

Fernandes, J., Martel-Pelletier, J., & Pelletier, J. (2002). The role of cytokines in osteoarthritis pathophysiology. *Biorheology, 1-2*(39): 237–246.

Fernandez-Ruiz, J., Romero, J., & Ramos, J. A. (2015). Endocannabinoids and neurodegenerative disorders: Parkinson's disease, Huntington's Corea, Alzheimer's Disease, and others. *Handb Exp Pharmacol, 231*: 233–259.

Finan, P. H., Buenaver, L. F., Bounds, S. C., Hussain, S., Park, R. J., Haque, U. J., Campbell, C. M., Haythornthwaite, J. A., Edwards, R. R., & Smith, M. T. (2013). Discordance between pain and radiographic severity in knee osteoarthritis: findings from quantitative sensory testing od central sensitization. *Arthritis Rheum, 65*(2): 363–372.

Fitzcharles, M. A., Clauw, D. J., Ste-Marie, P. A., & Shir, Y. (2013). The dilemma of medical marijuana use by rheumatology patients. *Arthritis Care Res, 66*(6): 797–801.

Fitzcharles, M. A., Baerwald, C., Ablin, J., & Hauser, W. (2016). Efficacy, tolerability and safety of cannabinoids in chronic pain associated with rheumatic disease (fibromyalgia syndrome, back pain, osteoarthritis, rheumatoid arthritis): A systematic review of randomized controlled trials. *Schmerz, 30*(1): 47–61.

Fitzcharles, M. A. & Hauser, W. (2016). Cannabinoids in the management of musculoskeletal or rheumatic diseases. *Curr Rheumatol Rep, 18*(12): 76.

Foxall, D. L., Brindle, K. M., Campbell, I. D., & Simpson, R. J. (1984). The inhibition of erythrocyte glyceraldehyde-3-phosphate dehydrogenase. In situ PMR studies. *Biochim Biophys Acta*, *804*(2): 209–215.

Freeman, M. A. & Wyke, B. (1967). The innervation of the knee joint. An anatomical and histological study in the cat. *J Anat, 101*(3): 505–532.

Fukuda S., Kohsaka, H., Takayasu, A., Yokoyama, W., Miyabe C., Harigai, M., Miyasaka, N., & Nanki, T. (2014). Cannabinoid receptor 2 as a potential therapeutic target in rheumatoid arthritis. *BMC Musculoskelet Disord, 15*: 275.

Gagliese, L. & Melzack, R. (1997). Chronic pain in elderly people. *Pain, 70*(1): 3–14.

Gaoni, Y., & Mechoulam, R. (1964). Isolation, structure, and partial synthesis of an active constituent of Hashish. *J Am Chem Soc*, *86*(8): 1646–1647.

Gauldie, S. D., McQueen, D. S., Pertwee, R., & Chessell, I. P. (2001). Anandamide activates peripheral nociceptors in normal and arthritic rat knee joints. *Br J Pharmacol*, *132*(3): 617–621.

Gear, A. R. (1974). Rhodamine 6G. A potent inhibitor of mitochondrial oxidative phosphorylation. *J Biol Chem, 249*(11): 3628–3637.

Gertsch, J. (2008). Anti-inflammatory cannabinoids in diet: towards a better understanding of CB(2) receptor action? *Commun Integr Biol, 1*(1): 26–28.

Ghosh, S., Wise, L. E., Chen, Y., Gujjar, R., Mahadevan, A., Cravatt, B. F., & Lichtman, A. H. (2013). The monoacylglycerol lipase inhibitor JZL184 suppresses inflammatory pain in the mouse carrageenan model. *Life Sci, 92*(8-9): 498–505.

Gobezie, R., Kho, A., Krastins, B., Sarracino, D. A., Thornhill, T. S., Chase, M., Millett, P. J., & Lee, D. M. (2007). High abundance synovial fluid proteome: distinct profiles in health and osteoarthritis. *Arthritis Res Ther, 9*(2): R36.

Goldring, M., Fukuo, K., Birkhead, J., Dudek, E., & Sandell, L. (1994). Transcriptional suppression by interleukin-1 and interferon-gamma of type II collagen gene expression in human chondrocytes. *J Cell Biochem, 54*: 85–99.

Goldring, M. B., Otero, M., Plumb, D. A., Dragomir, C., Favero, M., El Hachem, K., Hashimoto, K., Roach, H. I., Olivotto, E., Borzi, R. M., & Marcu, K. B. (2011). Roles of inflammatory and anabolic cytokines in cartilage metabolism: signals and multiple effectors converge upon MMP-13 regulation in osteoarthritis. *Eur Cell Mater, 21*: 202–220.

Goodwin, W., McCabe, D., Sauter, E., Reese, E., Walter, M., Buckwalter, J. A., & Martin, J. A. (2010). Rotenone prevents impact-induced chondrocyte death. *J Orthop Res, 28*(8): 1057–1063.

Griffioen, M. A., Dernetz, V. H., Yang, G.S., Griffith, K. A., Dorsey, S. G., & Renn, C. L. (2015). Evaluation of dynamic weight bearing for measuring nonevoked inflammatory hyperalgesia in mice. *Nurs Res, 64*: 81-87.

Gronblad, M., Konttinen, Y. T., Korkala, O., Liesi, P., Hukkanen, M., & Polak, J. M. (1988). Neuropeptides in synovium of patients with rheumatoid arthritis and osteoarthritis. *J Rheumatol, 15*(12): 1807–1810.

Gronblad, M., Konttinen, Y. T., Korkala, O., Liesi, P., Hukkanen, M., & Polak, J. M. (1988). Neuropeptides in the synovium of patients with rheumatoid arthritis and osteoarthritis. *J Rheumatol, 15*: 1807–1810.

Guermazi, A., Roemer, F. W., Hayashi, D., Crema, M. D., Niu, J., Zhang, Y., Marra, M. D., Katur, A., Lynch, J. A., El-Khoury, G. Y., Baker, K., Hughes, L. B., Nevitt, M. C., & Felson, D. T. (2011). Assessment of synovitis with contrast-enhanced MRI using a whole-joint semiquantitative scoring system in people with, or a high risk of, knee osteoarthritis: the MOST study. *Ann Rheum Dis, 70*(5): 805–811.

Guindon, J., & Hohmann, A. G. (2009). The endocannabinoid system and pain. *CNS Neurol Disord Drug Targets, 8*(6): 403–421.

Guindon, J., Guijarro, A., Piomelli, D., & Hohmann, A. G. (2011). Peripheral antinociceptive effects of inhibitors of monoacylglycerol lipase in a rat model of inflammatory pain. *Br J Pharmacol, 163*(7): 1464–1478.

Hanus, L., Breuer, A., Tchilibon, S., Shiloah, S., Goldenberg, D., Horowitz, M., Pertwee, R. G., Ross, R. A., Mechoulam, R., & Fride, E. (1999). HU-308: a specific agonist for CB2, a peripheral cannabinoid receptor. *Proc Natl Acad Sci USA, 96*(25): 14228–14233.

Hammell, D., Zhang, L., Ma, F., Abshire, S., McIlwrath, S., Stinchcomb, A., & Westlund, K. (2016). Transdermal cannabidiol reduces inflammation and pain-related behaviours in a rat model of arthritis. *Eur J Pain, 20*(6): 936–948.

Harris, W. H. (1986). Etiology of osteoarthritis of the hip. *Clin Orthop Rel Res,* (213): 20–33.

Heppelmann, B. & Pawlak, M. (1997). Sensitisation of articular afferents in normal and inflamed knee joints by substance P in the rat. *Neurosci Lett, 223*(2): 97–100.

Heppelmann, B. & McDougall, J. J. (2005). Inhibitory effect of amiloride and gadolinium on fine afferent nerves in the rat knee: evidence of mechanogated ion channels in joints. *Exp Brain Res, 167*(1): 114–118.

Hernandez-Torres, G., Cipriano, M., Heden, E., Bjorklund, E., Canales, A., Zian, D., Feliu, A., Mecha, M., Guaza, C., Fowler, C. J., Ortega-Gutierrez, S., & Lopez-Rodriguez. (2014). A reversible and selective inhibitor of monoacylglycerol lipase ameliorates multiple sclerosis. *Angew Chem Int Ed Engl, 53*(50): 13765–13770.

Hildebrand, C., Oqvist, G., Brax, L., & Tuisku, F. (1991). Anatomy of the rat knee joint and fibre composition of a major articular nerve. *Anat Rec, 229*(4): 545–555.

Hill, C. L., Hunter, D. J., Niu, J., Clancy, M., Guermazi, A., Genant, H., Gale, D., Grainger, A., & Conaghan, P. (2007). Synovitis detected on magnetic resonance imaging and its relation to pain and cartilage loss in knee osteoarthritis. *Ann Rheum Dis, 66*(12): 1599–1603.

Horner, G. & Dellon, A. L. (1994). Innervation of the human knee joint and implications for surgery. *Clin Orthop Relat Res, 465*(301): 221–226.

Huggins, J. P., Smart, T. S., Langman, S., Taylor, L., & Young, T. (2012). An efficient randomised, placebo-controlled clinical trial with the irreversible fatty acid amide hydrolase-1 inhibitor PF-04457845, which modulates endocannabinoids but fails to induce effective analgesia in patients with pain due to osteoarthritis of the knee. *Pain, 153*(9): 1837–1846.

Iannotti, F. A., Hill, C. L., Leo, A., Alhusaini, A., Soubrane, C., Mazzarella, E., Russo, E., Whalley, B. J., Di Marzo, V., & Stephens, G. J. (2013). Nonpsychotropic plant cannabinoids, cannabidivarin (CBDV) and cannabidiol (CBD), activate and desensitize transient receptor potential vanilloid 1 (TRPV1) channels in vitro: potential for the treatment of neuronal hyperexcitability. *ACS Chem Neurosci, 5*: 1131–1141.

Idris, A. I., Hof, R. J., Greig, I. R., Ridge, S. A., Baker, D., Ross, R. A., & Ralston, S. H. (2005). Regulation of bone mass, bone loss and osteoclast activity by cannabinoid receptors. *Nat Med, 11*(7): 774–779.

Idris, A. I. & Ralston, S. H. (2010). Cannabinoids and Bone: Friend or Foe? *Calcif Tissue Int, 87*(4): 285–297.

Ignatowska-Jankowska, B. M., Ghosh, S., Crowe, M. S., Kinsey, S. G., Niphakis, M. J., Abdullah, R. A., Tao, Q., O'Neal, S. T., Walentiny, D. M., Wiley, J. L., Cravatt, B. F., & Lichtman, A. H. (2014). *In vivo* characterization of the highly selective monoacylglycerol lipase inhibitor KML29: Antinociceptive activity without cannabimimetic side effects. *Br J Pharmacol, 171*(6): 1392–1407.

Imamura, M., Imamura, S. T., Kaziyama, H. H., Targino, R. A., Hsing, W. T., de Souza, L. P., Cutait, M. M., Fregni, F., & Camanho, G. L. (2003). Impact of nervous system hyperalgesia on pain, disability, and quality of life in patients with osteoarthritis: a controlled analysis. *Arthritis Rheum, 59*(10): 1424–1431.

Iuvone, T., Esposito, G., Esposito, R., Santamaria, R., Di Rosa, M., & Izzo, A. A. (2004). Neuroprotective effect of cannabidiol, a non-psychoactive component from Cannabis sativa, on beta-amyloid-induced toxicity in PC12 cells. *J Neurochem, 89*(1): 134–141.

Iuvone, T., Esposito, G., De Fillippis, D., Scuderi, C., & Steardo, L. (2009). Cannabidiol: a promising drug for neurodegenerative disorders? *CNS Neurosci & Ther, 1*: 65–75.

Ivanavicius, S. P., Ball, A. D., Heapy, C. G., Westwood, F. R., Murray, F., & Read, S. J. (2007). Structural pathology in a rodent model of osteoarthritis is associated with neuropathic pain: increased expression of ATF-3 and pharmacological characterisation. *Pain, 128*(3): 272–282.

Ivie, T. J., Bray, S. C., & Salo, P. T. (2002). Denervation impairs healing of the rabbit medial collateral ligament. *J Orthop Res, 20*(5): 990–995.

Janusz, M. J., Hookfin, E. B., Heitmeyer, S. A., Woessner, J. F., Freemont, A. J., Hoyland, J. A., Brown, K. K., Hsieh, L. C., Almstead, N. G., De, B., Natchus, M. G., Pikul, S., & Taiwo, Y. O. (2001). Moderation of iodoacetate-induced experimental osteoarthritis in rats by matrix metalloproteinase inhibitors. *Osteoarthr Cartil, 9*(8): 751–760.

Jensen, L. K. & Eenberg, W. (1996). Occupation as a risk factor for knee disorders. *Scand J Work Environ Health, 22*(3): 165–175.

Ji, R. R., Gereau, R. W., Malcangio, M., & Strichartz, G. R. (2009). MAP kinase and pain. *Brain Res Rev, 60*(1): 135–148.

Kalant, H. (2001). Medicinal use of cannabis: history and current status. *Pain Res Manag, 6*(2): 80–91.

Kapoor, M., Martel-Pelletier, J., Lajeunesse, D., Pelletier, J. P., & Fahmi, H. (2011). Role of proinflammatory cytokines in the pathophysiology of osteoarthritis. *Nat Rev Rheumatol, 7*(1): 33–42.

Kaptanoglu, E., Palaoglu, S., Surucu, H. S., Hayran, M., & Beskanokli, E. (2002). Ultrastrucutral scoring of graded acut spinal cord injury in the rat. *J Neurosurg, 97*(Suppl 1): 49–56.

Kapur, A., Zhao, P., Sharir, H., Bai, Y., Caron, M. G., Barak, L. S., & Abood, M. E. (2009). Atypical responsiveness of the orphan receptor GPR55 to cannabinoid ligands. *J Biol Chem*, *284*(43): 29817–29827.

Karimian, S. M., McDougall, J. J., Ferrell, W. R. (1995). Neuropeptidergic and autonomic control of the vasculature of the rat knee joint revealed by laser Doppler perfusion imaging. *Exp Physiol, 80*(30): 341–348.

Kawasaki, Y., Kohno, T., Zhuang, Z. Y., Brenner, G. J., Wang, H., Van Der Meer, C., Befort, K., Woolf, C. J., & Ji, R. R. (2004). Ionotropic and metabotropic receptors, protein kinase A, protein kinase C, and Src contribute to C-fiber-induced ERK activation and cAMP response element-binding protein phosphorylation in dorsal horn neurons, leading to central sensitization. *J Neurosci, 24*(38): 8310–8321.

Kelly, S., Chapman, R. J., Woodhams, S., Sagar, D. R., Turner, J., Burston, J. J., Bullock, C., Paton, K., Huang, J., Wong, A., McWilliams, D. F., Okine, B. N., Barrett, D. A., Walsh, D. A., & Chapman, V. (2015). Increased function of pronociceptive TRPV1 at the level of the joint in a rat model of osteoarthritis pain. *Ann Rheum Dis, 74*(1): 252–259.

Khalil, Z. & Helme, R. (1996). Sensory peptides as neuromodulators of would healing in aged rats. *J Gerontol A Biol Sci Med Sci, 51*(5): B354–361.

Kidd, B. L., & Urban, L. A. (2001). Mechanisms of inflammatory pain. *Br J Anaesth*, *87*(1), 3–11.

Kinsey, S. G., Long, J. Z., O'Neal, S. T., Abdullah, R. A., Poklis, J. L., Boger, D. L., Cravatt, B. F., & Lichtman, A. H. (2009). Blockade of endocannabinoid-degrading enzymes attenuates neuropathic pain. *J Pharmacol Exper Therapeut, 330*(3): 902–910.

Kinsey, S. G., Wise, L. E., Ramesh, D., Abdullah, R., Selley, D. E., Cravatt, B. F., & Lichtman, A. H. (2013). Repeated low-dose administration of the monoacylglycerol lipase inhibitor JZL184 retains cannabinoid receptor type 1-mediated antinociceptive and gastroprotective effects. *J Pharmacol Exp Ther, 345*(3): 492–501.

Konttinen, Y. T., Rees, R., Hukkanen, M., Gronblad, M., Tolvanen, E., Gibson S. J., Polak, J. M., & Brewerston, D. A. (1990). Nerves in inflammatory synovium: immunohistochemical observations on the adjuvant arthritis rat model. *J Rheumatol, 17*(12): 1586–1591.

Krasnokutsky, S., Belitskaya-Levy, I., Bencardino, J., Samuels, J., Attur, M., Regatte, R., Rosenthal, P., Greenberg, J., Schweitzer, M., Abramson, S. B., & Rybak, L. (2011). Quantitative magnetic resonance imaging evidence of synovial proliferation is associated with radiographic severity of knee osteoarthritis. *Arthritis Rheum, 63*(10): 2983–2991.

Krustev, E., Reid, A., & McDougall, J. J. (2014). Tapping into the endocannabinoid system to ameliorate acute inflammatory flares and associated pain in mouse knee joints. *Arthritis Res. Ther., 16*(5): 437

Krustev, E., Rioux, D., & McDougall, J. J. (2015). Mechanisms and mediators that drive arthritis pain. *Curr Osteoporos Rep, 13*(4): 216–224.

Krustev, E., Muley, M. M., & McDougall, J. J. (2017). Endocannabinoids inhibit neurogenic inflammation in murine joints by a non-canonical cannabinoid receptor mechanism. *Neuropeptides, 64:* 131-135.

Kujala, U. M., Kettunen, J., Paananen, H., Aalto, T., Battie, M. C., Impivaara, O., Videman, T., & Sarna, S. (1995). Knee osteoarthritis in former runners, soccer players, weight lifters, and shooters. *Arthritis Rheum, 38*(4): 539–546.

LaPorta, C., Bura, S. A., Aracil-Fernández, A., Manzanares, J., & Maldonado, R. (2013). Role of CB1 and CB2 cannabinoid receptors in the development of joint pain induced by monosodium iodoacetate. *Pain*, *154*(1): 160–174.

La Rana, G., Russo, R., D'Agostino, G., Sasso, O., Raso, G. M., Iacono, A., Meli, R., Piomelli, D., & Calignano, A. (2008). AM404, an anandamide transport inhibitor, reduces plasma extravasation in a model of neuropathic pain in rat: Role for cannabinoid receptors. *Neuropharmacology*, *54*(3): 521–529.

Latremoliere, A. & Woolf, C. J. (2009). Central sensitization: a generator of pain hypersensitivity by central neural plasticity. *J Pain, 10*(9): 895–926.

Lee, Y. C., Lu, B., Bathon, J. M., Haythornthewaite, J. A., Smith, M. T., Page, G. G., & Edwards, R. R. (2011). Pain sensitivity and pain reactivity in osteoarthritis. *Arthritis Care Res, 63*(3): 320–327.

Levick, J. R. (1979). An investigation into the validity of subatmoshperic pressure recordings from synovial fluid and their dependence on joint angle. *J Physiol, 289*: 55–67.

Li, H. (1974). An archaeological and historical account of cannabis in China. *Economic Botany, 28*:437–448.

Lin, Q., Peng, Y. B., Willis, W. D. (1996). Inhibition of primate spinothalamic tract neurons by spinal glycine and GABA is reduced during central sensitisation. *J Neurophysiol, 76*(2): 1005–1014.

Lundblad, H., Kreicbergs, A., & Jansson, K. A. (2008). Prediction of persistent pain after total knee replacement for osteoarthritis. *J Bone Joint Surg Br, 90*(2): 166–171.

Lynch, M. E, & Campbell, F. (2011). Cannabinoids for treatment of chronic non-cancer pain; a systematic review of randomized trials. *Br J Clin Pharmacol, 72*(5): 735–744.

Maccarrone, M., Bab, I., Bíró, T., Cabral, G. A., Dey, S. K., Di Marzo, V., Konje, J. C., Kunos, G., Mechoulam, R., Pacher, P., Sharkey, K. A., & Zimmer, A. (2015). Endocannabinoid signaling at the periphery: 50 years after THC. *Trends Pharmacol Sci, 36*(5): 277–296.

Mack, A. Marijuana as medicine?: the science beyond the controversy. In: Joy, J. E. Ed.). Washington, D.C.: National Academy Press; 2001.

Mahboubi, M. (2017). Mentha spicata as natural analgesia for treatment of pain in osteoarthritis patients. *Complement Ther Clin Pract, 26*: 1–4.

Maini, R. N. & Feldmann, M. (1998). Similarities in the mechanisms of action of pulse corticosteroids and anti-tumor necrosis factor alpha therapy in rheumatoid arthritis. *Arthrit Rheumat, 41*(3):565–565.

Malan, T. P., Ibrahim, M. M., Deng, H., Liu, Q., Mata, H. P., Vanderah, T., Porreca, F., & Makriyannis, A. (2001). CB2 cannabinoid receptor-mediated peripheral nociception. *Pain, 93*(3): 239–245.

Malek, N., Mrugala, M., Makuch, W., Kolosowska, N., Przewlocka, B., Binkowski, M., Czaja, M., Morera, E., Di Marzo, V., & Starowicz, K. (2015). A multi-target approach for pain treatment: dual inhibition of fatty acid amide hydrolase and TRPV1 in a rat model of osteoarthritis. *Pain, 156*(5): 890–903.

Malfait, A. M., Galily, R., Sumariwalla, P. F., Malik, A. S., Andreakos, E., Mechoulam, R., & Feldmann, M. (2000). The nonpsychoactive cannabis constituent is an oral anti-arthritic therapeutic in murine collagen-induced arthritis. *Proc Natl Acad Sci, 97*(17): 9561–9566.

Mapp, P. I., Walsh, D. A., Garrett, N. E., Kidd, B. L., Cruwys, S. C., Polak, J. M., & Blake, D. R. (1994). Effect of three animal models of inflammation on nerve fibres in the synovium. *Ann Rheum Dis, 53*(4): 240–246.

Mapp, P. I. (1995). Innervation of the synovium. *Ann Rheum Dis, 54*(5): 398–403.

Mapp, P. I & Walsh, D. A. (2012). Mechanisms and targets of angiogenesis and nerve growth in osteoarthritis. *Nat Rev Rheumatol, 8*(7): 390–398.

Maresz, K., Pryce, G., Ponomarev, E. D., Marsicano, G., Croxford, J. L., Shriver, L. P., Ledent, C., Cheng, X., Carrier, E. J., Mann, M. K., Giovannoni, G., Pertwee, R. G., Yamamura, T., Buckley, N. E., Hillard, C. J., Lutz, B., Baker, D., & Dittel, B. N. (2007). Direct suppression of CNS autoimmune inflammation via the cannabinoid receptor CB1 on neurons and CB2 on autoreactive T cells. *Nat Med, 13*(4): 492–497.

Martel-Pelletier, J., Pelletier, J. P., & Fahmi, H. (2003). Cyclooxygenase-2 and prostaglandins in articular tissues. *Semin Arthritis Rheum, 33*(3):155–167.

Martindale, J. C., Wilson, A. W., Reeve, A. J., Chessell, P., & Headley, P. M. (2007). Chronic secondary hypersensitivity of dorsal horn neurones following inflammation of the knee joint. *Pain, 133*(1-3): 79–86.

Matsuda, L. A., Lolait, S. J., Brownstein, M. J., Young, A. C., & Bonner, T. I. (1990). Structure of a cannabinoid receptor and functional expression of the cloned cDNA. *Nature*, *346*(6284), 561–564.

Mbvundula, E. C., Bunning, R. A., & Rainsford, K. (2005). Effects of cannabinoids on nitric oxide production by chondrocytes and proteoglycan degradation in cartilage. *Biochem Pharmacol,* 69(4): 635–640.

McDougall, J. J., Karimian, S. M., & Ferrell, W. R. (1994). Alteration of substance P-mediated vasodilatation and sympathetic vasoconstriction in the rat knee joint by adjuvant-induced inflammation. *Neurosci Lett*, *174*(2): 127–129.

McDougall, J. J., Karimian, S. M., & Ferrell, W. R. (1995). Prolonged alteration of vasoconstrictor and vasodilator responses in rat knee joints by adjuvant monoarthritis. *Exp Physiol*, *80*(3), 349–357.

McDougall, J. J., Bray, R. C., & Sharkey, K. A. (1997). Morphological and immunohistochemical examination of nerves in normal and injured collateral ligaments of rat, rabbit, and human knee joints. *Anat Rec, 248*(1): 29–39.

McDougall, J. J., Yeung, G., Leonard, C. A., & Bray, R. C. (2000). A role for calcitonin gene-related peptide in rabbit knee joint ligament healing. *Can J Physiol Pharmacol, 78*(7): 535–540.

McDougall, J. J. (2001). Abrogation of alpha-adrenergic vasoactivity in chronically inflamed rat knee joints. *Am J Physiol Regul Integr Comp Physiol, 281*(3): R821–827.

McDougall, J. J., Yu, V., & Thomson, J. (2008). *In vivo* effects of CB_2 receptor-selective cannabinoids on the vasculature of normal and arthritic rat knee joints. *Br J Pharmacol, 153*(2): 358–366.

McDougall, J. J. (2009). Cannabinoids and Pain Control in the Periphery. In B. Cairns (Ed.), Peripheral Receptor Targets for Analgesia: Novel Approaches to Pain Management. Hoboken, NJ: John Wiley and Sons, pp. 325–345.

McDougall, J. J., Andruski, B., Schuelert, N., Hallgrimsson, B., & Matyas, J. R. (2009). Unravelling the relationship between age, nociception and joint destruction in naturally occurring osteoarthritis of Dunkin Hartley guinea pigs. *Pain, 141*(3): 222–232.

McDougall, J. J. (2011). Peripheral analgesia: Hitting pain where it hurts. *Biochemica Et Biophysica Acta (BBA) Molec Basis Dis, 1812*(4): 459–467.

McDougall, J. J., Albacete, S., Schuelert, N., Mitchell, P. G., Lin, C., Oskins, J. L., Biu, H., & Chambers, M. G. (2017). Lysophosphatidic acid provides a missing link between osteoarthritis and joint neuropathic pain. *Osteoarthr Cartil, 25*(6): 926–934.

McHugh, D. (2012). GPR18 in microglia: implications for the CNS and endocannabinoid system signalling. *Br J Pharmacol, 167*(8): 1575-1582.

McInnes, I. B., & Schett, G. (2007). Cytokines in the pathogenesis of rheumatoid arthritis. *Nat Rev Immunol, 7*(6): 429–442.

McPartland, J. M. (2008). Expression of the endocannabinoid system in fibroblasts and myofascial tissues. *J Bodywork Movement Therap, 12*(2): 169–182.

Mechoulam, R., & Gaoni, Y. (1965). Hashish. IV. The isolation and structure of cannabinolic, cannabidiolic and cannabigerolic acids. *Tetrahedron, 21*(5): 1223–1229.

Mechoulam, R., Ben-Shabat, S., Hanus, L., Ligumsky, M., Kaminski, N. E., Schatz, A. R., Gopher, A., Almog, S., Martin, B. R., & Compton, D. R. (1995). Identification of an endogenous 2-monoglyceride, present in canine gut, that binds to cannabinoid receptors. *Biochem Pharmacol, 50*(1): 83–90.

Mechoulam, R. & Ben-Shabat, S. (1999). From gan-zi-gun-nu to anandamide and 2-arachidonoylglycerol: the ongoing story of cannabis. *Nat Prod Rep, 16*: 131–143.

Mogil, J. S. (2009). Animal models of pain: progress and challenges. *Nat Rev Neurosci, 10*(4): 283–294.

Moreton, B. J., Tew, V., das Nair, R., Wheeler, M., Walsh, D. A., & Lincoln, N. B. (2015). Pain phenotype in patients with knee osteoarthritis: classification and measurement properties of painDETECT and self-report Leeds assessment of neuropathic symptoms and signs scale in a cross-sectional study. *Arthritis Care Res, 67*(4): 519–528.

Mousa, S. A., Straub, R. H., Schafer, M., & Stein, C. (2007). Beta-endorphin, met-enkephalin and corresponding opioid receptors within synovium of patients with joint trauma, osteoarthritis and rheumatoid arthritis. *Ann Rheum Dis, 66*(7): 871–879.

Munro, S., Thomas, K. L., & Abu-Shaar, M. (1993). Molecular characterization of a peripheral receptor for cannabinoids. *Nature, 365*(6441): 61–65.

Nackley, A. G., Makriyannis, A., & Hohmann, A. G. (2003). Selective activation of cannabinoid CB(2) receptors suppresses spinal fos protein expression and pain behaviour in a rat model of inflammation. *Neuroscience, 119*(3): 747–757.

Naidu, P. S., Kinsey, S. G., Guo, T. L., Cravatt, B. F., & Lichtman, A. H. (2010). Regulation of inflammatory pain by inhibition of fatty acid amide hydrolase. *J Pharmacol Exper Therapeut, 334*(1): 182–190.

Neelakantan, H., Tallarida, R. J., Reichenbach, Z. W., Tuma, R. F., Ward, S. J., & Walker, E. A. (2015). Distinct interactions of cannabidiol and morphine in three nociceptive behavioural models in mice. *Behav Pharmacol, 26*(3): 304–314.

Nettelbladt, E. and Sundblad, L. (1959). Protein patterns in synovial fluid and serum in rheumatoid arthritis and osteoarthritis. *Arthritis Rheum, 2*: 144–151.

Neugebauer, V., & Schaible, H.-G. (1988). Peripheral and spinal components of the sensitization of spinal neurons during an acute experimental arthritis. *Agents Actions*, *25*(3–4): 234–236.

O'Brien, M., Philpott, H. T., & McDougall, J. J. (2017). Understanding osteoarthritis pain through animal models. *Clin Exp Rheumatol, 107*(5): 47-52.

Orita, S., Ishikawa, T., Miyagi, M., Ochiai, N., Inoue, G., Eguchi, Y., Kamoda, H., Arai, G., Toyone, T., Aoki, Y., Kubo, T., Takahashi, K., & Ohtori, S. (2011). Pain-related sensory innervation in monoiodoacetate-induced osteoarthritis in rat knees that gradually develops neuronal injury in addition to inflammatory pain. *BMC Musculoskelet Disord*, *12*: 134.

Orlowsky, E. W., & Kraus, V. B. (2015). The role of innate immunity in osteoarthritis: when our first line of defense goes on the offensive. *J Rheumatol, 42*: 363–371.

Pacher, P. (2006). The Endocannabinoid System as an Emerging Target of Pharmacotherapy. *Pharmacolog Rev*, *58*(3): 389–462.

Pazos, M. R., Mohammed, N., Lafuente, H., Santos, M., Martinez-Pinilla, E., Moreno, E., Valdizan, E., Romero, J., Pazos, A., Franco, R., Hillard, C. J., Alvarez, F. J., & Martinez-Orgado, J. (2013). Mechanisms of cannabidiol neuroprotectionin hypoxic-ischemic newborn pigs: role of 5HT(1A) and CB2 receptors. *Neuropharmacology, 71*: 282–291.

Pelletier, J. P., Martel-Pelletier, J., & Abramson, S. B. (2001). Osteoarthritis, an inflammatory disease: potential implication for the selection of new therapeutic targets. *Arthritis Rheum, 44*: 1237–1247.

Pertwee, R. G. (2005). Pharmacological actions of cannabinoids. *Handb Exp Pharmacol, 168*: 1–51.

Philpott, H. T., O'Brien, M., & McDougall, J. J. (2017). Attenuation of early phase inflammation by cannabidiol prevents pain and nerve damage in rat osteoarthritis. *Pain*: In Press.

Philpott, H. T. & McDougall, J. J. (2017). Arthritis and the endocannabinoid system. In: Kelly, M. E., Lehmann, C., & Zhou, J. (Eds). The Endocannabinoid System in Local and Systemic Inflammation. Morgan-Claypool, pp. 73-88.

Pitcher, G. M., Ritchie, J., & Henry, J. L. (1999). Paw withdrawal threshold in the von Frey hair test is influenced by the surface on which the rat stands. *J Neurosci Methods, 87*(2): 185–193.

Poole, A. R. (1999). An introduction to the pathophysiology of osteoarthritis. *Front Biosci, 4*(4): D662–670.

Pryce, G., Riddall, D. R., Selwood, D. L., Giovannoni, G., & Baker, D. (2015). Neuroprotection in experimental autoimmune encephalomyelitis and progressive multiple sclerosis by cannabis-based cannabinoids. *J Neuroimmune Pharmacol, 10*: 281–292.

Pugh, G., Welch, S. P. & Bass, P. P. (1994). Modulation of free intracellular calcium and cAMP by morphine and cannabinoids, alone and in combination in mouse brain and spinal cord synaptosomes. *Pharmacol Biochem Behav, 49:* 1093–1100.

Pugh, G., Smith, P. B., Dombrowski, D. S. & Welch, S. P. (1996). The role of endogenous opioids in enhancing the antinociception produced by the combination of delta 9–tetrahydrocannabinol and morphine in the spinal cord. *J Pharmacol Exp Ther, 279*: 608–616.

Qu, C., King, T., Okun, A., Lai, J., Fields, H. L., & Porreca, F. (2011). Lesion of the rostral anterior cingulate cortex eliminates the aversiveness of spontaneous neuropathic pain following partial or complete axotomy. *Pain*, *152*(7): 1641–1648.

Quadros, A. U., Pinto, L. G., Fonseca, M. M., Kusuda, R., Cunha, F. Q., & Cunha, T. M. (2015). Dynamic weight bearing is an efficient and predictable method for evaluation of arthritic nociception and its pathophysiological mechanisms in mice. *Sci Rep, 5*: 14648.

Ramer, R., Bublitz, K., Freimuth, N., Merkord, J., Rohde, H., Haustein, M., Borchet, P., Schmuhl, E., Linnebacher, M., & Hinz, B. (2012). Cannabidiol inhibits lung cancer cell invasion and metastasis via intercellular adhesion molecule-1. *FASEB J, 26*(4): 1535–1548.

Resstel, L. B. M., Tavares, R. F., Lisboa, S. F. S., Joca, S. R. L., Correa, F. M. A., & Guimaraes, F. S. (2009). 5-HT1A receptors are involved in the cannabidiol-induced attenuation of behavioural and cardiovascular responses to acute restraint stress in rats. *Br J Pharmacol, 156*(1): 181–188.

Richardson, J. D., Aanonsen, L., & Hargreaves, K. M. (1998). Antihyperalgesic effects of spinal cannabinoids. *Europ J Pharmacol, 345*(2): 145–153.

Richardson, D., Pearson, R. G., Kurian, N., Latif, M. L., Garle, M. J., Barrett, D. A., Kendall, D. A., Scammell, B. E., Reeve, A. J., & Chapman, V. (2008). Characterisation of the cannabinoid receptor system in synovial tissue and fluid in patients with osteoarthritis and rheumatoid arthritis. *Arthritis Res Ther, 10*(2): R43.

Robinson, W. H., Lepus, C. M., Wang, Q., Raghu, H., Mao, R., Lindstrom, T. M., & Sokolove, J. (2016). Low-grade inflammation as a key mediator of the pathogenesis of osteoarthritis. *Nat Rev Rheumatol, 12*(10): 580–592.

Roemer, F. W., Crema, M. D., Trattnig, S., & Guermazi, A. (2011). Advances in imaging of osteoarthritis and cartilage. *Radiology, 260*(2): 332–354.

Romero-Sandoval, E. A., Horvath, R. J., & DeLeo, J. A. (2008). Neuroimmune interactions and pain: focus on glial-modulating targets. *Curr Opin Investig Drugs, 9*(7): 726–734.

Russo, E. B., Burnett, A., Hall, B., & Parker, K. K. (2005). Agonistic properties of cannabidiol at 5-HT1a receptors. *Neurochem Res, 30*(8): 1037–1043.

Russo, E. B. (2007). History of cannabis and its preparations in saga, science, and sobriquet. *Chem Biodivers, 4*(8): 1614–1648.

Russo, E. B. (2011). Taming THC: potential cannabis synergy and phytocannabinoid-terpenoid entourage effects. *Br J Pharmacol, 163*(7): 1344–1364.

Russo, E. B. (2016). Beyond cannabis: Plants and the endocannabinoid system. *Trends Pharmacolo Sci, 37*(7): 594–605.

Ryberg, E., Larsson, N., Sjogren, S., Hjorth, S., Hermansson, N. O., Leonova, J., Elebring, T., Nilsson, K., Drmota, T., & Greasley, P. J. (2007). The orphan receptor GPR55 is a novel cannabinoid receptor. *Br J Pharmacol, 152*(7): 1092–1101.

Ryz, N. R., Remillard, D. J., & Russo, E. B. (2017). Cannabis roots: a traditional therapy with future potential for treating inflammation and pain. *Cannabis Cannabinoid Res, 2*(1): 210–216.

Sagar, D. R., Staniaszek, L. E., Okine, B. N., Woodhams, S., Norris, L. M., Pearson, R. G., Garle, M. J., Alexander, S. P., Bennett, A. J., Barrett, D. A., Kendall, D. A., Scammell, B. E., & Chapman, V. (2010). Tonic modulation of spinal hyperexcitability by the endocannabinoid receptor system in a rat model of osteoarthritis pain. *Arthritis Rheum, 62*(12): 3666–3676.

Saklatvala, J. (1986). Tumour necrosis factor alpha stimulates resorption and inhibits synthesis of proteoglycan in cartilage. *Nature, 322*: 547–549.

Scanzello, C. R., McKeon, B., Swaim, B. H., DiCarlo, E., Asomugha, E. U., Kanda, V., Nair, A., Lee, D. M., Richmond, J. C., Katz, J. N., Crow, M. K., & Goldring, S. R. (2011). Synovial inflammation in patients undergoing arthroscopic meniscectomy: molecular characterization and relationship to symptoms. *Arthritis Rheum, 63*(2): 391–400.

Scanzello, C. R., & Goldring, S. R. (2012). The role of synovitis in osteoarthritis pathogenesis. *Bone*, *51*(2), 249–257.

Schaible, H. G. & Schmidt, R. F. (1985). Effects of an experimental arthritis on the sensory properties of fine articular afferent units. *J Neurophysiol, 54*(5): 1109–1122.

Schaible, H. G. & Schmidt, R. F. (1988). Time course of mechanosensitivity changes in articular afferents during a developing experimental arthritis. *J Neurophysiol, 60*(6): 2180–2195.

Schaible, H. G. (2006). Peripheral and Central Mechanisms of Pain Generation. In: Stein, C. Ed Analgesia. Handbook of Experimental Pharmacology, vol 177. Springer, Berlin, Heidelberg, pp. 3–28.

Schaible, H. G., Richter, F., Ebersberger, A., Boettger, M. K., Vanegas, H., Natura, G., Vazquez, E., & Segond von Banchet, G. (2009). Joint pain. *Exp Brain Res, 196*(1): 153–162.

Schomberg, D., Ahmed, M., Miranpuri, G., Olson, J., & Resnick, D. (2012). Neuropathic pain: role of inflammation, immune response, and ion channel activity in central injury mechanisms. *Ann Neurosci, 19*(3): 125–132.

Schuelert, N., & McDougall, J. J. (2009). Grading of monosodium iodoacetate-induced osteoarthritis reveals a concentration-dependent sensitization of nociceptors in the knee joint of the rat. *Neurosci Lett, 465*(2): 184–188.

Schuelert, N., Zhang, C., Mogg, A., Broad, L., Hepburn, D., Nisenbaum, E., Johnson, M. P., & McDougall, J. (2010). Paradoxical effects of the cannabinoid CB2 receptor agonist GW405833 on rat osteoarthritic knee joint pain. *Osteoarthr Cartil, 18*(11): 1536–1543.

Schuelert, N., Johnson, M. P., Oskins, J. L., Jassal, K., Chambers, M. G., & McDougall, J. J. (2011). Local application of the endocannabinoid hydrolysis inhibitor URB597 reduces nociception in spontaneous and chemically induced models of osteoarthritis. *Pain, 152*(5): 975–981.

Schumacher, M. A. (2010). TRP channels in pain and inflammation: Therapeutic opportunities. *Pain Pract, 10*(3): 185–200.

Schwarz, H., Blanco, F., & Lotz, M. (1994). Anandamide, an endogenous cannabinoid receptor agonist inhibits lymphocyte proliferation and induces apoptosis. *J Neuroimmunol, 55*(1): 107–115.

Scott, D., Wolfe, F., & Huizinga, T. (2010). Rheumatoid arthritis. *Lancet, 376*(9746): 1094–1108.

Scuderi, C., Steardo, L., & Esposito, G. (2014). Cannabidiol promotes amyloid precursor protein ubiquitination and reduction of beta amyloid expression in SHSY5APP+ cells through PPARγ involvement. *Phytother Res, 28*(7): 1007–1013.

Seely, K. A., Brents, L. K., Franks, L. N., Rajasekaran, M., Zimmerman, S. M., Fantegrossi, W. E., & Prather, P. L. (2012). AM-251 and rimonabant act as direct antagonists at mu-opioid receptors: implications for opioid/cannabinoid interaction studies. *Neuropharmacology*, *63*(5): 905–915.

Sheng, W. S., Hu, S., Min, X., Cabral, G. A., Lokensgard, J. R., & Peterson, P. K. (2004). Synthetic cannabinoid WIN55,212-2 inhibits generation of inflammatory mediators by IL-1beta-stimulated human astrocytes. *Glia, 49*(2): 211–219.

Skou, S. T., Graven-Nielsen, T., Rasmussen, S., Simonsen, O. H., Laursen, M. B., & Arendt-Nielsen, L. (2014). Facilitation of pain sensitization in knee osteoarthritis and persistent post-operative pain: a cross-sectional study. *Eur J Pain, 18*(7): 1024–1031.

Smith, M., Triantafillou, S., Parker, A., Youssef, P. and Coleman, M. (1997). Synovial membrane inflammation and cytokine production in patients with early osteoarthritis. *J Rheumatol, 24*: 365–371.

Smith, F. L., Cichewicz, D., Martin, Z. L., & Welch, S. P. (1998). The enhancement of morphine antinociception in mice by delta9–tetrahydrocannabinol. *Pharmacol Biochem Behav, 60*: 559–566.

Sohn, D., Sokolove, J., Sharpe, O., Erhart, J., Chandra, P., Lahey, L., Lindstrom, T. M., Hwang, I., Boyer, K. A., Andriacchi, T. P., & Robinson, W. H. (2012). Plasma proteins present in osteoarthritic synovial fluid can stimulate cytokine production via toll-like receptor 4. *Arthritis Res Ther, 14*(1): R7.

Sokoloff, L. (1987). Aging and degenerative disease affecting cartilage. In Hall, B. K. ed. Cartilage. New York Academic Press, pp. 110–141.

Sokolove, J., & Lepus, C. M. (2013). Role of inflammation in the pathogenesis of osteoarthritis: latest findings and interpretations. *Ther Adv Musculoskelet Dis*, *5*(2): 77–94.

Sotocinal, S. G., Sorge, R. E., Zaloum, A., Tuttle, A. H., Martin, L. J., Wieskopf, J. S., Mapplebeck, J. C. S., Wei, P., Zhan, S., Zhang, S., McDougall, J. J., King, O. D., & Mogil, J. S. (2011). The rat grimace scale: a partially automated method for quantifying pain in the laboratory rat via facial expressions. *Mol Pain, 7*: 55.

Svizenska, I., Dubovy, P., & Sulcova, A. (2008). Cannabinoid receptors 1 and 2 (CB1 and CB2), their distribution, ligands and functional involvement in nervous system structures—a short review. *Pharmacol Biochem Behav, 90*(4): 501–511.

Tam, J., Ofek, O., Fride, E., Ledent, C., Gabet, Y., Muller, R., Zimmer, A., Mackie, K., Mechoulam, R., Shohami, E., & Bab, I. (2006). Involvement of neuronal cannabinoid receptor, CB1, in regulation of bone mass and bone remodeling. *Mol Pharmacol, 70*(3): 786–792.

Tam, J., Trembovler, V., Marzo, V. D., Petrosino, S., Leo, G., Alexandrovich, A., Regev, E., Casap, N., Shteyer, A., Ledent, C., Karsak, M., Zimmer, A., Mechoulam, R., Yirmiya, R, Shohami, E., & Bab, I. (2007). The cannabinoid CB1 receptor regulates bone formation by modulating adrenergic signaling. *FASEB J, 22*(1): 285–294.

Thakur, M., Rahman, W., Hobbs, C., Dickenson, A. H., & Bennett, D. L. (2012) Characterisation of a peripheral neuropathic component of the rat monoiodoacetate model of osteoarthritis. *PloS One, 7*(3): e33730.

The Arthritis Society of Canada. (2013). Arthritis Facts and Figures. Retrieved from https://arthritis.ca/understand-arthritis/arthritis-facts-figures.

Thomas, A., Baillie, G. L., Phillips, A. M., Razdan, R. K., Ross, R. A., & Pertwee, R. G. (2007). Cannabidiol displays unexpectedly high potency as an antagonist of CB1 and CB2 receptor agonists in vitro. *Br J Pharmacol, 150*(5):613–623.

Torres, L., Dunlop, D. D., Peterfy, C., Guermazi, A., Prasad, P., Hayes, K. W., Song, J., Cahue, S., Chang, A., Marshall, M., & Sharma, L. (2006). The relationship between specific tissue lesions and pain severity in persons with knee osteoarthritis. *Osteoarthr Cartil, 14*(10): 1033–1040.

Trouvin, A. & Perrot, S. (2017). Pain in osteoarthritis. Implications for optimal management. *Joint Bone Spine, S1297-319X*(17): 30156–2.

Tun, K., Cemil, B., Gurcay, A. G., Kaptanoglu, E., Sargon, M. F., Tekdemir, I., Comert, A., & Kanpolat, Y. (2009). Ultrastructural evaluation of pulsed radiofrequency and conventional radiofrequency lesions in rat sciatic nerve. *Surg Neurol, 72*(5): 496–500.

van Laar, M., Pergolizzi, J. V., Mellinghoff, H., Merchante, I. M., Nalamachu, S., O'Brien, J., Perrot, S., & Raffa, R. B. (2012). Pain treatment in arthritis-related pain: beyond NSAIDs. *Open Rheumatol J, 6*: 320–330.

Varga, A., Nemeth, J., Szabo, A., McDougall, J. J., Zhang, C., Elekes, K., Pinter, E., Szolcsanyi, J., & Helyes, Z. (2005). Effects of the novel TRPV1 receptor antagonist SB366791 in vitro and in vivo in the rat. *Neurosci Lett, 385*: 137–142.

Vera, G., Cabezos, P. A., Martin, M. I., & Abalo, R. (2013). Characterization of cannabinoid-induced relief of neuropathic pain in a rat model of cisplatin-induced neuropathy. *Pharmacol Biochem Behav, 105*: 205–212.

Vestweber, D. (2015). How leukocytes cross the vascular endothelium. *Nat Rev Immunol, 15*(11): 692–704.

Wang, Q., Rozelle, A., Lepus, C., Scanzello, C., Song, J., Larsen, D., Crish, J. F., Bebek, G., Ritter, S. Y., Lindstrom, T. M., Hwang, I., Wong, H. H., Punzi, L., Encarnacion, A., Shamloo, M., Goodman, S. B., Wyss-Coray, T., Goldring, S. R., Banda, N. K., Thurman, J. M., Gobezie, R., Crow, M. K., Holers, V. M., Lee, D. M., & Robinson, W. H. (2011) Identification of a central role for complement in osteoarthritis. *Nat Med, 17*(12): 1674–1679.

Ward, S. J., McAllister, S. D., Kawamura, R., Murase, R., Neelakantan, H., & Walker, E. A. (2014). Cannabidiol inhibits paclitaxel-induced neuropathic pain through 5-HT$_{1A}$ receptors without diminishing nervous system function or chemotherapy efficacy. *Br J Pharmacol, 171*(3): 636–645.

Watkins, L. R. & Maier, S. F. (2002). Beyond neurons: Evidence that immune and glial cells contribute to pathological pain states. *Physiol Rev, 82*(4): 981–1011.

Wedge, J. H., Wasylenko, M. J., & Houston, C. S. (1991). Minor anatomic abnormalities of the hip joint persisting from childhood and their possible relationship to idiopathic osteoarthritis. *Clin Orthrop, 264*: 122–128.

Welch, S. P., Thomas, C. & Patrick, G. S. (1995). Modulation of cannabinoid–induced antinociception after intracerebroventricular versus intrathecal administration to mice: possible mechanisms for interaction with morphine. *J Pharmacol Exp Ther, 272*: 310–321.

Welch, S. P. & Eads, M. (1999). Synergistic interactions of endogenous opioids and cannabinoid systems. *Brain Res, 848*: 183–190.

Wernecke, C., Braun, H. J., & Dragoo, J. L. (2015). The effect of intra-articular corticosteroids on articular cartilage. *Orthop J Sports Med, 3*(5): 2325967115581163.

Weydt, P., Hong, S., Witting, A., Moller, T., Stella, N., & Kliot, M. (2005). Cannabinol delays symptom onset in SOD1 (G93A) transgenic mice without affecting survival. *Amyotroph Lateral Scler Other Motor Neuron Disord, 6*: 182–184.

Whiteside, G. T., Gottshall, S. L., Boulet, J. M., Chaffer, S. M., Harrison, J. E., Pearson, M. S., Turchin, P. I., Mark, L., Garrison, A. E., & Valenzano, K. J. (2005). A role for cannabinoid receptors, but not endogenous opioids, in the antinociceptive activity of the CB2-selective agonist, GW405833. *Eur J Pharmacol, 528*(1-3): 65–72.

Whitting, P. F., Wolff, R. F., Deshpande, S., Di Nisio, M., Duffy, S., Hernandez, A. V., Keurentjes, C., Lang, S., Misso, K., Ryder, S., Schmidlkofer, S., Westwood, M., & Kleijnen, J. (2015). Cannabinoids for medical use: a systematic review and meta-analysis. *JAMA, 313*(24): 2456–2473.

Whyte, L. S., Ryberg, E., Sims, N. A., Ridge, S. A., Mackie, K., Greasley, P. J., Ross, R. A., & Rogers, M. J. (2009). The putative cannabinoid receptor GPR55 affects osteoclast function *in vitro* and bone mass *in vivo. Procee. Nat Acad Sci, 106*(38): 16511–16516.

Witkamp, R., & Meijerink, J. (2014). The endocannabinoid system: an emerging key player in inflammation. *Curr Opin Clin Nutr Metab Care, 17*(2): 130–138.

Woolf, C. J. & Thompson, S. W. (1991). The induction and maintenance of central sensitization is dependent on N-methyl-D-aspartic acid receptor activation: implications for the treatment of post-injury pain hypersensitivity states. *Pain, 44*(3): 293–9.

Woolf, C. J., Ma, Q. P., Allchorne, A., & Poole, S. (1996). Peripheral cell types contributing to the hyperalgesic action of nerve growth factor in inflammation. *J Neurosci, 16*(8): 2716-2723.

Woolf, C. J. & Salter, M. W. (2000). Neuronal plasticity: increasing the gain in pain. *Science, 288*(5472): 1765–1769.

Wu, C. W., Morrell, M. R., Heinze, E., Concoff, A. L., Wollaston, S. J., Arnold, E. L., Singh, R., Charles, C., Skovrun, M. L., FitzGerald, J. D., Moreland, L. W., & Kalunian, K. C. (2005). Validation of American College of Rheumatology classification criteria for knee osteoarthritis using arthroscopically defined cartilage damage scores. *Semin Arthritis Rheum, 35*(3): 197–201.

Wylde, V., Palmer, S., Learmonth, I. D., & Dieppe, P. (2012). Somatosensory abnormalities in knee OA. *Rheumatology (Oxford), 51*(3): 535–543.

Wylde, V., Sayers, A., Lenguerrand, E., Gooberman-Hill, R., Pyke, M., Beswick, A. D., Dieppe, P., & Blom, A. W. (2015). Preoperative widespread pain sensitization and chronic pain after hip and knee replacement: a cohort analysis. *Pain, 156*(1): 47–54.

Xu, H., Cheng, C. L., Chen, M., Manivannan, A., Cabay, L., Pertwee, R. G., Coutts, A., & Forrester, J. V. (2007). Anti-inflammatory property of the cannabinoid receptor-2-selective agonist JWH-133 in a rodent model of autoimmune uveoretinitis. *J Leukoc Biol, 82*(3): 532–541.

Yao, B. B., Hsieh, G. C., Frost, J. M., Fan, Y., Garrison, T. R., Daza, A. V., Grayson, G. K., Zhu, C. Z., Pai, M., Chandran, P., Salyers, A. K., Wensink, E. J., Honore, P., Sullivan, J. P., Dart, M. J., & Meyer, M. D. (2008). In vitro and in vivo characterization of A-796260: a selective cannabinoid CB2 receptor agonist exhibiting analgesic activity in rodent pain models. *Br J Pharmacol, 153*(2): 390–401.

Yates, M. L. & Barker, E. L. (2009). Inactivation and bioransformation of the endogenous cannabinoids anandamide and 2-arachidonoylglycerol. *Mol Pharmacol, 76*(1): 11–17.

Zehentbauer, F. M., Moretto, C., Stephen, R., Thevar, T., Gilchrist, J. R., Pokrajac, D., Richard, K. L., & Kiefer, J. (2014). Fluorescence spectroscopy of rhodamine 6G: concentration and solvent effects. *Spectochim Acta A Mol Biomol Spectrosc, 121*: 147–151.

Zhao, Y., Yuan, Z., Liu, Y., Xue, J., Tian, Y., Liu, W., Zhang, W., Shen, Y., Xu, W., Liang, X., & Chen, T. (2010). Activation of cannabinoid CB2 receptor ameliorates atherosclerosis associated with suppression of adhesion molecules. *J Cardiovasc Pharmacol, 55*: 292–298.

Zias, J., Stark, H., Sellgman, J., Levy, R., Werker, E., Breuer, A., & Mechoulam, R. (1993). Early medical use of cannabis. *Nature*, *363*(6426): 215.

Zygmunt, P. M., Petersson, J., Andersson, D. A., Chuang, H., Sorgard, M., Di Marzo, V., Julius, D., & Hogestatt, E. D. (1999). Vanilloid receptors on sensory nerves mediate the vasodilator action of anandamide. *Nature, 400*: 452–457

Appendix

A1

Copyright Clearance Center

RightsLink®

Home | Create Account | Help

Title: Attenuation of early phase inflammation by cannabidiol prevents pain and nerve damage in rat osteoarthritis.

Author: Holly Philpott, Melissa O'Brien, and Jason McDougall

Publication: Pain

Publisher: Wolters Kluwer Health, Inc.

Date: Sep 18, 2017

Copyright © 2017, (C) 2017 International Association for the Study of Pain

LOGIN

If you're a copyright.com user, you can login to RightsLink using your copyright.com credentials. Already a RightsLink user or want to learn more?

License Not Required

This request is granted gratis and no formal license is required from Wolters Kluwer. Please note that modifications are not permitted. Please use the following citation format: author(s), title of article, title of journal, volume number, issue number, inclusive pages and website URL to the journal page.

BACK | CLOSE WINDOW

A2

Re: Rights & Permissions Request
🔄 Reply all | ⌄   🗑 Delete   Junk | ⌄   •••   ✖

JC   **Joe Cho <cho@morganclaypool.com>**   👍   🔄 Reply all | ⌄
       Mon 10-16, 4:00 PM
       Holly Philpott ⌄

Inbox

Flag for follow up. Start by October-16-17. Due by October-16-17.

You replied on 2017-10-16 4:09 PM.

Hi Holly!
I remember you of course, from earlier this year. Yes, absolutely you can have permission to re-use this figure. So long as you can attribute the original publication in which the figure appeared, you are free to use it as you wish! And, if you could include the DOI in the credit line, that would be ideal! (so that readers can be directed to the original publication)

https://doi.org/10.4199/C00151ED1V01Y201702ISP074

Thanks so much for your email, and best of luck with your masters thesis!

Cheers,
joe

Joe Cho
Executive Editor
Colloquium Digital Library of Life Sciences
Morgan & Claypool Publishers
1210 Fifth Avenue, Suite 250
San Rafael, CA 94901
(415) 785-8003
cho@morganclaypool.com
https://www.linkedin.com/pub/joe-cho/34/a52/756